Design, Synthesis, and Evaluation of Insulin Bioconjugates for the Application of Enhanced Basal and Glucose-Responsive Activity

by

Abel Bryan Cortinas

B.S. Chemical Engineering
Texas Tech University, 2012

M.Sc. Chemical Engineering Practice
Massachusetts Institute of Technology, 2014

Submitted to the Department of Chemical Engineering in Partial Fulfillment of the Requirements for the Degree of

DOCTOR OF PHILOSOPHY

at the

MASSACHUSETTS INSTITUTE OF TECHNOLOGY

September 2018

Signature redacted

Signature of Author: .....
Abel B. Cortinas
Department of Chemical Engineering
September 6, 2018

Signature redacted

Certified by: .....
Daniel G. Anderson
Samuel A. Goldblith Professor of Applied Biology,
Chemical Engineering and Health Sciences & Technology
Thesis Supervisor

Signature redacted

Accepted by: .....
Patrick S. Doyle
Robert T. Haslam Professor of Chemical Engineering
Chairman, Committee for Graduate Students

Design, Synthesis, and Evaluation of Insulin Bioconjugates for the Application of Enhanced Basal and Glucose-Responsive Activity

by

Abel Bryan Cortinas

Submitted to the Department of Chemical Engineering on September 6, 2018 in Partial Fulfillment of the Requirements for the Degree of Doctor of Philosophy.

Abstract

Since its discovery by Banting and Best, the administration of exogenous insulin to control blood glucose levels has been a primary method of treatment for severe cases of diabetes mellitus. Several decades of insulin engineering and development has led to the clinical introduction of two broadly classified categories of protein therapies: prandial and basal insulins. Although these developments have had profound effects on disease management with respect to insulin-dependent diabetes, the overall strategy for development has historically been restricted to rational design criteria based on static pharmacodynamic profiles, profiles that are inherently naïve to physiological changes in the diabetic patient. As a result, stringent patient-dependent regimens are the standard of care with regard to glycemic monitoring and management. When coupled with issues such as patient noncompliance, severe hypoglycemia, as well as the adverse health effects that result from chronic mismanagement of hyperglycemia, it is obvious that there are still major hurdles that must be overcome to properly treat the disease.

Herein, we introduce innovative strategies aimed towards the advancement of novel insulin bioconjugate design and development for enhanced long-term efficacy and glucose-responsive activity. First, we develop a class of unimolecular, glucose-responsive insulin conjugates towards the design of a state-responsive, patient-dependent therapy. Optimization of this system resulted in the identification of a lead candidate, Ins-PL-4FPBA, capable of (1) glucose-mediated changes in solubility for long-term sequestration and intelligent depot formation, (2) superior safety in comparison to clinically used long-acting insulins, and (3) glucose-responsive pharmacokinetic and pharmacodynamic activity in both healthy and diabetic animal models.

Next, we pioneer the first design and synthesis strategy of a novel class of sugar-responsive insulin conjugates, with the ultimate goal of developing an insulin bioconjugate capable of sugar-mediated receptor binding interactions. In this effort, we created dynamically cyclized insulin conjugates that were found to exhibit enhanced chemical stability and superior thermal stability relative to the native protein, as well as sugar-mediated destabilization, suggesting the potential to exploit the insulin receptor binding mechanism.

Lastly, we focus on improving basal activity of the insulin protein by utilizing a novel class of zwitterionic insulin polymer conjugates towards the generation of ultra long-acting insulin therapies. The resulting library is demonstrated to afford equivalent biological potency relative to native human insulin, augmented thermal and chemical stability capable of withstanding thermal aggregation for over 80 days, as well as ultra long-acting basal insulin potential.

Thesis Supervisor: Daniel G. Anderson
Title: Samuel A. Goldblith Associate Professor

Acknowledgements

The completion of this Ph.D. would not have been possible without the countless contributions and support of numerous individuals. To begin, I would first like to thank my advisor and mentor, Prof. Dan Anderson, for giving me the amazing opportunity to join such an incredible group of scientists and visionaries. I also want to thank the members of my Thesis Committee, Prof. Bob Langer and Prof. Michael Strano, for your invaluable discussions, whether they were based in science, career development, or general mentorship. Your unparalleled support has been greatly appreciated and I look forward to continuing our professional relationship in the future.

It has been an honor and a privilege to work with such talented scientists in the Anderson and Langer labs, many of whom have also served as my mentors throughout my academic journey. I would like to personally thank Abigail Lytton-Jean for taking me under her wing during my first couple of months in the lab. I also want to gratefully thank Amy Lin, Ben Tang, Danny Chou, and especially Matt Webber for offering their mentorship, guidance, and training during the initial years of my Ph.D., the results of which ultimately inspired my overall thesis work. I want to particularly acknowledge and thank the following individuals, some of them collaborators, all of them friends, as well as the many more that I have had the great fortune and opportunity to interact and work with over the past several years: Kevin Daniel, Lisa Volpatti, Amanda Facklam, Volkan Yesilyurt, Lavanya Thapa, Kaitlyn Sadtler, Asha Patel, Owen Fenton, Jimmy Kaczmarek, Natasha Nukolova, Adam Behrens, Yulia Rybakova, Elena Smekalova, Omar Khan, Robert Dorkin, Sid Jhunjhunwala, Danya Lavin, James Dahlman, Piotr Kowalski, Luke Rhym, Benny Larson, Chandra Bhattacharya, Arnab, Rudra, Luke Ceo, Arijit Basu, Heloise Ragelle, Mark Tibbit, Eric Appel, Faryal Mir, Jun Yang, Arturo Vegas, Rose Kanasty, Suman Bose, Matthias Oberli, Keith Hearon, and Lisa Freed. I have also been extremely fortunate to have mentored and worked with an amazing group of undergraduate students throughout my time at MIT -- Fabin Girma, Steven Truong, and Morgan Matranga – all of whom have demonstrated a great capacity as scientists and through whom I have learned just as much. I especially want to thank Tara Fawaz for her incredible work and contribution in keeping the Anderson Lab running so smoothly.

As for my fellow ChemE classmates, many of you have become lifelong friends outside of the classroom and have been an everlasting source of support and inspiration. I am eternally grateful and forever in your debt for all your time, consideration, and help that you gave me during our first crazy year here at MIT. Specifically, I want to thank Manish Shetty, Kevin Kauffman, Hok Hei Tam, Paul Bisso, Chibueze Amanchukwu, Ankur Gupta, Elizabeth McLaughlin Perea, Nick Mozdzierz, Jen Lewis, Won-Jun Jo, Monique Kauke, and Sue Zanne Tan. I also want to thank a very specific group of Distinguished Alumni from this class, specifically Jose Gomez, Harry Watson, Chad Hunter, Justin Nelson, and Isaac Roes. I have thoroughly enjoyed the friendship we have created, all of the adventures we have taken (and look forward to the many more to come), as well as the shenanigans that ensued and the memories we have made (and subsequently forgotten).

Next, I want to thank my undergraduate research advisor, Prof. Micah Green, for the amazing mentorship and training that helped me become the scientist I am today, as

well as for your encouragement and guidance in applying to my dream school, MIT. I also want to pay special tribute to my first academic mentors: Mr. Mac Willson and Mrs. Teresa Hollums. I will always consider you my family, and I thank you for helping to kindle my initial passions for science and, more broadly, STEM. It is because of your countless hours of teaching, tutoring, support, guidance, and love that encouraged me to whole-heartedly pursue my academic dreams, and for that I am eternally grateful and forever indebted.

Finally, I would like to thank my family, to whom this thesis is dedicated. To my Mom and Grandma, thank you for your unconditional love, support, patience, and compassion. Thank you for being my champions and fierce advocates, yours are the shoulders that I have stood on, and have gained support from, when I needed it most. Dad, thank you for always being there for me, regardless of time, day, or condition. You have always been a pillar of support for me and have shaped the person I am today. To John, Andrea, Popo, Roy, and Princess (our family dog), I love you all very much and I thank you for being my support system, and for always being there for me. Also, to all my wonderful cousins -- of which a complete list would require a separate chapter of its own -- I want to pay tribute to Joseph, Kylub, Raelene, Andrew, Eric, Alyson, Jessica, and Jane, I love you all. Additionally, I want to thank my best friends from back home -- Reggie Martinez, Anthony Herrera, Robert Beuning, and Michael Flores. Regardless of where life has taken us, or the distance between us at any given time, thank you for your amazing friendship and for all the laughs and experiences, I will always cherish our relationship. Lastly, I want to thank Olesya, you are such an amazing individual and the life we have built together over these past (almost) two years has been absolutely incredible. I cannot wait to see where our future takes us and to see how our (cat/dog) family grows in the near future. I love you.

This PhD would not have been possible without the invaluable support and encouragement of countless family members, friends, and colleagues. Thank you to everyone, past and present.

Table of Contents

List of Figures

List of Tables

Chapter 1: Background and Significance

Portions of the work presented in this chapter were published as:

N. A. Bakh, A. B. Cortinas, M. A. Weiss, R. S. Langer, D. G. Anderson, Z. Gu, S. Dutta, M. S. Strano, Glucose-responsive insulin by molecular and physical design, *Nat. Chem.* **9**, 937–943 (2017).

1.1 *Motivation and Current Challenges in Insulin-Based Therapy*

Since its discovery by Banting and Best in 1922, the administration of exogenous insulin to control blood glucose levels has been a primary method of treatment for severe cases of diabetes mellitus.[1–3] Diabetes mellitus in all its forms is a global epidemic affecting over 400 million individuals worldwide, with that number projected to grow to more than 600 million by 2045.[4] The majority of globally prevalent cases of diabetes can be segmented into two main categories: Type I and Type II diabetes. Although the pathology of Type I and Type II diabetes is fundamentally different and very complicated, with Type I characterized by the severe destruction of all insulin-producing β cells in the pancreas, and Type II characterized by a resistance to the insulin naturally administered in the body, both often necessitate chronic insulin therapy to manage glycemic fluctuations experienced throughout the day. Despite the series of advancements over the past several decades aimed at improving insulin's relatively low therapeutic index, including the commercial introduction of a number of excipients for increased protein stability and performance, as well as a number of engineered insulin therapies, euglycemic control that autonomously mimics the healthy pancreas remains a challenging objective for both current and envisioned diabetes technologies.[5–8] Engineering efforts have historically focused on modifying the primary structure of the native insulin protein to provide more precisely-tuned pharmacodynamics, the results of which have largely resulted in the clinical introduction of two, broadly classified categories of protein therapies: prandial and basal insulins. Prandial insulin therapies, which primarily serve to rapidly offset spikes in blood sugar, utilize several different principles aimed at reducing the tendency of insulin monomers to self-associate into dimers and hexamers. These

mechanisms include exploiting charge repulsion (insulin aspart), decreasing interfacial hydrophobicity, removing the metal-ion binding site, interfering with hydrophobic contacts and β-sheet formation (insulin lispro), as well as steric hindrance.[9] Conversely, basal insulin therapies, which serve as a long-acting source of insulin supply, utilize strategies for enhancing protraction. These mechanisms include alteration of the isoelectric point (insulin glargine), acylation with hydrophobic residues that undergo albumin binding (insulin detemir, insulin lithocholic acid conjugates), or the strengthening of protein hexameric, or multi-hexameric, association (Co(III)-insulin hexamer, perfluoroalkyl chain insulin, insulin degludec).[10–15] More recently, efforts have aimed at diversifying rational design principles to better address some of the challenges of current insulin therapies, such as resolving the disproportionate bolus exposure of administered insulin to peripheral versus hepatic tissues through engineering tissue-specific binding to the liver (Insulin-A, Insulin-B, Insulin-327), as well as increased thermal and chemical stability for long-term storage, administration, and efficacy (single-chain insulin).[16–18] Although considerable developments have been made with regard to tuning the selectivity and pharmacodynamics of insulin, the vast majority of these engineering endeavors have continued to focus on rational design criteria based on static pharmacodynamic profiles that are inherently naïve to physiological changes in the diabetic patient.

The goal of this Thesis is to introduce innovative strategies for the design, synthesis, and development of novel unimolecular insulin constructs capable of enhanced basal activity as well as glucose responsive efficacy. The concept of a glucose responsive insulin (GRI) has been a recent objective of diabetes technology, with the major feature of the GRI being its ability to modulate its potency, concentration, or dosing relative to a

patient's dynamic glucose concentration, thereby approximating aspects of a normally functioning pancreas. The prospect of a GRI, capable of dynamic, patient-dependent activity, remains both a grand challenge and a long-standing goal of diabetes care and possesses immense promise in improving the management of diabetes mellitus. However, a number of challenges must be addressed and overcome before GRI technology can become a realizable therapy that can achieve effective, widespread clinical application, some of which will be discussed in the following sections.

1.1.1 Learning from Nature: Biomimetic GRI Formulations

The concept of mimicking natural systems in engineering design is not new. However, the GRI as a dynamic therapeutic is meant to plug into an obviously dynamic, complex biochemical signaling network. In this case, the target to imitate is the secretion of insulin from pancreatic β-cells. To this end, many existing GRI concepts center around the loading and controlled release of native insulin triggered by hyperglycemic conditions from a host matrix. Historically, this has involved two basic types. In one, glucose binds and directly triggers a change in insulin release through some morphology change, such as swelling, shrinking or disruption. Enabling materials for this include concanavalin A (ConA; a glucose-binding protein originally extracted from the jack-bean) or phenylboronic acid (PBA)-incorporated materials.[19] The first glucose-responsive insulin delivery system was developed in 1979[20], where an elevated glucose level led to competitive binding of free glucose with binding sites of the ConA-polysaccharide matrix, causing the dissociation of the complex and subsequent release of encapsulated sugar-conjugated insulin. The challenge of translating ConA-mediated GRI formulation mainly involves the host immunological responses to non-native ConA.[21] PBA is known for its

ability to form complexes with polyol molecules such as glucose.[19,22] Typically, hydrogels made from copolymers with a hydrophilic backbone and PBA pendants can exhibit reversible volume changes in response to changing glucose levels, leading to the triggered release of insulin. One challenge is that the *p*Ka of PBA (8-9) is considerably higher than that of the physiological pH. PBA with electron-withdrawing moieties are therefore used to activate morphology change under a neutral pH.[23] Despite this, few studies have been demonstrated *in vivo* utilizing formulations integrated with PBA.

The other type often associates with glucose oxidase (GOx)-based enzymatic reaction:

$$\text{Glucose} + O_2 + H_2O \xrightarrow{\text{GOx}} \text{Gluconic Acid} + H_2O \quad (1)$$

With a progressively activated manner, a hyperglycemic state promotes the decrease of local pH level[24,25], which subsequently induces swelling, shrinking, degradation or dissociation of pH-sensitive matrices, leading to enhanced insulin release.[26–28] For example, the acidic environment can enhance the solubility of lysine-modified insulin,[24] trigger the collapsing or swelling of hydrogels crosslinked by polymers that can be readily protonated[25,28–31], or dissociate nanoparticles assembled from pH-sensitive materials[27]. However, it remains a challenge to lower the physiological pH to levels that trigger morphology transition within a short period of time *in vivo*, especially in a buffered physiological environment. How to achieve fast response *in vivo,* with pharmacokinetic profiles similar to that of the normal pancreatic β-cells, has therefore become a central question for engineering GRI formulations.[19] A rational design includes further development of ultra acid-sensitive materials as well as exploration of new response mechanisms, which could effectively improve response speed. For example, a hypoxia-

sensitive vesicle-based GRI delivery strategy has recently been exploited, leveraging the hypoxic condition generated during the enzymatic reaction.[32] Inspired by the responsiveness of natural vesicles (or granules) inside β-cells, such synthetic vesicles loaded with insulin can rapidly dissociate upon hyperglycemicia, compared to pH-activated vesicles. This formulation is also compatible with loading into a microneedle-array patch for painless administration.

In addition to increasing the rate of response, another important design criterion for improving the performance of current GRI formulations includes engineering the reliability of the response. To date, the glucose-responsive and repeatable pulsatile release profiles of synthetic formulations have yet to be reliably demonstrated *in vivo*, either due to irreversible disruption of formulations or depletion of insulin. A biomimetic design, learning from the β-cell GRI secretion system would facilitate improvement. In healthy individuals, the rate of insulin release through β-cells varies over a range of at least two orders of magnitude and is prompted in two release phases by relatively small changes in blood glucose concentration (4-8 mM)[33]. The mechanism involves metabolic coupling actions associated with insulin granule vesicles. Furthermore, the potential for inducing hypoglycemia as a result of unexpected release of a large amount of insulin remains a critical issue. Co-delivery of glucagon as a safeguard in a bio-responsive manner could potentially offer a solution. However, identifying an appropriate biomarker trigger for achieving controlled release of glucagon remains elusive in addition to glucagon's extreme instability. Finally, for formulations consisting of new materials, how to optimize biocompatibility without systemic and long-term toxicity is always a concern. These all require further tailoring material design and exploring innovations in discovering

response mechanisms. Importantly, to expedite translation of GRI systems, appropriate animal models integrated with the continuous glucose monitoring systems (CGMSs) should be thoroughly tested to obtain detailed dynamic glucose-responsive information for guiding optimization and clinic translation.

1.1.2 Molecular Modeling as a Tool for GRI Design

Recent work has introduced the concept of GRI molecular design and evaluation utilizing the mathematical framework of the state machine in an effort to develop *in silico* methods for identification of potential GRI constructs.[34,35] A state machine is an entity capable of basic computation, and there exists a rich, mathematical framework within which to analyze their workings.[36] Treating the design and synthesis of a GRI as a state machine allows one to leverage the advances in computation and simulation of the human endocrine system that have come about as a part of the Artificial Pancreas effort.[37–41] Reducing a GRI to a state machine allows a mathematical representation to be developed which encompasses a number of critical parameters to GRI synthesis. These state machines can then be interfaced with physiological compartmental models of glucose and insulin metabolism to investigate the effect of varying GRI parameters on blood glucose levels. Through exploring this parameter space, a goal for optimal GRI parameters could be developed for several different GRI types, which can help guide in the synthesis of such insulins.

A physiological compartment model of glucose and insulin metabolism developed by Sorensen[42] and further refined by Bisker et al.[43] divides the body into various well mixed compartments such as the brain, heart and lungs, liver, kidney, gut, adipose, and muscle tissue. Solutes circulate through the capillary volumes and are free to diffuse to

the interstitial volumes. The equations for a generic compartment with capillary and interstitial volumes are as follows:

$$V_{kc}^{s}\frac{dC_{kc}}{dt}=Q_{k}\left(C_{H}\ -C_{kc}\right)-\frac{V_{ki}^{s}}{T_{k}^{s}}\left(C_{kc}\ -C_{ki}\right)-r_{suc}+r_{spc}+v_{s}r_{GRI} \tag{2}$$

$$V_{ki}^{s}\frac{dC_{ki}}{dt}=\frac{V_{ki}^{s}}{T_{k}^{s}}\left(C_{kc}\ -C_{ki}\right)-r_{sui}+r_{spi}+v_{s}r_{GRI} \tag{3}$$

where *V*, *C*, and *Q* stand for the volume, concentration and flowrate of each compartment, respectively. The superscript *s* stands for the type of solute, the subscript *k* denotes the compartment, and the subscripts *c* and *i* denote capillary or interstitial space respectively. *T* is the transcapillary diffusion time, *r* is the reaction rate and the subscripts *u* and *p* are the uptake and production, respectively, of the solute. r_{GRI} is the rate of reaction for the GRI and v_s is the stoichiometric ratio for each solute. Despite the novel approach, significant theoretical and experimental work needs to be conducted in order to validate and specialize the aforementioned, generalized equations to be specifically applicable to a GRI candidate in the various *in vivo* environments utilized by experimentalists in preclinical development as well as in the clinic. For example, the Sorensen model has several limitations. The parameters in the model are based on a healthy 70 kg male, which makes it difficult to account for patient variability.[42] Additionally, the model also has difficulty capturing metabolic abnormalities, such as insulin resistance, which can occur in some patients.[42] Finally, the model cannot be extended to animals, such as rodents, where GRIs are tested experimentally, making it difficult to predict current GRI experimental data. Alternatively, the framework of utilizing the GRI as a state machine can potentially be applied to other GRI approaches, such as those relying on polymeric

release mechanisms to aid in the synthesis of a new generation of therapeutics.[27,28,44–46] However, the molecular modeling required to describe such polymer based GRIs is significantly more complicated than the simple chemical reaction presented above for a freely circulating GRI and more work needs to be done on that front. Nonetheless, by overlaying pharmacokinetic models with mathematical GRI constructs, future research efforts may be able to stimulate and accelerate progress in this field by using rational targets to replace the current, broadly empirical approaches to GRI development that resort immediately to time-consuming and costly iterative chemical synthesis as well as extensive animal testing.

1.2 *Insulin Molecules with Engineered Glucose Recognition*

Recent efforts have attempted to incorporate the dynamic functionalities of a "synthetic" pancreas within a single protein or protein complex, although this has proven to be challenging by many metrics.[47] In regard to carbohydrate recognition moieties, certain classes of proteins have garnered much consideration in the context of integration into multi-component, glucose-responsive systems. Those of note in addition to ConA and GOx include other glucose-converting enzymes such as glucodehydrogenase and hexokinases.[48] Although a major advantage of these reporter proteins lies in the selectivity and specificity offered with respect to glucose, due to the presence of multivalent binding architectures, a major disadvantage in the context of synthesizing glucose-responsive properties within a single peptide is the size and complexity of such proteins. Additionally, the fact that there are currently no clinically available, intelligent, materials-based release systems for diabetes therapy, despite almost half-a-century of

intense research, can be a reminder of the overwhelming hurdles, both engineering and regulatory, that have yet to be overcome.[49] Conversely, the number of examples demonstrating proof-of-principle, unimolecular, insulin-based protein systems attempting abiotic functionality is surprisingly scarce.[8,47,50] Nevertheless, the potential for such a unimolecular GRI, possessing patient-dependent pharmacodynamics as opposed to the currently observed static profiles, possesses paradigm-shifting implications in the realm of diabetes therapies.

1.2.1 Boronic Acids as a Synthetic Alternative for Glucose Recognition

An attractive alternative for the carbohydrate binding motif for unimolecular GRI design can potentially utilize synthetic, small molecule boronic acids for sugar recognition.[51,52] Boronic acids are Lewis acids which have been shown to form fast, reversible covalent bonds to *cis*-1,2 or *cis*-1,3 diols such as glucose, and offer a diverse framework from which to incorporate carbohydrate recognition while potentially offering a minimal change to overall size and tertiary structure.[22,53–55] Despite the fact that selectivity of boronic acids is significantly lower than its protein counterparts, several examples exist demonstrating the successful utilization of aryl boronic acids possessing carbohydrate-specific binding affinities in physiologically relevant ranges (2-30mM), although an accurate efficacious range of concentrations in the context of GRIs still remains ambiguous due to the abundance of non-glucose carbohydrates existing in both healthy and diabetic individuals as well as mechanism-dependent kinetics.[48,56–62]

1.2.2 Practical Limitations for Scalable GRI Production

In the context of GRI synthesis, production of insulin and its analogues is largely dominated by recombinant DNA (rDNA) protein expression at the commercial scale,

providing unprecedented quantities of the diabetic therapy primarily through utilization of either yeast or bacteria as the biomanufacturing unit.[63,64] Despite the advancements in rDNA technology, severe shortcomings present themselves from the perspective of GRI synthesis mainly through the accessibility of unnatural diversity in design, including the incorporation of non-native amino acids, synthetic probes, or pharmacological agents.[65] Total synthesis has attempted to improve this, with the current state-of-the-art approaching yields of 25%.[66,67] Unfortunately, the majority of total synthesis schemes involve harsh oxidation conditions during protein folding, which could prove deleterious to redox-sensitive reagents such as boronic acids.[67–69] Although some developments have aimed at ameliorating these issues, further improvements are necessary in order to realize the full opportunity of GRI synthesis capabilities beyond the academic setting, and will ultimately have to compete with rDNA biosynthesis in order to ascertain a viable, commercial product. [70–72,66,73,74]

1.2.3 Recent Advances in GRI Development

Despite the relatively low number of unimolecular GRI's present in the literature to-date, compared to the highly active area of polymeric or multi-component release systems that has occurred since the late 1970s, the examples that do exist possess enormous potential in providing an initial framework through which to evaluate and further expand design criteria for future constructs.[8,50] Pioneering studies involving bioconjugation of boronic acid to the insulin protein first demonstrated the resulting conjugate's ability to bind to glucose *in vitro*, albeit under supraphysiological conditions using a model polymeric system (Figure 1. 1a) and *in vivo* validation yet to be demonstrated.[75] Further work expanding on insulin bioconjugates utilized boronate- gluconate motifs for multi-

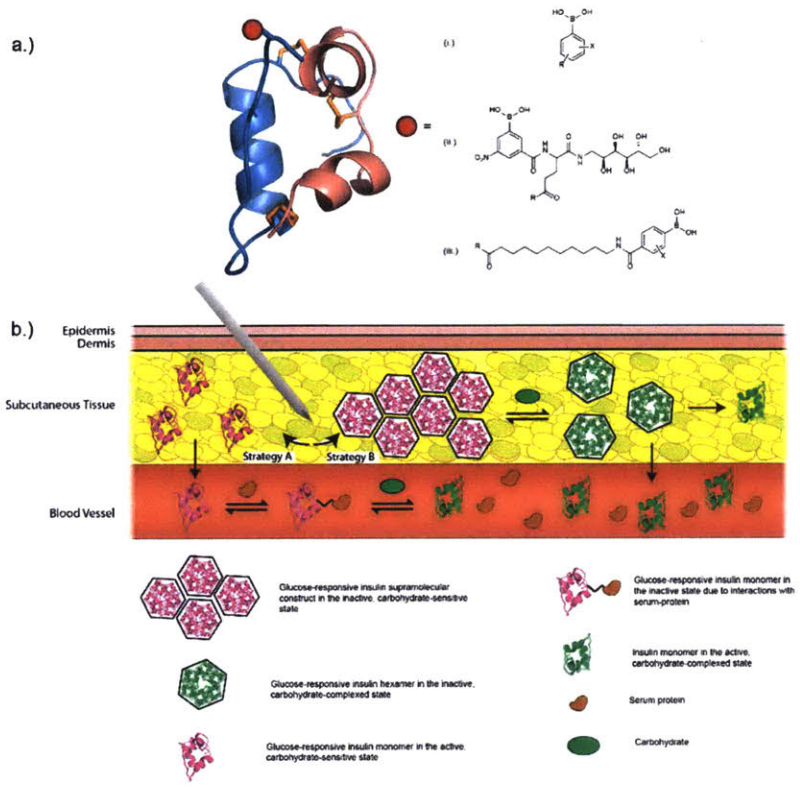

Figure 1. 1 Glucose responsive insulin constructs and mechanisms-of-action. (a) Representation of insulin bioconjugates demonstrating various designs of boronic acid-based motifs for glucose-responsive engineering (X = electron-withdrawing groups; R represents the conjugation site to the insulin protein); (b) Depiction of the various methods of protraction envisioned from the described glucose-responsive insulin constructs from literature, ranging from (Strategy A) glucose-responsive monomeric insulin and its various possible interactions with the in vivo environment, from glycoproteins present in the subcutaneous tissue to serum-binding proteins found in the blood stream, to (Strategy B) glucose-responsive supramolecular complexation of insulin for long-term, carbohydrate-dependent protraction.

hexamerization and revealed the formation of high molecular weight self-assemblies capable of dose-dependent disassembly in the presence of carbohydrates *in vitro*, although under special formulation and non-physiologically relevant conditions (Figure 1. 1b).[76] Recently, the first demonstration of glycemic control in a biologically relevant diabetic mouse model was observed for aliphatic PBA-insulin bioconjugates, capable of glucose-responsive bioavailability that mimics the functionality of a healthy pancreas under glycemic challenge when compared to native insulin and a clinically-used basal

insulin (Figure 1. 1c).[77] These efforts have inspired and guided innovation aimed towards creating an abiotic, pancreas-mimicking insulin. It is envisioned that future generations continue these engineering efforts in creating design strategies aimed at glucose-mediated bioavailability (i.e. protraction of either the monomeric or complexed state), potency (i.e. leveraging receptor-binding interactions in a carbohydrate-dependent manner), or any combination of the aforementioned designs to engineer the perfect insulin with respect to specificity, stability, reliability, and dynamic response.

1.2.4 Summary and Perspective

Overall, this section intends to (1) underline the existing paradigm in glycemic management for treating insulin-dependent diabetes, as well as (2) highlight both the obstacles and the recent progress of emerging concepts and novel approaches currently spurring innovation in the field of glucose responsive insulin technology. Although the concept of a unimolecular glucose-responsive insulin has been a recent objective of diabetes technology, significant progress has been made over the past several years, with momentum continuously growing. The molecular embodiments designed and developed thus far have made large strides in progressing the field; however, despite the significant progress, there are still numerous hurdles yet to be overcome, both engineering and regulatory. This point is further supported and emphasized by the fact that there are currently no clinical examples of glucose-responsive insulin technology available today despite active research and development since the 1970s. Coupled with the resources (e.g. infrastructure and capital) that would be necessary to drive the development of a glucose-responsive insulin from preclinical development through regulatory approval, as well as the immense competition faced by the many incumbent

organizations (e.g. Sanofi, Novo Nordisk, Eli Lilly) currently developing and commercializing non-glucose-responsive insulin therapies, the prospect of achieving the designation and status of the "first" glucose-responsive insulin therapy to reach patients is daunting.

Despite these obstacles, and many more, it is important to re-iterate the paradigm shifting implications that a glucose-responsive insulin possesses, as well as the need for its continuous improvement to advance the technology towards a clinically viable therapy. The prospect of a state-responsive therapy in the diabetes space has immense, positive potential for all stakeholders. It is envisioned that the use of a truly glucose-responsive insulin therapy has the potential to improve the lives of insulin-dependent diabetics around the world. Such a therapy could improve patient compliance and disease management through successful targeting and achievement of glycemic goals due to its state-responsive nature, as well as significantly decrease the direct and indirect costs (both financial- and health-based) that results due to improper management of severe hypoglycemia and chronic hyperglycemia. Ultimately, glucose-responsive insulin technology possesses the potential to revolutionize and replace current standards-of-care in insulin-treatment for diabetics around the world, and further development of the technology is paramount towards its success and global relief of the disease.

1.3 *Thesis Overview*

In summary, the work presented in this Thesis aims to advance the field of glucose-responsive insulin therapies towards the development of an autonomous glycemic treatment for insulin-dependent diabetes. Notably, our efforts have focused on the

innovative design, synthesis, and characterization of novel molecular embodiments for a unimolecular insulin technology capable of enhanced basal and glucose-responsive activity. Ultimately, our goal is to elucidate new strategies for the chemical modification and engineering of the native insulin protein. These strategies aim to synergistically incorporate aspects of organic, inorganic, and analytical chemistry, as well as molecular biology and pharmacology, to integrate functional aspects of the healthy pancreas onto the insulin protein in order to create a one-size-fits-all insulin therapy. To that effect, the Thesis is divided into the following sections:

In **Chapter 2**, we utilize a rational screen-based design strategy to synthesize and develop a novel class of unimolecular glucose-responsive insulin conjugates. The resulting library of GRI candidates afforded several unique conjugates, each capable of varying degrees of glucose-responsivity to the diabetic environment. Theoretically, every synthesized candidate was afforded varying degrees of glucose-responsivity, and therefore the potential to be pursued as an independent GRI therapeutic candidate. However, further optimization of the library system led to the identification of one lead GRI candidate, Ins-PL-4FPBA, capable of several desired properties envisioned to be necessary for a clinically translatable GRI: glucose-mediated solubility, safety, and activity. The rational-screen-based strategy we conceived here, which led to the identification and optimization of the synergistic properties afforded for Ins-PL-4FPBA, is envisioned to potentially accelerate preclinical development of future GRI candidates towards the generation of a long-term, state-responsive insulin therapy.

In **Chapter 3**, we pioneer the first design and synthesis strategy for a novel class of sugar-responsive insulin conjugates, with the ultimate goal of developing a state-

responsive therapy capable of sugar-mediated receptor binding interactions. Unlike previous iterations of GRI technologies, boronic acid motifs were incorporated with polyol sugar analogues independently and in parallel to the same insulin protein in a site-selective manner. In this effort, we created dynamically cyclized insulin bioconjugates found to exhibit enhanced chemical stability (> 50%) and superior thermal stability (> 100%) relative to the native protein. Remarkably, when introduced to the sugar sorbitol, reversion in chemical stability was observed, suggesting the reversible nature of the boronic acid-polyol interactions and the implications it has, due to the functional similarity in the mechanisms involved with insulin denaturation and insulin receptor activation, towards developing a GRI capable of sugar-mediated receptor binding interactions. When assessed *in vitro*, it was found that the library of conjugates demonstrated varying degrees of native potency retention; whereas, in an *in vivo* diabetic mouse model, glucose-correcting efficacy was determined to be completely retained for select conjugates, regardless of *in vitro* activity.

In **Chapter 4**, we focus on improving basal activity of the insulin protein by utilizing a novel class of zwitterionic insulin polymer conjugates towards the generation of ultra long-acting insulin therapies. The resulting library is demonstrated to afford equivalent biological potency relative to native human insulin, augmented thermal and chemical stability capable of withstanding thermal aggregation for over 80 days, as well as ultra long-acting basal insulin potential. Interestingly, one candidate in particular, Ins-PC, demonstrates the capability of enhanced protraction and *in vivo* activity comparable to a pegylated insulin, inspired by ultra long-acting insulin peglispro. Overall, it is envisioned that zwitterionic functionalization of insulin could provide a potentially improved

therapeutic strategy for the development of ultra long-acting insulin therapeutics for diabetes management.

In **Chapter 5**, we conclude the Thesis by summarizing its contents and by providing a future outlook for the field of unimolecular glucose-responsive insulin therapy.

Chapter 2: Unimolecular Glucose-Responsive Insulin Conjugates for Glucose-Mediated solubility, Safety, and Efficacy

The work presented in this chapter is in preparation for publication:

A. B. Cortinas, L. S. Thapa, S. D. Truong, R. S. Langer, D. G. Anderson, Unimolecular glucose-responsive insulin conjugates for glucose-mediated solubility, safety, and efficacy. *In preparation.*

2.1 Introduction

Diabetes mellitus is a devastating disease that has steadily risen in prevalence over the decades, currently affecting more than 400 million individuals globally and with that number projected to increase to more than 600 million by 2045.[4] Diabetes is characterized across all forms by the common phenotype of hyperglycemia, or elevated blood glucose levels; however, severe cases of the disease force a subset of patients to self-monitor their blood sugar and self-administer exogenous insulin multiple times a day in an attempt to mimic aspects of the normally functioning pancreas.[78,79] While the benefits of maintaining tight glycemic control has been shown to decrease the risk of a myriad of health complications, enormous hurdles such as poor patient compliance, as well as the fact that intensification of insulin therapy regimens adversely increases the risk of severe hypoglycemia, remain to be overcome.[80–83]

Due to insulin's relatively low and narrow therapeutic index, efforts to engineer the protein have largely focused on modifying its primary structure as a means of attempting to tune more precise and predictable pharmacokinetic (PK) and pharmacodynamic (PD) profiles.[69,84,85] The outcome of such efforts have led to the introduction of two broad categories of insulin analogues over the past two decades that currently serve as the state-of-the-art for diabetes patients: prandial (fast-acting) and basal (long-acting) insulins.[6,8,63,86] Prandial insulins, such as insulin aspart (Novo Nordisk), insulin lispro (Eli Lilly), and insulin glulisine (Sanofi), provide patients with fast-acting glucose-correcting activity through the use of various protein dimer and hexamer destabilization mechanisms, allowing for rapid absorption and activity.[84,87] Basal insulins, such as insulin glargine (Sanofi), insulin detemir (Novo Nordisk), and insulin degludec (Novo Nordisk),

offer prolonged release that allows for delayed absorption and extended activity based on various protraction mechanisms that include enabling subcutaneous precipitation through the alteration of the protein's isoelectric point, enabling serum-protein binding, and enabling multi-hexamer complexation, respectively.[11,88–90] Taken in combination, prandial and basal insulin therapies offer insulin-dependent diabetics a means of approximating the release profiles of a functional pancreas. However, despite the numerous improvements in overall glycemic management observed for patients as a result of the administration of one or more of the aforementioned insulin analogues, better therapies are still needed.[91] More specifically, efforts-to-date have aimed at ameliorating specific clinical issues such as patient variability and the inherent risks of hypoglycemia through focusing on rational design criteria that optimizes static PK and PD profiles.[14,16–18,89,92,93] As a result, all the aforementioned insulins are unsusceptible to responding to physiological changes in the patient. In consideration of these issues and complications, coupled with the steady rise over the years in the number of diabetic patients requiring insulin medication, the need for a unimolecular glucose-responsive insulin (GRI) therapy, possessing the potential for state-responsive behavior as opposed to dose-responsive, is more pressing than ever.[8,35,94]

Large strides have been made with regard to progressing the design and development of unimolecular glucose-responsive insulins under *in vitro* and *in vivo* settings, all of which have demonstrated the potential impact of current constructs and the possibilities for further expanding on their frameworks.[34,35] Reported iterations to-date have incorporated inorganic boronic acids as the sugar-sensing moiety, in large part due to their relatively low impact on overall molecular weight and insulin tertiary structure, the ability to

reversibly bind to saccharides in the millimolar concentration range, as well as their diverse structural framework from which to incorporate glucose recognition and response.[48,53] Early examples introduced the application of boronic acids, either alone or in conjunction with a saccharide motif, to provide glucose-responsive insulin behavior and release *in vitro*.[75,76] And although these systems demonstrated the ability for polymeric formulation and multi-hexamer assembly under simulated saccharide stimulation, the afforded glucose-responsive mechanisms ultimately proved to be physiologically irrelevant with *in vivo* validation yet to be determined. Most recently, boronic acids were used in conjunction with an aliphatic hydrocarbon chain to afford long-lasting, glucose-responsive activity *in vivo*, the results of which demonstrated glycemic control over a therapeutically relevant range of doses and timescales compared to clinical standards.[77] Although the direct mechanism of action was ultimately not verified, the construct improved upon earlier iterations with regard to design and efficacy, and highlighted a very important aspect necessary for the improvement of GRI constructs, safety. Moving forward, rational design criteria that focuses on synergistically combining aspects of potency, efficacy, glucose-responsive mechanism-of-action, as well as safety, must be taken into consideration for the successful development of next-generation GRI constructs.

Herein, we develop a class of unimolecular, glucose-responsive insulin conjugates designed to afford glucose-dependent solubility, safety, and activity towards the generation of a long-term, state-responsive insulin therapy. Design rationale utilized a screen-based approach whereby a small library of phenylboronic acids were incorporated into an isoelectric-point-shifting oligopeptide, inspired by insulin glargine, composed of an

oligo-lysine homopolymer. Optimization of this system afforded a smart depot construct capable of both shifting the isoelectric point of insulin for subcutaneous precipitation while also providing a means of re-solubilization under hyperglycemic concentrations of glucose. Evaluation of the optimized lead candidate in a normoglycemic *in vivo* mouse model revealed significant reduction in risk of hypoglycemia relative to clinically used insulins, even under supraphysiological dose conditions, as well as demonstrated dynamic, glucose-dependent PK bioavailability and safety. In a Type 1 diabetic mouse model, the glucose-correcting activity of the lead candidate under physiologically relevant doses was shown to withstand repeat glucose challenges over a 10.5-h period relative to clinically used insulins, as well as revealed a response profile matching that of the healthy pancreas. Taken together, the described strategy is envisioned to provide an innovative framework for the development of enhanced, and potentially clinically-relevant, glucose-responsive insulin constructs towards the application of autonomous glycemic management for insulin-dependent diabetes.

2.2 *Design and Characterization of the Insulin Core Unit*

The unimolecular glucose-responsive insulin (GRI) design (Figure 2. 1) consists of two main components. The first component is the Insulin-DBCO core molecule (Figure 2. 1a), which serves as the biologically-active protein scaffold intended for facile incorporation into a copper-free click chemistry synthesis scheme. Utilizing N-hydroxysuccinimide (NHS) coupling chemistry under basic conditions, a dibenzocyclooctyne (DBCO) group bearing a short hydrocarbon linker was chemically conjugated to the ε-amine on the B29 lysine residue of the insulin protein, as previously

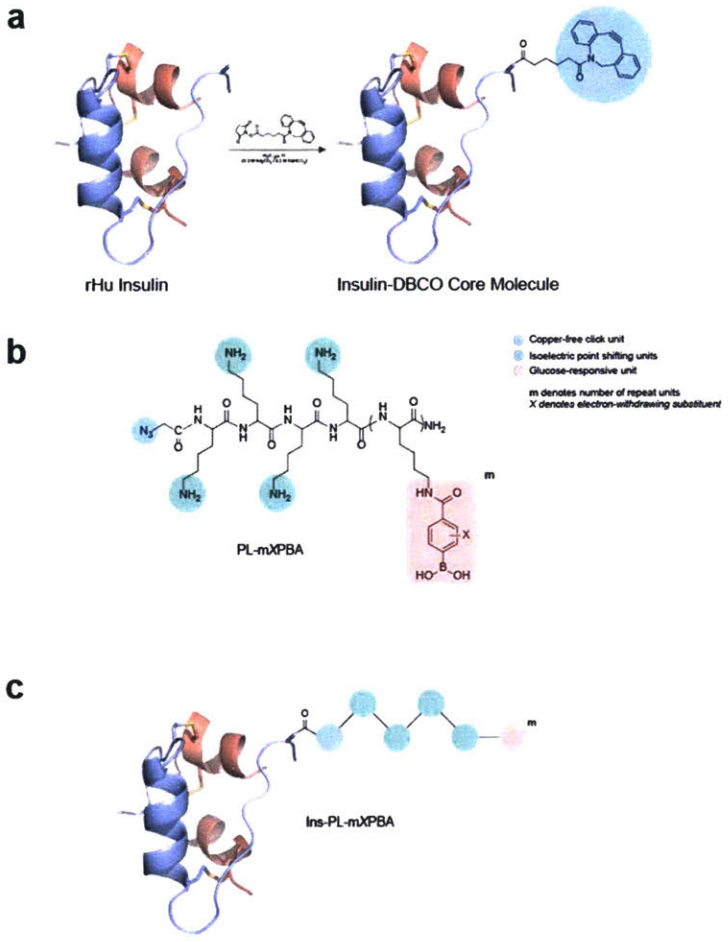

Figure 2. 1 Design of the unimolecular glucose-responsive insulin construct. (a) Reaction of the DBCO small molecule to the ε-amine on the B29 lysine residue of native human insulin for site-preferential conjugation and synthesis of the Insulin-DBCO core molecule. (b) Generalized structure of the isoelectric-point-shifting, glucose-responsive oligopeptide unit. (c) Generalized structure of the unimolecular, isoelectric-point-shifted, glucose-responsive insulin bioconjugate.

described.[75,77] Purification and characterization of the Insulin-DBCO core molecule was performed to validate site-selective mono conjugation to the B29 lysine residue (Figure A. 1). In addition, clinical control insulin detemir was synthesized and characterized in a similar manner, with myristic acid NHS ester used as the small molecule reagent, as previously described (Figure A. 2).[77]

2.3 *Rational Design of the Glucose-Responsive Oligopeptide Construct*

To develop the second component of the unimolecular GRI, the glucose-responsive oligopeptide unit (Figure 2. 1b), a rational screen-based approach was utilized whereby phenylboronic acids (PBAs) were screened and selected for incorporation into an oligopeptide scaffold. The oligopeptide scaffold was synthesized utilizing solid-phase peptide synthesis (Figure A. 3) and is comprised of three distinct regions: (1) the copper-free click chemistry handle; (2) the isoelectric-point-shifting region; and (3) the glucose-responsive region. For facile incorporation into a copper-free click chemistry reaction scheme, an azido group was incorporated into the N-terminus of the oligopeptide to serve as the reactive handle for the Insulin-DBCO core molecule. The isoelectric-point-shifting region, inspired by insulin glargine, is comprised of four lysine residues that increases the net charge of the insulin protein, thereby raising the isoelectric point of human insulin from 5.4 to the more physiologically relevant 7.4, as previously demonstrated.[1,24] For the glucose-responsive region, rational screening of a small library of PBA small molecules (Figure 2. 2a) was conducted both individually as well as after incorporation into the oligopeptide unit (Figure 2. 2b). Inorganic boronic acids are Lewis acids that are known to be capable of reversible covalent interactions with *cis*-1,2 or *cis*-1,3 diols (for example glucose) and serve as an attractive option for biomolecular incorporation of inorganic glucose-recognition.[53,59] Additionally, there exists a rich body of literature describing the augmentation effects on saccharide-sensing due to the presence of electron-withdrawing substituents proximal to the boronic acid motif, (for example the primary amines present on the lysine residues of the oligopeptide).[48,95–97] The basis for choosing the selected PBAs is based on their respective pKa values being close to physiological pH, which has

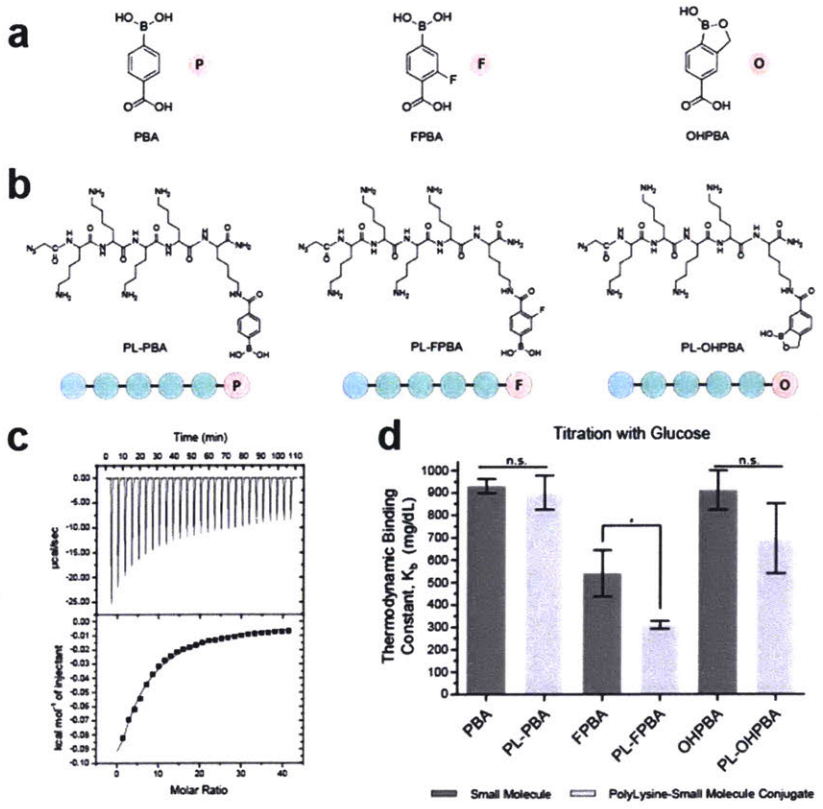

Figure 2. 2 Characterization of phenylboronic acid constructs. (a) Structures of the phenylboronic acid small molecules selected for their pKa values being close to a physiologically relevant pH; pKa (PBA) ~ 7.8, pKa (FPBA) ~ 7.2, pKa (OHPBA) ~ 7.2.[23,56,98] (b) Structures of the oligopeptide-incorporated PBA molecules. (c) Representative ITC data for the titration of glucose to the various PBA constructs. The top data set profile of power versus time was integrated to yield the bottom data set profile of molar enthalpy versus the ratio of glucose:PBA construct. (d) Thermodynamic binding constants of all PBA constructs in complex with glucose. Mean ± S.D. ($n \geq 3$). n.s. $P > 0.05$, * $P < 0.05$ (two-tailed, unpaired t-test).

been shown to be associated with their potential binding capability to saccharides.[23,56,98] For these reasons, investigation of the individual PBAs along with the oligopeptide-incorporated PBAs was carried out using isothermal titration calorimetry (Figure 2. 2c, Figure A. 4) to determine the baseline thermodynamic binding constants along with any potential electron-withdrawing enhancements observed as a function of conjugation to the oligopeptide. Binding constant measurements (Figure 2. 2d) of the individual PBA small molecules revealed that the fluorinated PBA (FPBA) possessed a thermodynamic

binding constant closest to the physiological regime, bordering the extreme end of the hyperglycemic concentration range. Additionally, after incorporation into the oligopeptide unit, there was no statistically significant enhancement of binding constants as a result of proximal electron-withdrawing groups for any PBA except FPBA. As a result, the FPBA small molecule was selected as the glucose-sensing component to be implemented for further optimization of the glucose-responsive oligopeptide unit.

2.4 *In Vitro Assessment of the Glucose-Responsive Insulin Conjugates*

To further optimize the glucose-responsive oligopeptide unit, the effects of varying the number of FPBA small molecules present on the oligopeptide scaffold was investigated (Figure 2. 3a). The primary motivations for systematic examination of this parameter was to determine whether further enhancements in binding constant were realizable, as well as to assess the implications of those enhancements in creating an insulin conjugate capable of glucose-mediated solubility towards the development of a long-term, intelligent GRI depot. Incrementally increasing the total number of FPBA molecules per oligopeptide resulted in proportional enhancements in thermodynamic binding constants as measured by ITC (Figure 2. 3b), with the strongest binding constant belonging to the construct containing four FPBA molecules. Incorporation of the oligopeptide-FPBA constructs onto the Insulin-DBCO core molecule via bio-orthogonal copper-free click chemistry allowed for the facile synthesis of a novel class of GRI candidates to be further tested for dynamic solubility. The Insulin-DBCO core molecule

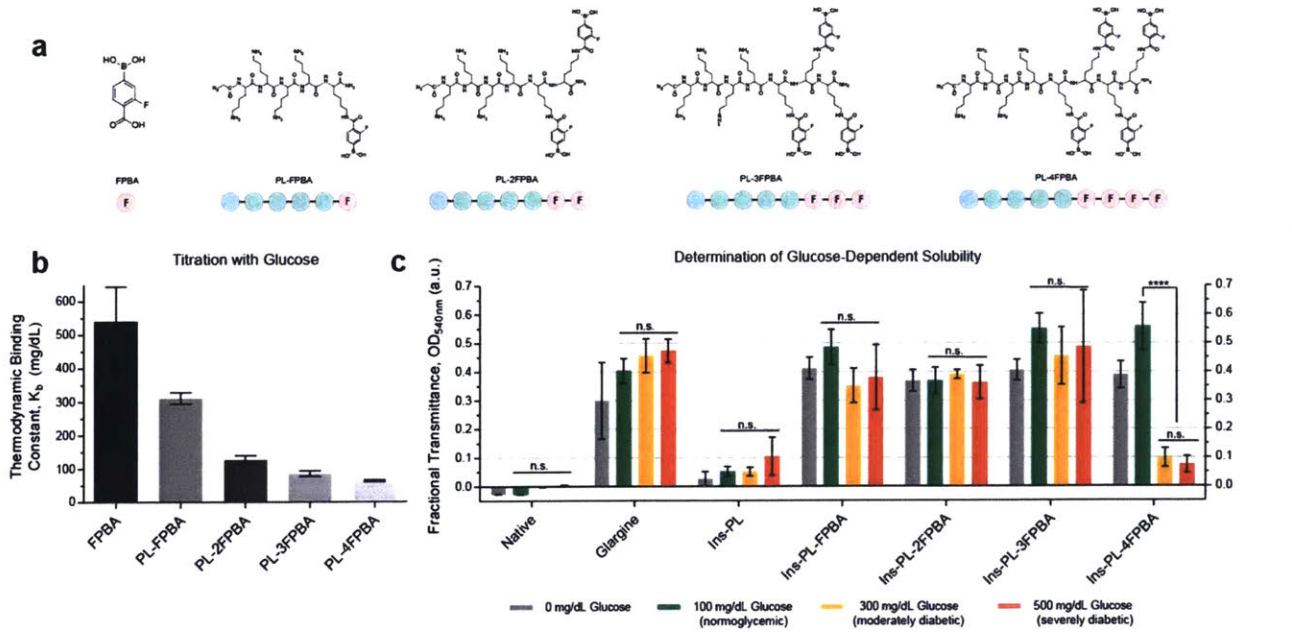

Figure 2. 3 **Oligopeptide unit optimization for glucose-mediated solubility.** (a) Structures of the FPBA constructs, incrementally increasing the total number of FPBA molecule per oligopeptide unit. (b) Thermodynamic binding constants of all FPBA constructs in complex with glucose. All thermodynamic binding constants are statistically different from one another. Mean ± S.D. ($n \geq 3$). Statistical differentiation is defined as $P < 0.05$ (two-tailed, unpaired t-test). (c) Measurement of potential glucose-mediated changes in solubility of insulin samples as quantified by solution transmittance. All statistical comparisons are made within the same sample group, across all non-zero glucose conditions. Mean ± S.D. ($n = 3$). n.s. $P > 0.05$, **** $P < 0.0001$ (two-tailed, unpaired t-test).

was reacted with each respective oligopeptide-FPBA construct via combining each copper-free click handle in solution, with conjugation validated using ESI mass spectrometry (Figure A. 5). To assess dynamic solubility, each GRI candidate, along with native human insulin and isoelectric-point-shifted insulin glargine used as controls, were monomerically formulated at insulin concentrations representative of clinical formulations (~ 1 mg/mL) at physiological pH (7.4) and at various concentrations of glucose (Figure 2. 3c). Transmittance was measured at 540 nm, a wavelength for which insulin has negligible absorbance, to detect changes in solubility as a function of glucose concentration. As expected, when exposed to non-physiological (0 mg/dL) and

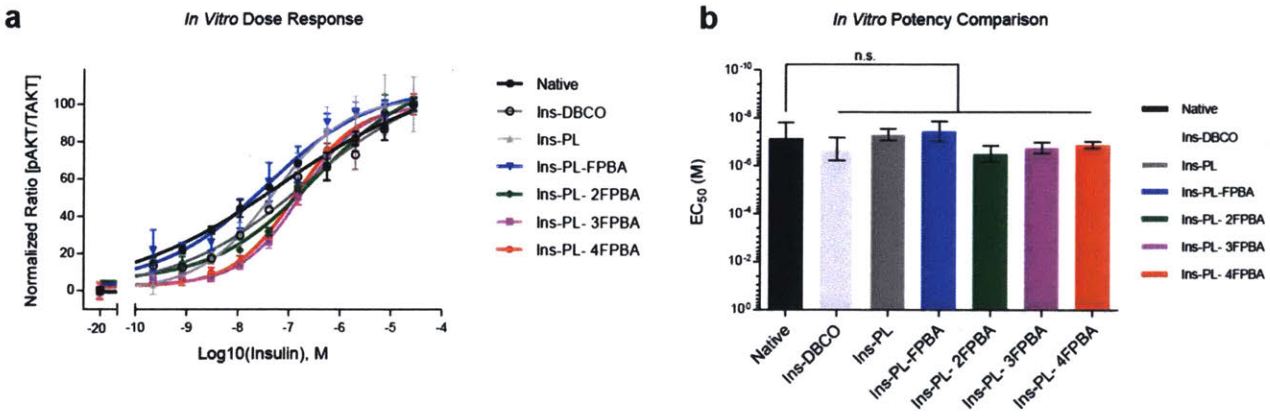

Figure 2. 4 *In vitro* cell-based functional characterization of synthesized insulin constructs. (a) *In vitro* cell stimulation assay for all insulin samples, measuring dose-responsive insulin receptor activation. Mean ± S.D. (n = 3). (b) Potency comparison via dose-response-derived EC50 values for all insulin constructs relative to the native protein. Mean ± 95% C.I. (n = 3). n.s. $P > 0.05$ (sum-of-squares F test).

normoglycemic (100 mg/dL) concentrations of glucose in solution, insulin glargine and all insulin conjugates precipitated to some degree, whereas native human insulin retained near-complete solubility.[99,100] Furthermore, increasing the glucose concentrations towards the moderate (300 mg/dL) and severely (500 mg/dL) hyperglycemic regimes did not have a marked effect on solubility for any clinical control or for Ins-PL, the experimental control consisting of Insulin-DBCO conjugated to an oligopeptide unit bearing no boronic acid motifs. Evaluation of each GRI candidate revealed only one construct, Ins-PL-4FPBA, to be capable of both precipitation under normoglycemic glucose concentrations as well as re-solubilization after exposure to moderately hyperglycemic concentrations of glucose (300 mg/dL). To further assess retention of biological potency, insulin receptor activation was measured for all insulin constructs (Figure 2. 4). For all synthesized conjugates, relative to native human insulin, no statistically significant loss of receptor-based potency was observed, suggesting no adverse biological effects as a result of the overall synthesis scheme.

2.5 *In Vivo Safety Assessment of the Glucose-Responsive Insulin Conjugates*

By definition, the non-diabetic normoglycemic mouse model provides an important environment through which to judge a glucose-responsive insulin construct. Therefore, to assess the state-responsive behavior of the optimized class of GRI conjugates, and to determine the safety implications of their design, escalating dose response studies were performed in healthy C57BL/6 mice. A total of two therapeutically relevant doses and one supraphysiological dose were selected to evaluate each insulin sample. Clinical dose definitions were used for all clinically relevant controls (human insulin, 1 IU = 5.97 nmol; insulin glargine, 1 IU = 6.00 nmol; insulin detemir, 1 IU = 24.0 nmol) while the dose definition of human insulin was used for all synthesized GRI constructs.[101–103] The extent by which each sample induced a hypoglycemic response was defined as a blood glucose concentration below 70 mg/dL. Quantification of hypoglycemia for each sample was calculated using the hypoglycemia index, a unitless metric measured by the drop from initial blood glucose concentration to the nadir (i.e., the lowest observed value) divided by the initial blood glucose concentration. A variation of this metric is used clinically to help diagnose incidence of hypoglycemia in diabetic patients.[104] As shown in Figure 2. 5a, the therapeutically relevant doses of 3 IU/kg and 5 IU/kg illustrate the differentiating effects of each insulin sample, with both native human insulin and insulin glargine inducing hypoglycemia. At a dose of 3 IU/kg, insulin detemir did not induce an average drop in blood glucose below 70 mg/dL but did border the threshold. Interestingly, at the same dose each GRI candidate achieved varying degrees of hypoglycemia protection (GRI sample, nadir: Ins-PL-FPBA, 82.2 mg/dL; Ins-PL-2FPBA, 86.2 mg/dL; Ins-PL-3FPBA, 100 mg/dL; Ins-PL-4FPBA, 120 mg/dL). Increasing the dose to 5 IU/kg demonstrated the

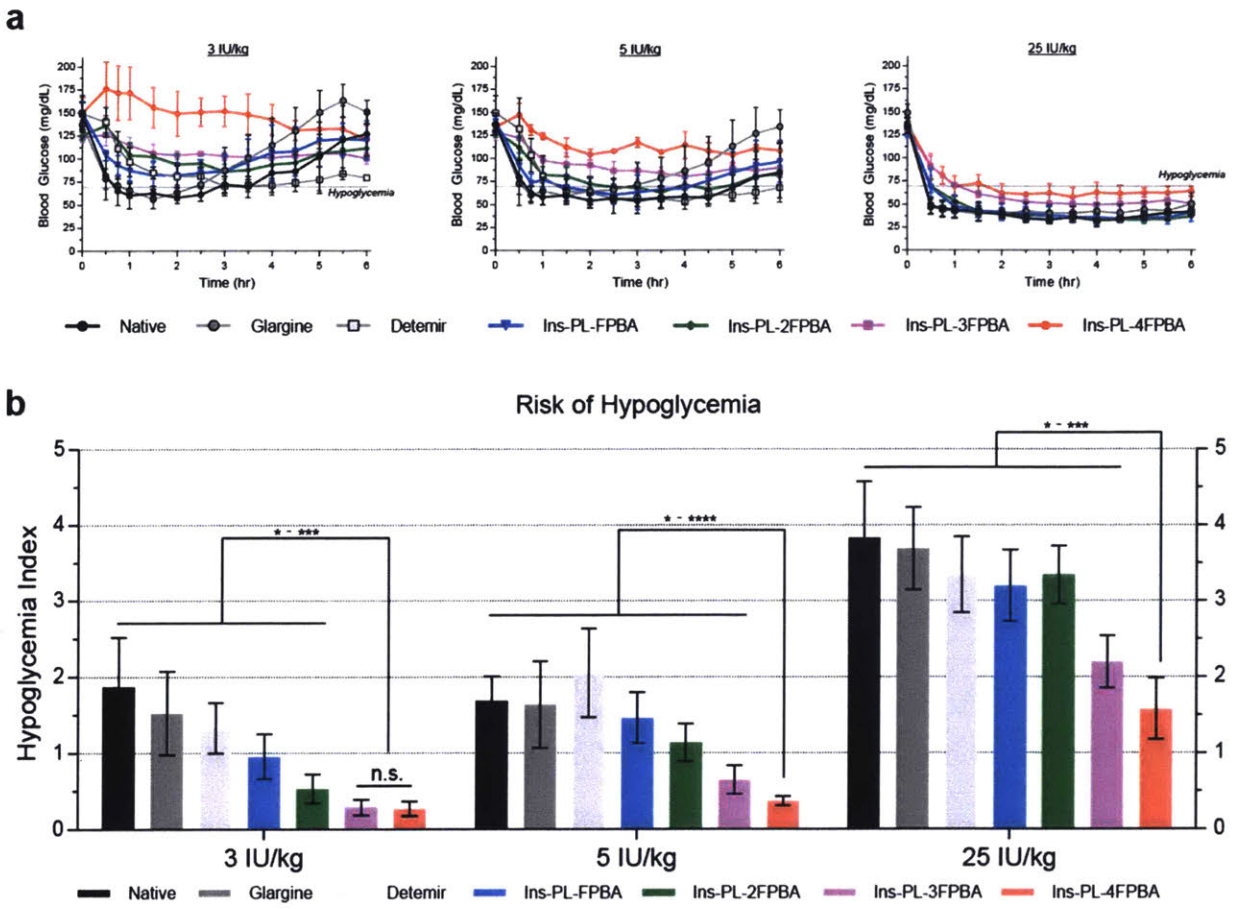

Figure 2. 5 In vivo safety assessment of optimized GRI candidates. (a) Blood glucose changes of healthy mice over time after subcutaneous administration of different insulin samples at clinical doses of 3 IU/kg and 5 IU/kg, and supraphysiological dose of 25 IU/kg. Mean ± S.D. (n ≥ 4). (b) Risk of hypoglycemia quantified by the hypoglycemia index, calculated from the difference between the initial blood glucose concentration and the nadir divided by the initial blood glucose concentration. Mean ± S.D. (n ≥ 4). n.s. $P > 0.05$, * $P < 0.05$, ** $P < 0.01$, *** $P < 0.001$, **** $P < 0.0001$ (two-tailed, unpaired t-test).

same trend, with all clinical controls as well as Ins-PL-FPBA and Ins-PL-2FPBA inducing hypoglycemia. Whereas, for the GRI candidates containing three and four FPBA molecules, Ins-PL-3FPBA and Ins-PL-4FPBA, hypoglycemia was not induced and Ins-PL-4FPBA did not drop blood glucose below 100 mg/dL. These results are reflected in the hypoglycemia index calculated for all samples at 3 IU/kg and 5 IU/kg (Figure 2. 5b). To assess the limits of hypoglycemia protection, the supraphysiological dose of 25 IU/kg was used. Under this condition, although all samples induced hypoglycemia (< 70 mg/dL),

it is important to note that all samples except Ins-PL-4FPBA induced clinically severe biochemical hypoglycemia (<50 mg/dL), a parameter designated to have significant clinical implications on cognitive impairment and mortality.[105] The level of hypoglycemia risk reduction at this supraphysiological dose condition is also significantly differentiable when compared to all other samples, with Ins-PL-4FPBA exhibiting the lowest risk of hypoglycemia at 25 IU/kg. Given the extreme nature of risk reduction in hypoglycemia across the tested doses, the Ins-PL-4FPBA candidate possesses significant potential in providing truly glucose-responsive behavior.

2.6 *In Vivo Screen and Evaluation of Glucose-Responsive Efficacy*

To evaluate each GRI candidate in an *in vivo* diabetic environment, a streptozotocin-induced insulin-deficient mouse model was prepared to screen each insulin conjugate and to identify a lead candidate (Figure 2. 6).[106] To distinguish between differences in potency of all samples, clinical definitions of dose were not used as in the *in vivo* safety studies. Instead, subcutaneous administration of each insulin was performed at the same molar concentration with the therapeutically relevant molar dose chosen to be equivalent to 5 IU/kg native human insulin (1 IU = 5.97 nmol). Within the first 3.5-h following insulin administration, all samples corrected blood glucose to normoglycemic levels. At 3.5-h an intraperitoneal glucose tolerance test (IPGTT) was administered with blood glucose levels measured for another 3.5-h timeframe. Notably, native human insulin and insulin glargine failed to correct blood glucose to within the normoglycemic range, whereas insulin detemir demonstrated minor correction but ultimately failed to recover. Of significance, all synthesized GRI candidates corrected blood glucose to within the normoglycemic regime

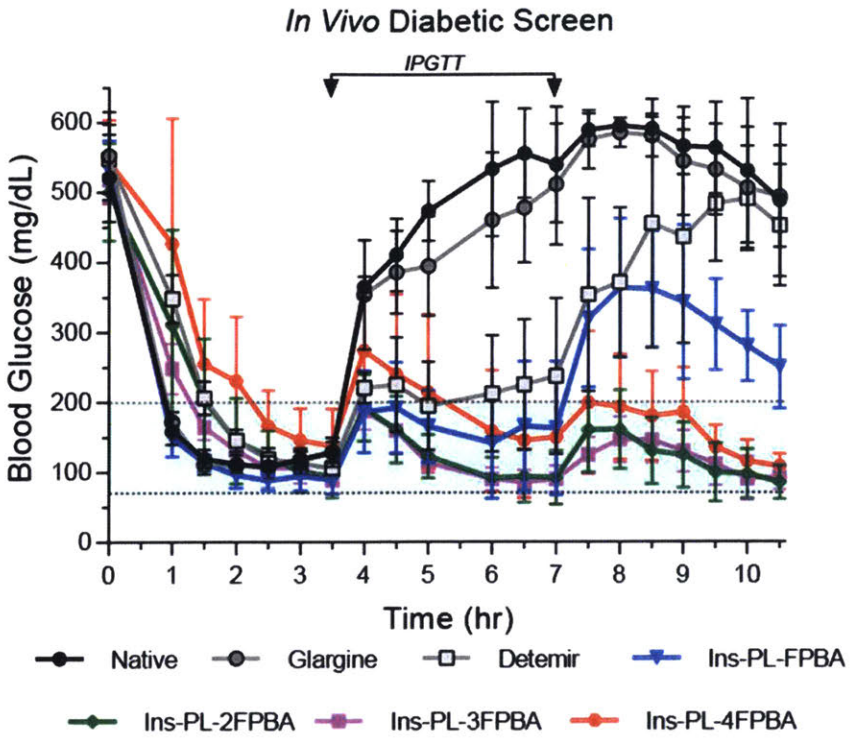

Figure 2. 6 *In vivo* diabetic screen of insulin samples. Experiment involved the administration of all insulin samples at equimolar concentrations, and with multiple intraperitoneal glucose tolerance test administered at 3.5-h and 7-h. Mean ± S.D. ($n \geq 3$).

after the first IPGTT. To further test long-term glucose-correcting efficacy, an additional IPGTT was administered at 7-h, after which all GRI candidates except for Ins-PL-FPBA corrected blood glucose back to pre-test conditions. Given the stark contrast in glucose-correcting efficacy observed for Ins-PL-4FPBA relative to clinical controls, in combination with the significantly reduced risk of hypoglycemia observed in healthy mice for the same dose, as well as the glucose-mediated solubility properties observed *in vitro*, this GRI conjugate was identified as the lead candidate for further evaluation.

To further establish glucose-mediated efficacy, a dose escalation study was performed for all clinical controls and for the best-performing GRI candidate, Ins-PL-4FPBA. To better assess potential clinical relevance and translation, clinical dose

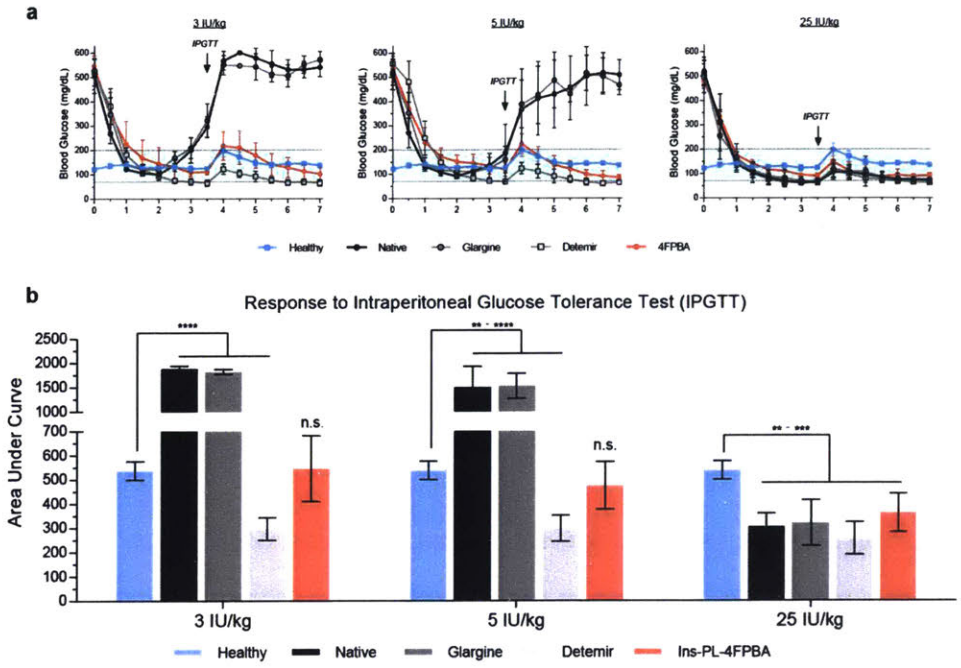

Figure 2. 7 *In vivo* diabetic dose escalation assessment of GRI lead candidate Ins-PL-4FPBA relative to clinical controls. (a) Blood glucose changes of diabetic mice over time after subcutaneous administration of different insulin samples at clinical doses of 3 IU/kg and 5 IU/kg, and supraphysiological dose 25 IU/kg. Mean ± S.D. ($n \geq 3$). (b) Responsiveness to IPGTT was calculated based on the area under the curve from 3.5-h to 7-h, with the baseline set at the 3.5-h blood glucose concentration. All statistical comparisons are with respect to the healthy pancreatic response. Mean ± S.D. ($n \geq 3$). n.s. $P > 0.05$, ** $P < 0.01$, *** $P < 0.001$, **** $P < 0.0001$ (two-tailed, unpaired t-test).

definitions were used for all insulin controls while the dose definition of native human insulin was used for Ins-PL-4FPBA, as in the *in vivo* safety assessment.[101–103] Dose concentrations of 3 IU/kg and 5 IU/kg were chosen to be therapeutically relevant, with the inclusion of one IPGTT was used to differentiate long-term efficacy relative to the healthy pancreatic response. As shown in Figure 2. 7a, native human insulin and insulin glargine began to correct blood glucose levels at 3 IU/kg and 5 IU/kg after subcutaneous administration but failed to maintain glucose-correcting efficacy before the IPGTT. After the IPGTT, blood glucose concentration returned to hyperglycemic conditions. For insulin detemir, although glucose-correcting efficacy was observed both before and after

administration of the IPGTT, blood glucose overcorrection and hypoglycemia were observed and sustained throughout the study for both 3 IU/kg and 5 IU/kg doses. Blood glucose overcorrection is further illustrated by comparison to the healthy pancreatic response profile (Figure 2. 7b). For Ins-PL-4FPBA, blood glucose correction to normoglycemia without induction of hypoglycemia was observed for doses of 3 IU/kg and 5 IU/kg, with the response profile shown to be statistically comparable to that of the healthy pancreatic response for both doses (Figure 2. 7b). When administered with the supraphysiological dose of 25 IU/kg, all insulin samples notably demonstrated glucose-correcting efficacy, but with the important distinction that all clinical controls induced sustained hypoglycemia. For Ins-PL-4FPBA, although overcorrection of blood glucose was observed when compared to the healthy pancreatic response, hypoglycemia was not induced and an average blood glucose concentration below 85 mg/dL was not observed throughout the study.

To better understand and elucidate the glucose-responsive behavior of the lead GRI candidate, Ins-PL-4FPBA, a healthy mouse model was utilized to measure glucose-mediated PK/PD profiles following a single subcutaneous administration of 5 IU/kg over a 7-h study, with the inclusion of one IPGTT at 3.5-h to directly measure glucose-responsivity. Clinical dose definitions were used for all insulin controls while the dose definition of native human insulin was used for Ins-PL-4FPBA, as in the *in vivo* safety assessment. As shown in Figure 2. 8, classical insulin PK absorption and elimination was observed as expected, with no demonstrable insulin responsivity observed as a result of the IPGTT.[6,107] Additionally, all clinical insulin controls induced hypoglycemia despite an almost order-of-magnitude difference in serum concentration relative to each other, with

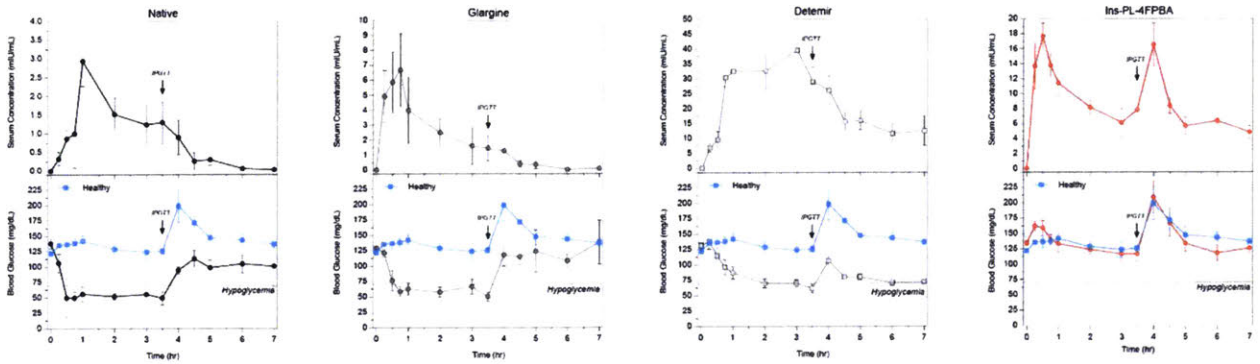

Figure 2. 8 *In vivo* bioavailability study. The experiment involved measuring pharmacokinetic serum insulin concentrations and pharmacodynamic blood glucose response of clinical insulin samples and the lead GRI candidate, Ins-PL-4FPBA, after subcutaneous administration at a dose of 5 IU/kg and subsequent IPGTT. Mean ± S.D. ($n \geq 3$).

native human insulin and insulin glargine experiencing diminished effects after the IPGTT and insulin detemir sustaining a hypoglycemic response both before and after the IPGTT. Interestingly, Ins-PL-4FPBA demonstrated observable absorption and apparent clearance before the IPGTT but did not exhibit any significant glucose-depressing effects relative to the healthy pancreatic response, despite serum concentrations being observably higher than that of native human insulin and insulin glargine. Once the IPGTT was administered, a glucose-responsive change in bioavailable serum insulin concentration was observed. Directly following the IPGTT at 3.5-h, the GRI serum concentration both increased to match the peak pre-test serum GRI concentration in response to the glucose challenge, as well as decreased to the pre-IPGTT serum levels observed directly preceding the glucose challenge. Overall, the GRI PK/PD profile of Ins-PL-4FPBA mirrored the change in glucose concentration observed in the healthy *in vivo* environment, demonstrating the ability to signifincatly change GRI serum concentration and therefore bioavailability in response to a glucose challenge while also eliminating the risk of hypoglycemia.

2.7 *Discussion and Conclusions*

Clinically available insulin therapies to-date have been developed and optimized using static PK/PD profile criteria that is intrinsically non-patient responsive. As a result, insulin-dependent diabetics are forced to continuously monitor fluctuations in their blood sugar profile throughout the day, a profile that can be as unique as the individual, and manually respond to those changes through injection of various exogenous insulins. Advances in insulin protein therapy have introduced novel long-acting therapies including albumin-binding insulin detemir (Novo Nordisk) and isoelectric-point-shifted insulin glargine, as well as ultra long-acting insulin degludec (Novo Nordisk) and recently terminated insulin peglispro (Eli Lilly).[108,109] Although the ultra long-acting insulins potentially reduces the injection frequency of insulin from twice-daily to once-daily, the risk of hypoglycemia and the systemic effect it has on initiating and properly maintaining an effective therapeutic regimen remains a major concern for insulin-dependent diabetics.[110,111] Research efforts aimed at developing an intelligent, glucose-responsive system capable of autonomous glycemic management have been largely restricted to the academic setting, with the vast majority of these systems utilizing multi-faceted constructs that usually depend on polymeric matrices, enzymes or large protein complexes, and large reservoirs of the active insulin protein. Disadvantages of this multi-component approach includes leakage, protein activity loss, as well as the increased possibility of failure for any given component and the effect that has on the entire system, just to name a few.[112,113]

To specifically address these issues, a class of unimolecular insulin conjugates were designed for long-lasting, autonomous glycemic management. First, with inspiration from

insulin glargine, the net charge of the designed GRI was shifted closer towards neutrality through the introduction of an oligo-lysine homopolymer. Furthermore, the oligopeptide contained inorganic, glucose-sensing phenylboronic acid molecules to introduce glucose-sensing capability. Optimization of this construct resulted in the ability of the lead GRI candidate, Ins-PL-4FPBA, to precipitate to a higher degree under physiological pH and clinically relevant formulation concentrations relative to insulin glargine. Interestingly, under exposure to moderate and severe diabetic concentrations of glucose *in vitro*, significant re-solubilization of Ins-PL-4FPBA was observed, suggesting the ability of the GRI to micro-precipitate and form a smart depot after subcutaneous administration as well as re-solubilize under hyperglycemic conditions in a patient-responsive manner.

Next, after verification of *in vitro* receptor potency, *in vivo* dose-escalation studies were performed in both normoglycemic healthy mice as well as in hyperglycemic diabetic mice in order to assess the extent of glucose-responsive behavior. In the healthy *in vivo* environment, Ins-PL-4FPBA exhibited noticeably diminished activity relative to clinical controls as well as all other GRI candidates, as demonstrated by comparison of the hypoglycemia index under the various dose conditions tested. Even more remarkably, at the supraphysiological dose of 25 IU/kg, the hypoglycemia index of Ins-PL-4FPBA was comparable to that of native insulin at the significantly lower doses of 3 IU/kg and 5 IU/kg. When introduced into a diabetic environment, a stark contrast in glucose-correcting efficacy was observed for Ins-PL-4FPBA under hyperglycemic conditions. Significantly higher potency was observed for Ins-PL-4FPBA when compared to clinical controls after exposure to repeat glucose-tolerance challenges over a 10.5-h screen. Additionally, dose-escalation studies revealed the glucose-correcting profile of Ins-PL-4FPBA to be

similar to that of the healthy pancreatic response for physiologically relevant doses. Furthermore, for the supraphysiological dose, Ins-PL-4FPBA did not induce hypoglycemia. Additional insight was provided by performing a PK/PD profile study of the lead candidate relative to clinical insulin controls in a healthy *in vivo* environment. After administration of the GRI, dynamic changes in concentration of Ins-PL-4FPBA was observed throughout the study, with glucose-mediated serum bioavailability directly observed after administration of an IPGTT. Interestingly, no adverse blood glucose depression effects were observed for the GRI as seen with all clinical insulin controls. This result is significant because it further demonstrates the direct ability of the GRI to respond to the *in vivo* environment and behave in a state-responsive manner as opposed to a dose-responsive. It is envisioned that combining the properties of glucose-mediated solubility, enhanced safety, and glucose-responsive efficacy will allow for the development of a GRI capable of once-daily or twice-weekly administration.

In conclusion, all the observations demonstrated that the lead GRI candidate, Ins-PL-4FPBA, has the potential to provide an innovative framework for the development of a truly unimolecular, glucose-responsive insulin therapy. This strategy revealed that the rational design of various aspects of the GRI therapy such as dynamic solubility, enhanced safety and reduced risk of hypoglycemia, as well as glucose-responsive potency, could ensure a long-term, clinically viable and efficacious glucose-responsive insulin for autonomous glycemic management in insulin-dependent diabetes.

2.8 *Materials and Methods*

Materials. All commercially available reagents and lab supplies were purchased from Sigma Aldrich unless otherwise specified. DBCO-C6-NHS Ester (Catalog # A102) and azidoacetic acid (Catalog # 1081) were purchased from Click Chemistry tools. 1-Hydroxy-1,3-dihydro-2,1-benzoxaborole-6-carboxylic acid (OHPHA, Catalog # 102303) and 4-Carboxy-3-fluorophenylboronic acid (FPBA, Catalog # 035568) were purchased from Matrix Scientific. All resins, amino acid derivatives, and activator reagents used for solid-phase peptide synthesis were purchased by Millipore Sigma. Recombinant human insulin was purchased from Life Technologies Corporation.

Synthesis of Insulin-DBCO Core and Insulin Detemir. Recombinant human insulin (100 mg, 17.22 μmol) was dissolved in a buffer containing 0.12 M $NaHCO_3$ and 0.12 M Na_2CO_3 (3 mL) at pH 11. The small molecule DBCO-C6-NHS ester (74.1 mg, 172.2 μmol) was dissolved in 1 mL of anhydrous DMSO and added to the gently stirred insulin solution in three increments (333 μL at 0 min, 20 min, and 40 min). After 60 min, 1 M CH_3NH_2 (1 mL) was added to the reaction mixture. The product was purified via reversed phase preparative HPLC using a 218TP1022 C18 column (2.2 cm ID × 25 cm L, 10 μm; Vydac), with a mobile phase gradient from 2% to 65% (vol/vol) of solvent B (0.043% trifluoroacetic acid/acetonitrile, 20/80) with solvent A (trifluoracetic acid/water, 0.05/99.95). Fractions were collected and lyophilized to provide a white product. The product was characterized by deconvolution electrospray ionization using a QSTAR hybrid Q-TOF, performed at the Koch Institute Swanson Biotechnology Center Biopolymers and Proteomics core. Whole protein MS for $C_{278}H_{400}N_{66}O_{79}S_6$ provided a molecular mass of 6121.6 Da (calculated, 6123.00 Da). Insulin detemir was synthesized and characterized in a similar manner, with

myristic acid NHS ester used as the small molecule reagent, as previously described.[77] Whole protein MS for $C_{271}H_{409}N_{65}O_{78}S_6$ provided a molecular mass of 6017.8 Da (calculated, 6017.99 Da).

To confirm site-specific, mono-conjugated modification on the ε-amine of the B29 lysine residue, purified Insulin-DBCO and insulin detemir were reduced using DTT, followed by alkylation of free thiols and subsequent protein digestion with trypsin. Proteomics analysis was performed using a QSTAR hybrid Q-TOF with tandem MS/MS analysis, with a search conducted for masses of the digested products with free amines at the N-terminal A1Gly, N-terminal B1Phe, and the ε-amine B29Lys positions, as well as for the DBCO and myristic acid small molecule-conjugated masses. All purification and characterization were performed at the Koch Institute Swanson Biotechnology Center Biopolymers and Proteomics core.

Synthesis of Glucose-Responsive Oligopeptide Constructs. All oligopeptides were synthesized with a Tribute-UV automated solid phase peptide synthesizer (Protein Technologies, Inc.) using Rink Amide MBHA Low Load polystyrene resin. Standard Fluorenylmethyloxycarbonyl (FMOC) chemistry was used with activation reagents HATU (P3 BioSystems) and 4-methylmorpholine (NMM) used in fivefold molar excess in anhydrous N,N-dimethylformamide (DMF). Amino acid derivative FMOC-Lys(Boc)-OH was used for oligopeptide backbone synthesis in combination with amino acid derivative Fmoc-Lys(Dde)-OH used for selective orthogonal lysine protection for phenylboronic acid derivatization. N,N′-Diisopropylcarbodiimide (DIC) and 1-Hydroxy-7-azabenzotriazole (HOAt) were used as activation reagents for azidoacetic acid and all phenylboronic acid molecules, with extended coupling times used specifically for azidoacetic acid and FPBA.

Post synthesis, resin was washed in dichloromethane (DCM) and dried prior to a two-hr cleavage with 95% trifluoracetic acid. Precipitation of all oligopeptides was carried out in cold diethyl ether, with washing steps carried out at least three times. The oligopeptide pellet was then isolated, aqueously reconstituted, and freeze dried. Crude oligopeptide product was purified via reverse phase preparative HPLC using a method similar to that of the Insulin-DBCO core and insulin detemir molecules. The product was characterized using matrix-absorption laser desorption instrument time-of-flight (MALDI-TOF, Bruker MicroFlex), performed at the Koch Institute Swanson Biotechnology Center Biopolymers and Proteomics core. Masses obtained were as follows: PL, expected 612.78, actual: 613.48; PL-PBA, expected 888.88, actual, 889.50; PL-FPBA, expected 906.87, actual 907.49; PL-OHPBA, expected 900.89; actual 901.46; PL-2FPBA, expected 1200.96, actual 1200.99; PL-3FPBA, expected 1495.05, actual 1495.80; PL-4FPBA, expected 1789.14, actual 1788.38.

Synthesis of Glucose-Responsive Insulin Conjugates utilizing Copper-Free Click Chemistry. Insulin-DBCO (10.0 mg, 1.63 μmol) was dissolved in a buffer containing 0.12 M $NaHCO_3$ and 0.12 M Na_2CO_3 (0.25 mL). For each oligopeptide construct, 0.25 mL of Insulin-DBCO was mixed with 0.25 mL of appropriate amount of oligopeptide stock solutions prepared in the same carbonate buffer. Ten moles excess (16.3 μmol) of each oligopeptide construct was used in each reaction to ensure complete conjugation of Insulin-DBCO. Directly after mixing, the reaction mixture was placed at 4°C overnight under gentle orbital shaking (50 rpm). The resulting insulin conjugates were used directly from the reaction mixture with no further purification performed to remove unreacted, excess oligopeptide. All products were characterized by deconvolution electrospray

ionization using a QSTAR hybrid Q-TOF, performed at the Koch Institute Swanson Biotechnology Center Biopolymers and Proteomics core. Masses obtained were as follows: Ins-PL, expected 6735.78, actual 6735.2; Ins-PL-FPBA, expected 7029.87, actual 7030.3; Ins-PL-2FPBA, expected 7323.96, actual 7288.2; Ins-PL-3FPBA, expected 7618.05, actual 7582.4; Ins-PL-4FPBA, expected 7912.14, actual 7876.7. It is noted that these masses are consistent with MS for PBA-modified peptides, where the double-dehydrated mass (i.e., −36) is observed due to gas phase anhydro formation of a boronic acid.[75]

Isothermal Titration Calorimetry (ITC). Titration experiments were carried out at 310.15 K, with all samples dissolved in PBS (1X) at pH 7.4, on a VP–ITC calorimeter from Microcal, Inc. For all phenylboronic acids, the small molecule PBAs were in the sample cell at a concentration of 3.0 mM, and glucose was in the injection syringe at a concentration of 600 mM. For oligopeptides bearing PBA molecules, the constructs were in the sample cell at a concentration of 0.25-3.0 mM, with glucose in the injection syringe at a concentration of 60-600 mM. The titration schedule consisted of consecutive injections of 10 μL over a duration of 20-seconds, with the interval between injections set at 240-seconds. Heats of dilution, measured by titrating glucose into the sample cell containing only buffer, were subtracted from each data set. All solutions were degassed prior to titration. The data were analyzed using Origin 7.0 software using the 'one-set-of-sites' binding model, which assumes the complexes do not interact with one another. All statistical comparisons were performed using two-tailed, unpaired t-tests (GraphPad Prism 6.0).

Measurement of Dynamic Solubility. Stock concentrations (816 μM) of each glucose-responsive insulin candidate were synthesized, as described above. Subsequently, each insulin sample was individually mixed with varying concentrations of glucose, prepared in 1 M HEPES, for final concentrations of 0 mg/mL, 1 mg/mL, 3 mg/mL, and 5 mg/mL glucose, final concentration of 172 μM for all insulin samples, and final pH of 7.4. Samples were plated at 30 μL per well (n = 3/group) in a black, clear-bottom 384-well plate (Thermo Scientific Nunc) and sealed with an optically clear and thermally stable seal (VWR). The plate was incubated at 4 °C overnight under gentle orbital shaking (50 rpm). After incubation the plate was equilibrated to room temperature and placed into an Infinite M1000 plate reader (Tecan Group), with absorbance readings collected at 540 nm to measure differences in transmittance as a result of precipitation and glucose-mediated re-solubilization. All statistical comparisons were performed using two-tailed, unpaired t-tests (GraphPad Prism 6.0).

In Vitro Insulin Receptor Activation. C2C12 cells were purchased from the American Type Culture Collection (ATCC) and confirmed free of mycoplasma contamination before use. Cells were cultured in Dulbecco's modified Eagle medium (DMEM) containing L-glutamine, 4.5 g/L D-glucose, and 110 mg/L sodium pyruvate, and supplemented with 10% FBS and 1% penicillin–streptomycin. Incubations occurred in a 5% CO_2/water-saturated incubator at 37 °C. Cells were seeded in 96-well plates at a density of 5,000 cells per well. Twenty-four hrs after plating, the cells were washed three times with 200 μL of DMEM containing L-glutamine, 4.5 g/L glucose, and 110 mg/L sodium pyruvate, and starved for at least 4 h at 37 °C in the same serum-free conditions. After 4 h, the media was removed, and cells were stimulated with 100 μL of insulin samples of various

concentrations for 30 min at 37 °C. After 30 min, cells were washed three times with 100 µL of cold Tris-buffered saline (1X), followed by lysing the cells for 10 min with 100 µL of cold Lysis Buffer (Perkin-Elmer). Levels of phosphorylated AKT 1/2/3 (Ser473) and Total AKT 1 were determined from cell lysates using the AlphaLISA SureFire ULTRA kits (Perkin-Elmer) according to the manufacturer's instructions. Intra-well normalized data of phosphorylated AKT 1/2/3 (Ser473) and Total AKT 1 were analyzed using GraphPad Prism 6.0, with dose–response curves fitted to a variable slope (four-parameter) stimulation model to determine the EC_{50} of each insulin sample, and statistical significance determined by an extra sum-of-squares F test for comparing the global fit statistics of LogEC50 for all samples relative to the native protein.

Mouse Models. All animal studies were conducted through protocols approved by the MIT animal care and use committee, following all institutional, state, and federal guidelines for the use of research animals. Male C57BL/6J mice, age 8 wk, were purchased from Jackson Laboratory and used as is for healthy mouse studies. For all diabetic mouse studies, after acclimation, mice were fasted overnight before intraperitoneal injection of 150 mg/kg STZ. Preparation of STZ for injection involved dissolving the chemical at a concentration of 15 mg/mL in sodium citrate buffer (114 mM, pH 4.5) immediately before injection. Food was withheld for 2 h post-injection, after which mice were allowed to eat and drink ad libitum. Glucose levels were monitored by peripheral tail vein bleeds using a portable glucose meter (Clarity Plus, Clarity Diagnostics) daily until unfasted glucose levels were >400 mg/dL.

***In Vivo* Studies.** For all healthy mouse studies, all mice were fasted overnight before initiating the study. Blood glucose concentration was measured at the beginning of each

study, and any mouse with a fasting blood glucose level > 200 mg/dL was triaged from the study. All insulin samples were prepared at a dose concentration of 5 IU/kg according to their respective clinical dose definition (human insulin, 1 IU = 5.97 nmol; insulin glargine, 1 IU = 6.00 nmol; insulin detemir, 1 IU = 24.0 nmol), with the clinical dose definition for human insulin used for all glucose-responsive insulin candidates. Mice were then randomized and injected, with all insulin samples administered subcutaneously. For the hypoglycemia assessment study, blood glucose concentration was measured for a total of 6 hrs, with the hypoglycemia index quantified as the difference between the initial and the nadir (i.e., lowest observed) blood glucose readings divided by the nadir. For the pharmacokinetic and pharmacodynamic study, blood was collected by terminal cardiac punctures for each timepoint, with serum isolated via centrifugation followed by subsequent analysis and quantification of serum insulin levels using an insulin ELISA kit (ALPCO) according to the manufacturer's instructions. Administration of the intraperitoneal glucose tolerance test (IPGTT) at 3.5 hrs was performed with a 1 g/kg glucose solution prepared in PBS (1X). For all diabetic mouse studies, STZ-induced diabetic mice were fasted overnight before initiating the study. Blood glucose concentration was measured at the beginning of the study, and any mouse with a fasting blood glucose level < 300 mg/dL was triaged from the study. Mice were then randomized and injected, with all insulin samples administered subcutaneously. For the potency-based diabetic screening study, insulin samples were administered at a molar dose equivalent of 5 IU/kg native human insulin (1 IU = 5.97 nmol). Blood glucose readings were collected every 30 min, with multiple IPGTTs administered at 3.5 and 7 hrs. For the IPGTT, 1 g/kg glucose was administered in PBS (1X). For the diabetic dose escalation

study, insulin samples were prepared at dose concentrations according to their respective clinical dose definition, with the clinical dose definition for human insulin used for all glucose-responsive insulin candidates. Mice were then randomized and injected, with all insulin samples administered subcutaneously. Blood glucose readings were collected every 30 min with an IPGTT administered at 3.5 hrs. For the IPGTT, 1 g/kg glucose was administered in PBS (1X). Responsiveness was quantified by measuring the area under the curve with a baseline set at 3.5-hr and integrating across a 3.5-hr window following the challenge. All statistical comparisons were performed using two-tailed, unpaired t-tests (GraphPad Prism 6.0).

2.9 *Acknowledgements*

This work was supported by a grant from the Leona M. and Harry B. Helmsley Charitable Trust Foundation (Grant No. 2017PG-T1D027). We acknowledge technical support from the Koch Institute Swanson Biotechnology Center and are specifically grateful for use of the Biopolymers & Proteomics Core Facility. Additionally, the Biophysical Instrumentation Facility for the Study of Complex Macromolecular Systems (NSF-0070319) is gratefully acknowledged.

Chapter 3: Engineering Dynamically Tethered Insulin Protein Conjugates Towards a Glucose-Responsive Therapy

The work presented in this chapter is in preparation for publication:

A. B. Cortinas, K. B. Daniel, L. S. Thapa, F. Girma, R. S. Langer, D. G. Anderson, Engineering Dynamically Thethered Insulin Protein Conjugates. *In preparation.*

3.1 *Introduction*

The concept of a unimolecular glucose-responsive insulin is attractive as a paradigm-shifting diabetes technology, especially in regard to the numerous and diverse possibilities in which glucose-responsive behavior can be engineered and exploited. Embodiments of unimolecular insulins explored to-date have incorporated boronic acid motifs onto the protein in an attempt to impart inorganic glucose-sensing ability and sequestration through various mechanisms. Due to the promiscuity of boronic acids to reversibly bind with *cis*-1,2 and *cis*-1,3 diols, exposure to the *in vivo* biological environment exposes boronic acids to the numerous immobilized diols found on various cellular architectures, including cell surface glycans, glycoproteins and glycosylated proteins found in the blood, as well as glycosaminoglycans, all of which are found throughout the body either in the healthy state or as a potential result of chronic hyperglycemia.[53,54,59,114] The reversible-covalent interactions that boronic acids possess provide these GRI constructs the ability to bind and sequester to these various diols found throughout the body, potentially increasing the half-life of the therapeutic relative to the native protein. More importantly, this reversibility allows for elevated glucose concentrations to compete with these interactions, providing a potential means for release of the GRI therapy under the hyperglycemic conditions of glucose commonly experienced in the diabetic state.

In addition to the sequestration model largely exploited in current GRI constructs, there exists an attractive, alternative approach that potentially exploits the hinge-opening mechanism through which insulin interacts with its receptor. Cross-species research into this mechanism through which insulin interacts with the insulin receptor has revealed

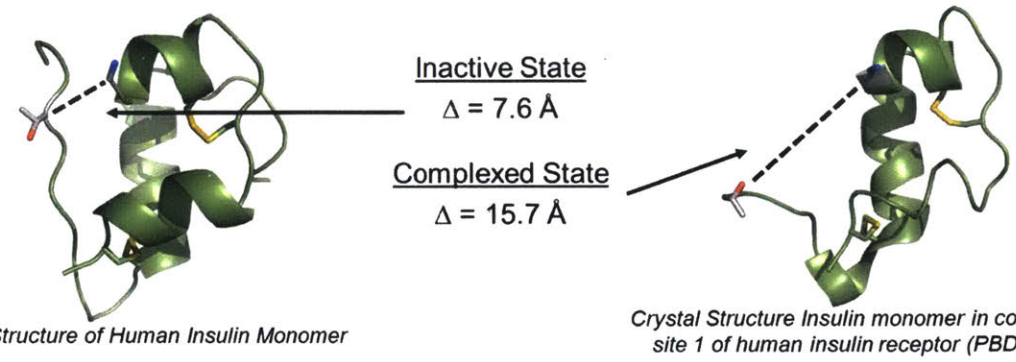

Figure 3. 1 Three-dimensional changes in native insulin structure during interaction with insulin receptor. The hinge-opening mechanism is highlighted and emphasized by the ~2X change in amino acid distance between the A1 glycine and B29 lysine residues of the closed, inactive state (*left*) and the open, complexed state (*right*).

insights into a specific condition through which the protein must change its three-dimensional structure and confirmation in a hinge-like manner to engage in insulin receptor binding and activation.[115] Perturbations of certain amino acid residues through covalent chemical modifications has further exposed important intramolecular interactions required for this unfolding, requiring the N-terminus of the A chain and the C-terminus of the B chain of insulin to be capable of displacement relative to each other (Figure 3. 1). Additionally, there exists engineered insulin analogues that utilize sterically-locked amino acids at locations critical for protein unfolding, forcing the engineered insulin to be either in the closed, inactive state (Figure 3. 1 left) or in the open, complexed state (Figure 3. 1 right). Insights provided by these insulin analogues reveal two important findings: (1) insulin locked in the closed, inactive state exhibits significantly enhanced stability but at the expense of a significant drop in potency and activity; (2) insulin locked in the open, complexed state exhibit retained native potency and activity, but significantly diminished stability.[116] These findings are further supported by protein models of the

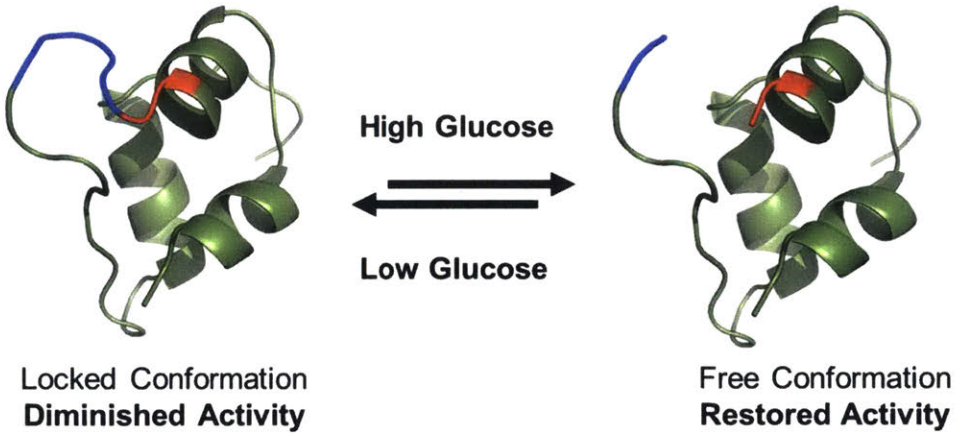

Figure 3. 2 Visual representation of envisioned mechanism of action for desired glucose-responsive insulin. Glucose-responsive behavior is afforded by exploiting the ability of insulin to freely engage with the receptor, reversibly transitioning between the "locked" conformation under hypoglycemic or normoglycemic conditions and the "unlocked" or "free" conformation under hyperglycemic conditions. Insulin models adapted from PDB:2JZQ.

tethered state, created by synthesizing chemically cross-linked insulin derivatives and single-chain insulin analogs.[117–122] This information, in conjunction with additional supporting structural data, provides a motivation for investigating the ability to create an insulin conjugate that can reversibly lock into a non-binding (inactive yet highly stable) state under euglycemic and hypoglycemic conditions, as well as undergo glucose-mediated unlocking to unfold and allow for receptor engagement and stimulation under hyperglycemic conditions (Figure 3. 2).[117,119,123] Inter-chain cross-linking between these elements at low glucose concentration might impair receptor binding but enhance stability, whereas competitive displacement of the tether at high glucose concentrations might restore sufficient protein flexibility to enable high-affinity receptor stimulation. Design of such reversible, glucose-responsive tethers are envisioned to include a glucose-sensing element in one chain of the hormone and a saccharide, or saccharide mimic, in the other chain, which could, in principle, exploit the opening of the B-chain's N-

or C-terminal segments relative to the critical insulin receptor binding A1-A8 α-helix.[115] This scheme would thereby intrinsically couple insulin's receptor-binding interactions with potential saccharide-sensing while also enhancing the overall thermodynamic stability of the engineered insulin.[116] Although such schemes would be attractive in their simplicity and structural elegance, a challenge to the implementation of this strategy is posed by the non-linear relationship between insulin's receptor-binding affinity, its biological potency in vivo, and by the precise shape of the curve relating blood-glucose concentration to activity. [124,125]

Herein, we describe, to our knowledge, the first example of a chemically conjugated insulin protein capable of dynamic cyclization towards the generation of an insulin therapy possessing enhanced stability and potentially glucose-responsive, hinge-opening interactions. The design strategy involved the synthesis of a library of 24 insulin conjugates having two unique small molecules, a phenylboronic acid (PBA) and a polyol saccharide analogue, site-specifically conjugated to the A1 glycine and B29 lysine residues. Analysis of the synthesized library identified 14 insulin conjugates that demonstrated enhancements in chemical stability relative to the native protein, suggesting successful implementation of a dynamic tether through an intra-protein stabilization interaction between the PBA and polyol. Further study of thermal aggregation properties was carried out for a total of 10 conjugates, with all samples demonstrating an enhanced resistance to aggregation by at least 100%. Introduction of various diols into the chemical stability assay revealed the dynamic PBA-polyol interactions to be too strong for glucose to impose any dynamic competition. However, the use of sorbitol, due to the structural similarity to the polyol molecule, revealed the potential sugar-responsive, hinge-

opening nature of the insulin conjugate. The use of sorbitol imposed a destabilizing effect that reverted one particular conjugate back towards its native stability, suggesting the potential for dynamic competition of the intra-protein PBA-polyol interaction and targeted, saccharide-induced protein unfolding. Lastly, *in vitro* cell-based potency and *in vivo* efficacy studies of select conjugates revealed the partial retention of receptor-binding activity as well as glucose-correcting activity. Overall, it is envisioned that the proposed strategy, with further improvement, could provide a potentially novel therapeutic strategy for the development of glucose responsive insulin therapeutics that exploit the receptor binding interaction for autonomous glycemic management.

3.2 *Design and Characterization of the Insulin Conjugate Library*

The protein conjugate design utilized a small library of phenylboronic acid and polyol sugar analogues as the basis for synthesizing the novel class of insulins (Figure 3. 3). Utilizing N-hydroxysuccinimide (NHS) coupling chemistry under basic conditions, the dynamically tethered insulin conjugates were synthesized by first conjugating one component (i.e. either the PBA or polyol first) to the ε-amine on the B29 lysine residue followed by subsequent conjugation of the other component to the A1 glycine residue of the insulin protein, an *in situ* adaptation of a previously described method.[75,77] Complete synthesis of the library resulted in 24 unique conjugates. Purification and characterization of the insulin conjugates was performed to validate whole protein conjugation as well as site-selective modification to the B29 lysine and A1 glycine residues (Figure A. 6). A complete list and nomenclature of which PBA and polyol sugar analogues are found for a specific conjugate is shown in Table 3. 1.

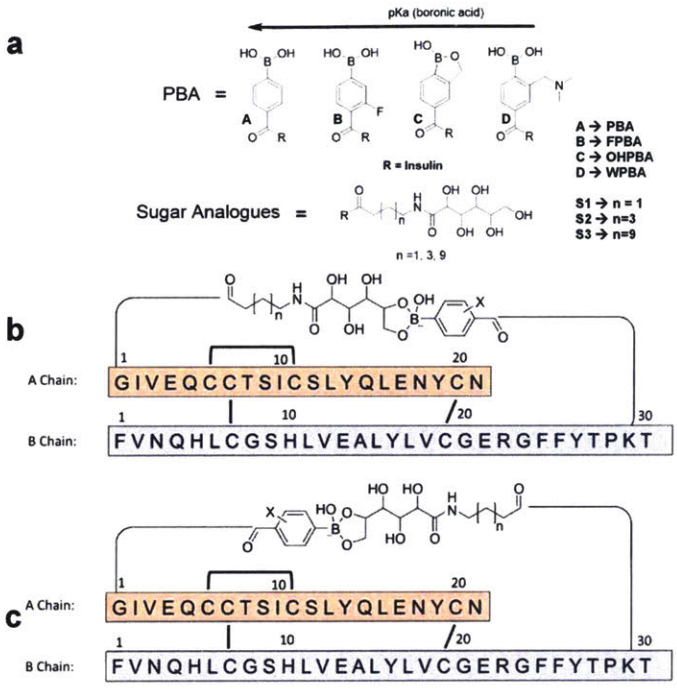

Figure 3. 3 Strategy for synthesizing dynamically-cyclized insulin conjugates. (a) Structures of the phenylboronic acid (PBA) and polyol sugar analogue small molecules used in the synthesis of the insulin conjugates. (b) Primary structure of insulin conjugates with PBA conjugated to the C-terminus of the B-chain and the polyol sugar analogue conjugated to the N-terminus of the A-chain. (c) Primary structure of insulin conjugates having the reverse orientation, with the polyol sugar analogue conjugated to the C-terminus of the C-terminus of the B-chain and the PBA conjugated to the N-terminus of the A-chain. A total of 24 conjugates are envisioned using this synthesis strategy.

Table 3. 1 Complete list of conjugates and their respective small molecule conjugations

Sample Name	A1 Glycine Conjugation	B29 Lysine Conjugation
C1	PBA	S2
C2	FPBA	S2
C3	OHPBA	S2
C4	WPBA	S2
C5	PBA	S1
C6	FPBA	S1
C7	OHPBA	S1
C8	WPBA	S1
C9	PBA	S3
C10	FPBA	S3
C11	OHPBA	S3
C12	WPBA	S3
C25	S2	PBA
C26	S2	FPBA
C27	S2	OHPBA
C28	S2	WPBA
C29	S1	PBA
C30	S1	FPBA
C31	S1	OHPBA
C32	S1	WPBA
C33	S3	PBA
C34	S3	FPBA
C35	S3	OHPBA
C36	S3	WPBA

3.3 *Chemical and Thermal Stability of the Synthesized Conjugates*

In order to determine whether any undesired effects of the synthesis conditions on the resulting conjugate existed, circular dichroism was employed as a means of measuring protein secondary structure conformation. As can be seen in Figure 3. 4a, two representative conjugates demonstrate virtually no loss in the alpha helical signature present in the native protein, indicating that the synthesis, purification, and characterization conditions have a miniscule effect on protein secondary structure. Furthermore, the stability of the native protein and the synthesized conjugates were determined by titration with the denaturant Guanidine HCl to measure the resulting change in the alpha helical signature (Figure 3. 4b), as previously described.[17,126] In conducting the denaturation study in this manner, implied thermodynamic quantities regarding the stability of the proteins can be determined, specifically the Gibbs Free Energy of Unfolding. As can be seen in Figure 3. 4b, there are qualitative differences in

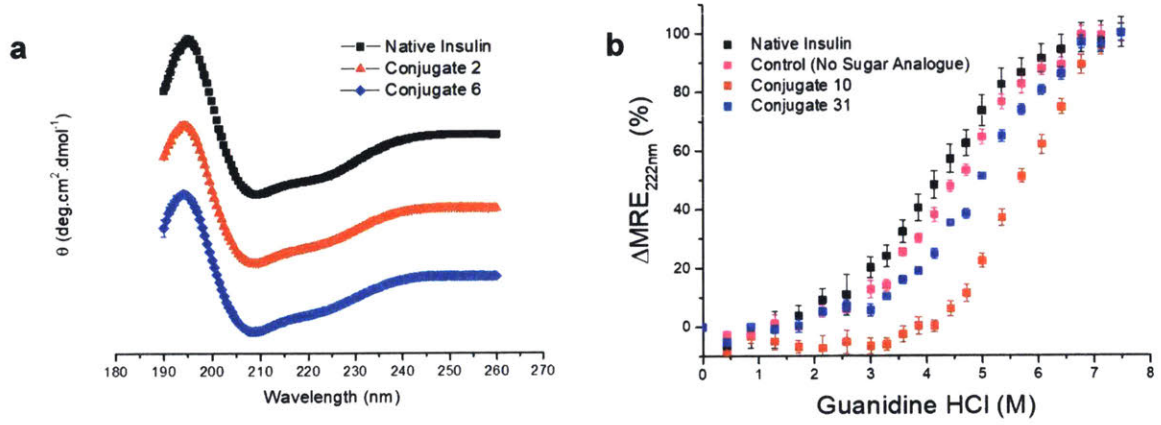

Figure 3. 4 Analytical characterization of the insulin conjugates. (a) Representative circular dichroism structures illustrating retention of alpha-helical secondary structure post-modification. Mean ± SD (n = 3). (b) Thermodynamic modeling of stability as a function of denaturant concentration using a two-state model of all tested conjugates. Denaturation study demonstrated evidence of dynamic covalent intra-protein interaction occurring between the boronic acid and polyol small molecules, illustrated by the shift of the curves to the right which signify enhancements in chemical stability. Mean ± SD (n = 3).

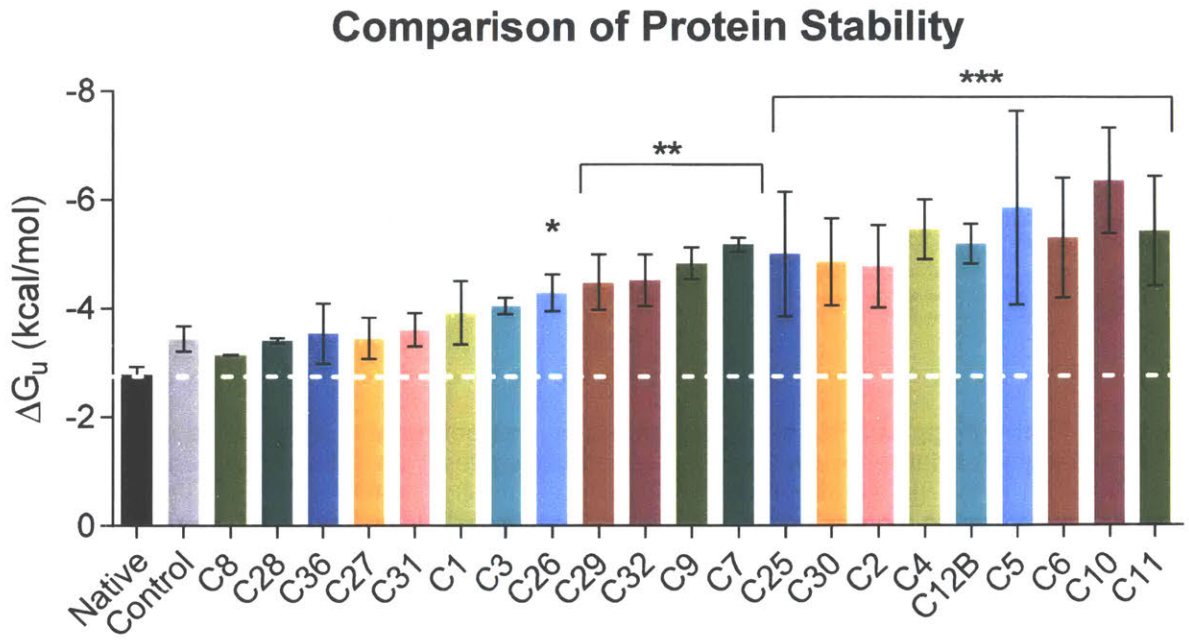

Figure 3. 5 Statistical comparison of resulting stability for the synthesized conjugates. Statistical increases in stability of certain conjugates is observed, suggesting the presence of a dynamic covalent interaction occurring between the boronic acid and polyol sugar analogue, despite being independently conjugated to the insulin protein. Mean ± S.D. (n = 3). * $P < 0.05$, ** $P < 0.01$, *** $P < 0.001$ (One-way ANOVA multiple comparisons test).

the stabilities between representative conjugates 10 and 31 compared to the native protein and a control conjugate. The control conjugate is structurally equivalent to C3, but is specifically lacking the respective alcohols found on the sugar analogue polyol backbone. Albeit indirect, the results of the denaturation study demonstrate the presence of an interaction occurring between the boronic acid and polyol small molecules, despite the fact that both small molecules were conjugated independently of each other without prior pre-complexation before the conjugate synthesis. This interaction is supported by the proposed mechanisms of insulin denaturation as given in the literature, which proposes that insulin unfolding and denaturation processes are initiated by the separation

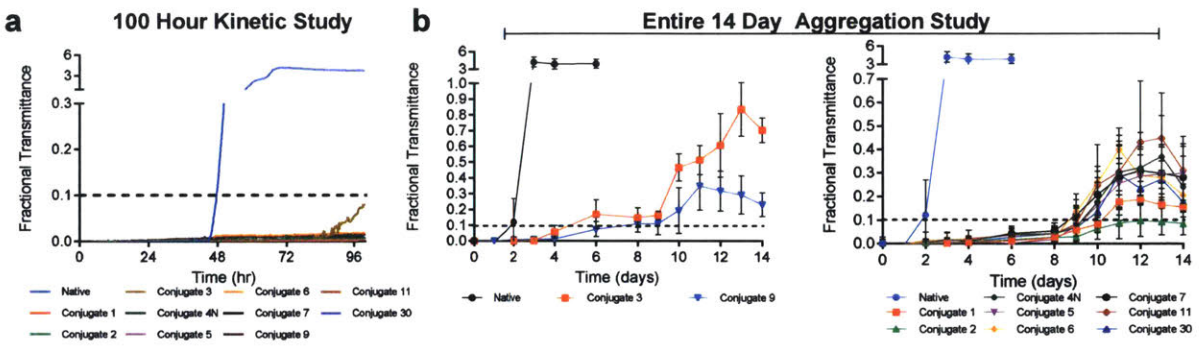

Figure 3. 6 Thermal aggregation study performed on a select number of insulin conjugates. (a) 100-hour kinetic study for native insulin and 10 selected conjugates, with native insulin aggregating after 48 hours. Mean (n = 3). (b) Aggregation data specifically for Conjugates 3 and 9 (*left*) demonstrating a moderate resistance to aggregation by at least 2 additional days compared to native insulin, and aggregation data for all other conjugates (*right*) demonstrating enhanced stability to aggregation by at least 4 additional days, and at most 8 additional days, compared to native insulin. Mean ± SD (n = 3).

of the A-chain N-terminus and the B-chain C-terminus, the locations where insulin modification was targeted for these conjugates.[127,128] Statistical analysis was performed on the resulting stability curves, comparing the Gibb's Free Energy of Unfolding, and it was found that 14 of the conjugates were statistically more stable than the native protein and the respective control. The resulting analysis provided additional support of a statistically relevant basis for an intramolecular interaction occurring within the protein complex, as shown in Figure 3. 5. A thermal stability test was also conducted to determine whether the conjugates would resist aggregation under elevated temperature and agitation compared to the native protein.[129] As can be seen in Figure 3. 6 and Table 3. 2, all conjugates resisted aggregation by at least 4 days under extreme heat and agitation, compared to the native insulin protein that aggregated within 2 days, further demonstrating the presence of a stabilizing, intramolecular interaction. Furthermore, in order to demonstrate whether the intramolecular interaction between the boronic acid and

Table 3. 2 Compiled thermodynamic and aggregation data for select conjugates. Mean ± 95% C.I. (n = 3).

Species	ΔG_u (kcal/mol)	Aggregation Lag Time (days)
Conjugate 1	-3.93 (0.59)	10
Conjugate 2	-4.78 (0.76)	10
Conjugate 30	-4.85 (0.80)	10
Conjugate 4	-5.45 (0.55)	9
Conjugate 5	-5.85 (1.8)	9
Conjugate 6	-5.29 (1.1)	9
Conjugate 7	-5.17 (0.13)	9
Conjugate 11	-5.41 (1.0)	9
Conjugate 9	-4.83 (0.29)	6
Conjugate 3	-4.05 (0.15)	4
Native	-2.78 (0.15)	2

polyol has the potential to be diol-responsive, glucose and sorbitol were incorporated into the GHCl denaturation study to determine whether these diols could dynamically compete and displace the reversible covalent bond exhibited between the conjugated PBA and polyol and therefore decrease the observed stability of the synthesized conjugates. Such an effect would suggest direct competition with the PBA-polyol sugar analogue interaction, which would directly result in reverting the conjugate back towards native stability. An observed reversion such as this would indicate the desired lock-and-key mechanism directed towards the hinge-opening denaturation process, which is prevented by the dynamic PBA-polyol interaction. First, as shown in Figure 3. 7a, glucose was incorporated into the denaturation study at a relevant diabetic concentration of 500 mg/dL of glucose with Conjugate 2 to determine if any glucose-mediated destabilization was observed. As can be seen, there is no qualitative, and subsequently no quantitative, difference between the resulting stability curves. A second attempt was made utilizing sorbitol at 50 mg/mL, as can be seen in Figure 3. 7b and c. Sorbitol was chosen due to

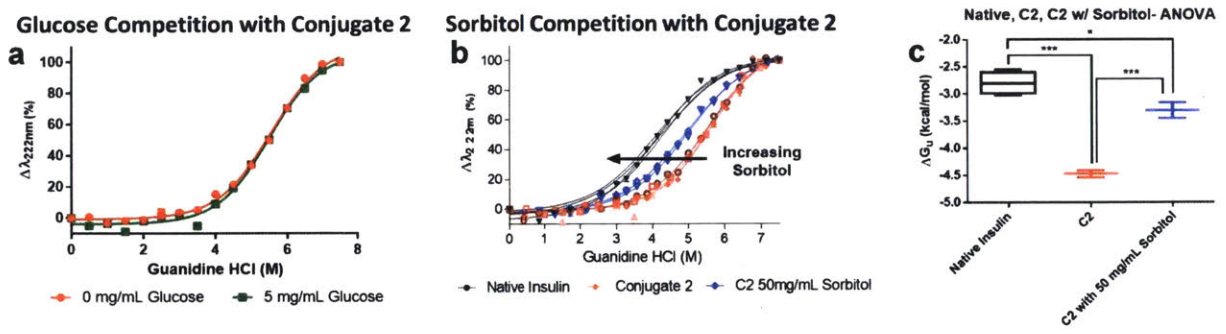

Figure 3. 7 Chemical denaturation studies incorporating saccharides for the determination of sugar-mediated destabilization. (a) Protein denaturation study involving Conjugate 2 both with and without 500 mg/dL glucose, demonstrating no significant qualitative or quantitative difference in the resulting implied thermodynamic Gibbs Free Energy of Unfolding. Mean ± SD (n = 3). (b) Protein denaturation study of Conjugate 2 with and without 5,000 mg/dL sorbitol as well as a reference of native insulin without sorbitol. The resulting data demonstrates a qualitative change in stability of Conjugate 2, shifting the stability curve towards that of the native protein. Mean ± SD (n = 3). (c) One-way ANOVA analysis comparing native insulin to Conjugate 2 alone, comparing Conjugate 2 to Conjugate 2 containing 5,000 mg/dL sorbitol, as well as comparing native insulin to Conjugate 2 containing 5,000 mg/dL sorbitol. The results ultimately demonstrate a shift in stability of Conjugate 2 towards that of the native protein as a function of sorbitol concentration. Mean ± SD (n = 3). * $P < 0.05$, ** $P < 0.01$, *** $P < 0.001$ (One-way ANOVA multiple comparisons test).

the structural similarity of this polyol to the sugar analogue conjugated to the insulin protein, therefore providing a higher likelihood of displacing the reversible, covalent PBA-polyol interaction. As can be seen, sorbitol demonstrated a statistically significant displacement of the resulting stability curve for Conjugate 2, reverting the more stable conjugate's stability curve back towards native insulin as a function of diol concentration. The following results demonstrate the potential for the synthesized conjugates to possess diol-responsive capabilities with regard to stability and unfolding, and therefore possess potential towards saccharide-induced receptor binding potency due to the processes between denaturation and receptor binding interaction having functional similarities.[116,127,128]

3.4 *Tertiary Structure Evaluation via X-Ray Diffraction*

In an attempt to directly visualize the tertiary structure of the synthesized conjugates, crystallization of selected conjugates was employed in order to perform x-ray diffraction (XRD) experiments. Crystals of Conjugate 3 were successfully grown using the hanging-drop method and subsequently isolated and diffracted to obtain relevant structure data (Figure 3. 8a), as previously described.[130–132] The data obtained from XRD was modeled to obtain the crystal structure information as shown in Figure 3. 8b and Table 3. 3. As can be seen in Figure 3. 8c, there is demonstration of little to no loss in tertiary structure compared to the native protein when structurally overlapped. Additional evidence from the molecular structure determination revealed that the crystal packing of the monomers in the crystal lattice resembled that of the native protein, demonstrating antiparallel alignment of the protein conjugates monomers with respect to each other. This antiparallel alignment signified the absence of intermolecular interactions due to the requisite alignment between the B29 position of one monomer and the A1 position of the neighboring monomer (Figure A. 7). Due to the antiparallel nature, this provides further evidence that the interactions observed, albeit indirectly observed in the stability assays with and without diols, suggest the presence of an intramolecular interaction. Unfortunately, the electron density of the small molecule conjugations was not detectable during the acquisition of XRD data, and therefore the boronic ester complex occurring in Conjugate 3 could not be directly visualized or modeled. Future experiments will focus on optimizing crystal packing conditions to ensure sufficient electron density visualization is acquired to model the boronic ester interactions.

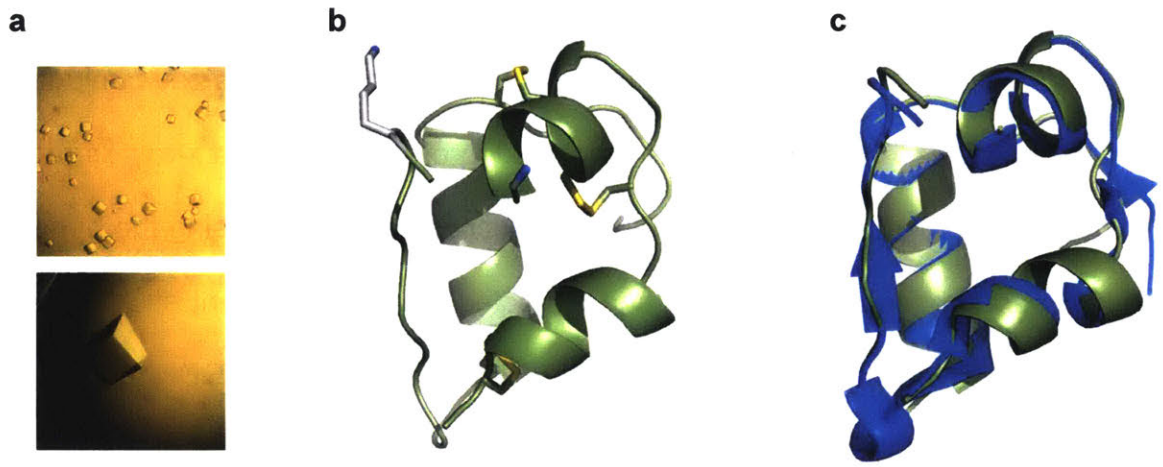

Figure 3. 8 Crystallization and subsequent diffraction of Conjugate 3 using XRD. (a) Protein crystals of Conjugate 3 obtained using the hanging-drop technique. (b) Mathematical model of Conjugate 3 obtained from XRD study. (c) Direct overlay of tertiary structures of Conjugate 3 with the native insulin monomer (PDB: 4EY1), demonstrating retention of tertiary structure and no adverse effects as a result of modification or purification processes.

Table 3. 3 Refinement parameters of Conjugate 3 molecular structure as determined using Phenix software suite.

Refinement Parameters	
Resolution (Å)	1.465
Completeness of Range (%)	96.8
R_{work} (%)	18.8
R_{free} (%)	21.3
Ramachandran Plot	98% favored 2% Allowed 0% Outliers
B-factor (%)	10.5
Space Group	$I2_13$

3.5 *In Vitro Potency and In Vivo Efficacy of Conjugates*

In order to assess receptor binding and activation potency of all synthesized conjugates, an *in vitro* cell-based assay that measured the relative ratio of phosphorylated AKT levels relative to total AKT levels as a result of insulin receptor stimulation was used. All 24 synthesized conjugates were initially screened and compared to native insulin in order to determine their relative *in vitro* potencies, as shown in Figure 3. 9. Representative dose response data can be seen in Figure 3. 9a, with the resulting EC_{50} concentrations shown in Figure 3. 9b as calculated with a four-parameter fit of the dose response data. From this data, notable conjugates that exhibit the most *in vitro* potency retention possess the WPBA small molecule, with no apparent correlation found for the polyol sugar analogue. Most notably, the lead conjugate was identified to be Conjugate 4 (C4) due to it possessing the largest EC_{50} concentration relative to all other conjugates tested. An *in vivo* assessment of select insulin conjugates using an STZ-induced Type 1 diabetic mouse model demonstrated retention of insulin efficacy, as shown in Figure 3. 10. Select Conjugates 4, 9, and 10 were injected at a concentration of 5 IU/kg subcutaneously (1 IU = 5.97 nmol). The corresponding blood glucose depression levels were measured over

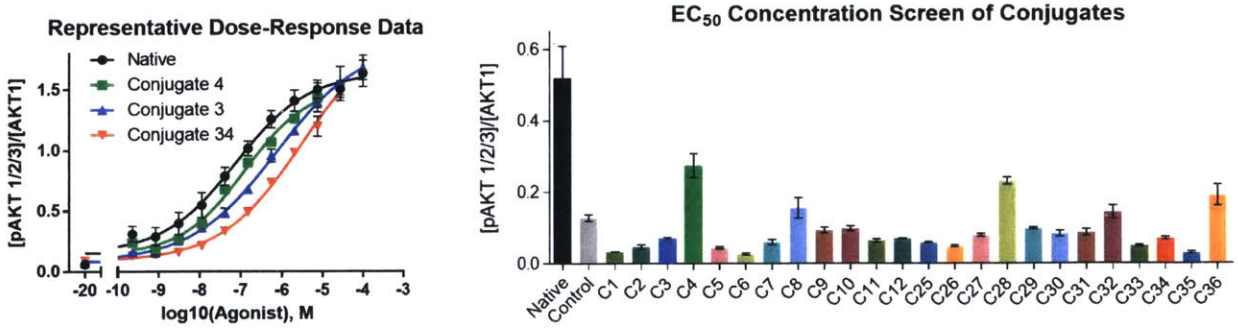

Figure 3. 9 *In vitro* characterization of insulin conjugates. (a) Representative dose-response data for selected conjugates. Mean ± SD (n = 3). (b) Potency comparison via dose-response-derived EC_{50} values for all insulin conjugates relative to the native protein using a four-parameter fit. Mean ± 95% C.I. (n = 3).

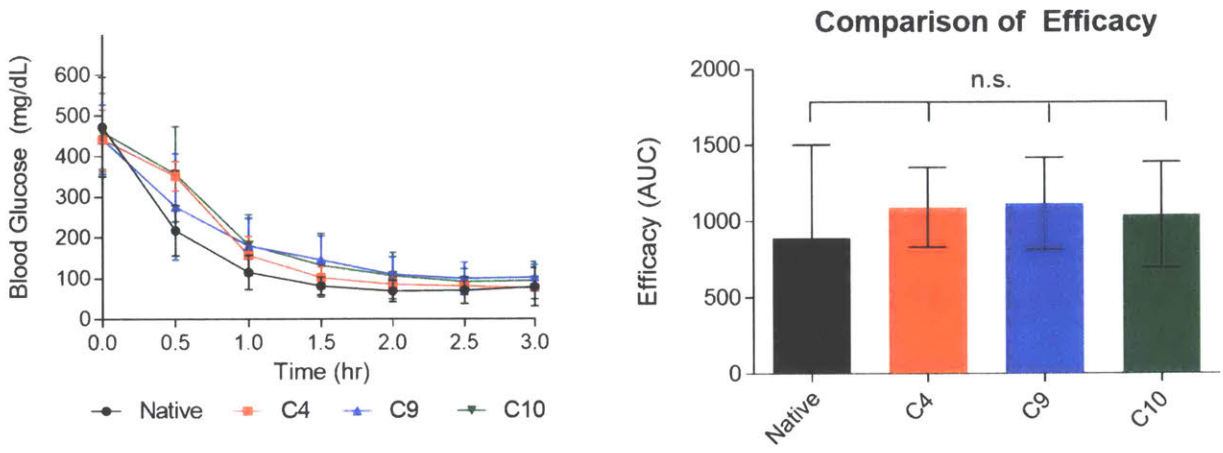

Figure 3. 10 *In vivo* diabetic study of select insulin conjugates. Experiment involved the subcutaneous administration of insulin samples at equimolar concentrations. Mean ± S.D. (n = 3). n.s. $P > 0.05$ (two-tailed, unpaired t-test).

the course of three hours (Figure 3. 10 *left*). Analysis of the area-under-the-curve for the entire duration of the experiment revealed statistically non-significant differences in *in vivo* efficacy, demonstrating equivalence in the ability to correct blood sugar in a diabetic mouse model over this timeframe (Figure 3. 10 *right*).

3.6 *Discussion and Conclusions*

Molecular embodiments of glucose-responsive insulin systems have thus far been largely restricted to multi-component arrangements that possess the following three components: (1) a scaffold that encloses the entire system, most often a polymer or polymeric complex; (2) large proteins or protein complexes that induce an environmental or microenvironmental change in the entire system to trigger a release response; and (3) large reservoirs of the active insulin protein. When optimized for a specific environment, and when working in concert, the overall glucose-responsive system in its many forms

has been demonstrated to adequately release insulin in response to changing concentrations of glucose. However, active research utilizing this specific approach for nearly 50 years has not yielded a clinical viable glucose-responsive insulin therapy. More recently, advances in the field have driven these glucose-responsive systems into unimolecular constructs that have utilized, in almost all cases, boronic acid motifs as the inorganic sugar sensing component. The universal theme for mechanism-of-action for these unimolecular glucose responsive insulins utilizes the boronic acid component to exploit its promiscuity in binding to almost any saccharide found within the body to sequester the protein until it can be competed against with hyperglycemic concentrations of glucose, a method that has found some success thus far.[77] No examples, to the best of our knowledge, currently exist that attempt to take advantage of the hinge-opening mechanism and change in three-dimensional conformation that the insulin protein must undergo in order to interact with the insulin receptor, an interaction that is necessary for both receptor binding and activation.

Herein, we develop a strategy that exploits the hinge-opening mechanism of action necessary for insulin to not only denature, but also interact with the insulin receptor, to create a novel class of dynamically tethered insulin protein conjugates exhibiting enhanced thermodynamic stability. First, through utilization of a small library of phenylboronic acids and synthesized polyol sugar analogues, a total of 24 insulin conjugates were synthesized by independently conjugating either the PBA or polyol sugar analogue to the C-terminus of the B chain while conjugating the other small molecule to the N-terminus of the A chain, and vice versa, thereby exploiting the two segments on the insulin protein that are critical for both stability and insulin receptor interactions. After

analytical characterization and verification of retained secondary structure after incorporation of both small molecules onto the insulin protein, an in-depth assessment of the insulin conjugate monomers was conducted to evaluate the chemical and thermal stabilities of the resulting modifications. Overall, 14 total conjugates were identified that exhibited statistically significant enhancements in thermodynamic stability relative to the native protein and a control conjugate lacking the polyol sugar as studied by a titration experiment with chemical denaturant GHCl. This result is significant because the data suggests not only successful implementation of both small molecules onto the protein via chemical conjugation, but more importantly that a dynamic interaction is occurring between both molecules on the same protein. The presence of a dynamic tether through an intra-protein stabilization interaction between the PBA and polyol is significant because it suggests the potential for further engineering and refining to create an insulin conjugate capable of sugar-mediated receptor binding through exploitation of the important hinge-opening mechanism.

Next, from the denaturation study, a total of 10 monomeric conjugates were identified to be studied using a thermal aggregation assay whereby all tested conjugates experienced continuous agitation and exposure to extreme temperatures (37 °C) reminiscent to that of distribution and transportation networks in developing countries lacking appropriate cold-chain infrastructure. As expected from the chemical denaturation studies, all tested conjugates demonstrated significantly enhanced resistance to thermal aggregation, with the least stable conjugate resisting aggregation by approximately 4 days, relative to 2 days with native human insulin, and the most stable conjugates resisting aggregation by approximately 10 days. These results are significant

because enhancements were observed without clinical formulation with zinc or any other excipient used to augment the native protein's stability.

To assess the sugar-responsive nature of the denaturation mechanism, and as a result the possibility to gain insight into the conjugate's potential for sugar-mediated receptor binding, two sugars were incorporated into the chemical denaturation study for Conjugate 2: glucose and sorbitol. When incorporating hyperglycemic concentrations of glucose (500 mg/dL) into the denaturation assay, no qualitative or quantitative effects were observed with respect to the stability profile, suggesting no dynamic interaction or competition of the dynamic tether with the sugar glucose. Next, sorbitol was incorporated into the chemical denaturation study to better probe the dynamic system, due to the structural similarities between sorbitol and the synthesized polyol sugar analogues chemically conjugated onto the insulin protein. Interestingly, in the presence of the sorbitol sugar, a significant shift in the stability profile of Conjugate 2 was observed and analyzed to be statistically significant when compared to the stability profile of Conjugate 2 in the absence of sorbitol. Even more remarkably, as a result of the sorbitol sugar, the stability curve of Conjugate 2 is shown to be reverted back towards the native insulin stability, suggesting that the observed stability enhancement is indeed reversible via simple introduction of the sugar. This result is significant because it further supports and demonstrates the potential of the conjugate to dynamically tether itself in the absence of the sugar, and therefore exhibit enhanced stability, but also reversibly untether itself in the presence of the sugar and revert to the native insulin protein stability properties. This property will be an important consideration when further designing the next generation of intelligent insulins capable of sugar-mediated receptor binding interactions. An attempt

was made to visualize and model the dynamic interaction via crystallization of Conjugate 3 followed by x-ray diffraction and mathematical modeling of the resulting structure, but the electron density was deemed too sparse to gain any insight.

Lastly, an *in vitro* potency screen of all conjugates followed by an *in vivo* efficacy study of select conjugates were conducted to measure biological functionality. From the *in vitro* screen, there was some evidence of receptor-binding potency and activation under hyperglycemic conditions of glucose. The candidates that demonstrated the highest retention of potency under these conditions were conjugates possessing the WPBA small molecule, irrespective of polyol sugar analogue. It is envisioned that the positive charge afforded by the WPBA under physiological conditions compensates for the positive charge lost from the primary amine present on the insulin protein needed for modification. These results demonstrate the potential for retained biological functionality with respect to the receptor binding interactions. From the *in vitro* screen, a select number of insulin conjugates were chosen to assess *in vivo* efficacy in a Type 1 diabetic moues model, including the lead candidate, Conjugate 4, and two conjugates that exhibited low potency retention, Conjugates 9 and 10. Overall, comparison of the area-under-the-curve of the glucose-correcting profiles of all conjugates revealed no statistical differences in biological efficacy, suggesting that all conjugates have glucose-correcting potential in the *in vivo* diabetic environment.

In conclusion, all the observations demonstrated that the novel class of dynamically-tethered insulin protein conjugates possess the potential to provide an innovative framework for further development of an insulin-based therapy capable of enhanced thermodynamic stability, both chemically and thermally, as well as the potential for sugar-

responsive receptor binding interactions and potency. It is envisioned that the demonstrated strategy will be further developed towards the generation of a clinically viable and efficacious sugar-responsive insulin for enhanced diabetes management.

3.7 *Materials and Methods*

Materials. All commercially available reagents and lab supplies were purchased from Sigma Aldrich unless otherwise specified. 1-Hydroxy-1,3-dihydro-2,1-benzoxaborole-6-carboxylic acid (OHPHA, Catalog # 102303) and 4-Carboxy-3-fluorophenylboronic acid (FPBA, Catalog # 035568) were purchased from Matrix Scientific. 2-(Dimethylaminomethyl)-4-carboxyphenylboronic acid pinacol ester (WPBA, Catalog # PN-4078) was purchased from Combi-Blocks. Recombinant human insulin was purchased from Life Technologies Corporation. For purification and characterization of the sugar analogues and control sugar analogue, normal and reverse phase chromatography was performed using a CombiFlash Rf 200 automated system from TeledyneISCO (Lincoln, NE, USA). Additionally, NMR spectra were recorded on a Varian FT 500 MHz NMR instrument.

Synthesis of 4-(2,3,4,5,6-Pentahydroxyhexanamido)butanoic acid (Sugar Analogue S1). Gluconic acid-α-D-lactone (0.75 g, 4.2 mmol) was dissolved in MeOH (20 mL). To this was added 4-Aminobutanoic acid (0.43 mg, 4.2 mmol) and the reaction was held at reflux for 18 h. The reaction mixture was then cooled to RT and the solvent was removed. The crude product was purified by reverse phase prep HPLC eluting a gradient of 1-100% acetonitrile in water (both contain 0.1% formic acid) to obtain the purified product in 32% yield (0.38 g, 1.3 mmol). ^{1}H NMR (500 MHz, DMSO-d_6): δ 7.70 (t, J = 6.0 Hz, 1H), 3.97

(d, J = 3.5 Hz, 1H), 3.89 (s, 1H), 3.56 (dd, J_1 = 11.5 Hz, J_2 = 3.0 Hz, 1H), 3.45 (m, 2H), 3.36 (dd, J_1 = 11.0 Hz, J_2 = 5.0 Hz, 1H), 3.09 (q, J = 6.5 Hz, 2H), 2.19 (t, J = 7.5 Hz, 2H), 1.63 (quint, J = 7.5 Hz, 2H).

Synthesis of 6-(2,3,4,5,6-Pentahydroxyhexanamido)hexanoic acid (Sugar Analogue S2). Gluconic acid-α-D-lactone (0.50 g, 2.8 mmol) was dissolved in MeOH (30 mL). To this was added 6-Aminohexanoic acid (0.37 mg, 2.8 mmol) and the reaction was held at reflux for 18 h. The reaction mixture was then cooled to RT and the solvent was removed via rotarty evaporation. The crude product was purified by reverse phase prep HPLC eluting a gradient of 1-100% acetonitrile in water (both contain 0.1% formic acid) to obtain the purified product in 26% yield (0.22 g, 0.7 mmol). ^{1}H NMR (500 MHz, DMSO-d_6): δ 7.62 (t, J = 6.0 Hz, 1H), 5.36 (brs, 1H), 4.45 (brs, 4H), 3.96 (d, J = 3.5 Hz, 1H), 3.88 (s, 1H), 3.56 (dd, J_1 = 11.0 Hz, J_2 = 3.0 Hz, 1H), 3.46 (m, 2H), 3.35 (m, 2H), 3.05 (m, 2H), 2.18 (t, J = 7.0 Hz, 2H), 1.47 (quint, J = 7.5 Hz, 2H), 1.40 (quint, J = 7.5 Hz, 2H), 1.23 (m, 2 H).

Synthesis of 12-(2,3,4,5,6-Pentahydroxyhexanamido)dodecanoic acid (Sugar Analogue S3). Gluconic acid-α-D-lactone (0.50 g, 2.8 mmol) was dissolved in MeOH (30 mL). To this was added 12-Aminododecanoic acid (0.60 mg, 2.8 mmol), followed by the slow addition of Et_3N (2.0 mL, 14.3 mmol) and the reaction was held at reflux for 18 h. The reaction mixture was then cooled to RT and the solvent was removed via rotarty evaporation. The resulting residue was dissolved in EtOAc (20 mL) and a precipitate formed. The resulting solid was filtered rinsing with copious amounts of EtOAc and MeOH (10 mL) to afford the pure product in 70% yield (0.78 g, 2.0 mmol). ^{1}H NMR (500 MHz, DMSO-d_6): δ 7.60 (t, J = 6.0 Hz, 1H), 3.96 (d, J = 4.0 Hz, 1H), 3.88 (s, 1H), 3.56 (dd, J_1

= 11.5 Hz, J_2 = 3.0 Hz, 1H), 3.45 (m, 2H), 3.35 (dd, J_1 = 10.5 Hz, J_2 = 5.5 Hz, 1H), 3.05 (m, 2H), 2.16 (t, J = 7.0 Hz, 2H), 1.46 (quint, J = 6.0 Hz, 2H), 1.39 (quint, J = 6.0 Hz, 2H), 1.23 (m, 14 H).

Synthesis of 6-Hexanamidohexanoic acid (Control Sugar Analogue). 6-Aminohexanoic acid (0.20 g, 1.5 mmol) was dissolved partially in MeOH (15 mL). To this was added Et_3N (0.64 mL, 4.5 mmol) and the mixture was cooled to 0 °C. Hexanoyl chloride (0.28 mL, 2.0 mmol) was slowly added over the course of 1 h. The reaction mixture was warmed to RT and the reaction was allowed to occur for 18 h. The solvent was then removed and the crude product was suspended in water (30 mL) and adjusted to pH 1 with 1 M HCl. The mixture was then extracted with EtOAc (3 x 50 mL). The organics were collected, dried over $MgSO_4$, filtered and evaporated to afford the pure product (0.34 g, 1.5 mmol) in >99% yield. ^{1}H NMR (500 MHz, DMSO-d_6): δ 6.55 (t, J = 5.5 Hz, 1H), 3.14 (q, J = 6.5 Hz, 2H), 2.25 (t, J = 7.5 Hz, 2H), 2.11 (t, J = 7.5 Hz, 2H), 1.54 (m, 4H), 1.44 (quint, J = 7.0 Hz, 2H), 2.24 (m, 6H), 0.80 (t, J = 7.0 Hz, 3H).

Synthesis of Insulin Conjugate Library. One day prior to performing the insulin conjugation reaction, the small molecules were activated overnight. Briefly, to create conjugates C1-C12, a 5X molar excess of the polyol sugar analogue small molecule (86.1 µmol) was activated with N,N′-dicyclohexylcarbodiimide (86.1 µmol) and N-hydroxysuccinimide (86.1 µmol) by combining all components into the same container and dissolving in DMSO (1 mL). The resulting mixture was allowed to stir at room temperature overnight. In parallel, a 10X molar excess of the phenylboronic acid small molecule (172 µmol) was activated with N,N′-dicyclohexylcarbodiimide (172 µmol) and N-hydroxysuccinimide (172 µmol) by combining all components into the same container

and dissolving in DMSO (1 mL). The resulting mixture was allowed to stir at room temperature overnight. To create conjugates C25-C36, the same procedure was used to activate the small molecules, but instead the phenylboronic acid small molecule was activated at a 5X molar excess and the polyol sugar analogue small molecule was activated at a 10X molar excess.

Immediately before initiating the reaction, recombinant human insulin (100 mg, 17.22 μmol) was dissolved in a buffer containing 0.12 M $NaHCO_3$ and 0.12 M Na_2CO_3 (3 mL) at pH 11. For synthesizing conjugates C1-C12, the reaction began by first adding the activated polyol sugar analogue small molecule to the gently stirred insulin solution in three increments (333 μL at 0 min, 20 min, and 40 min). At 60 min, the activated phenylboronic acid small molecule was then added to the gently stirred insulin solution in three increments (333 μL at 60 min, 80 min, and 100 min). After 120 min, 1 M CH_3NH_2 (1 mL) was added to the reaction mixture. The same procedure is followed for synthesizing C25-C36, except the order of adding the small molecules is reversed: first add the activated phenylboronic acid small molecule between time 0-40 min followed by addition of the activated polyol sugar analogue small molecule between time 60-100 min, after which 1 M CH_3NH_2 (1 mL) is added at time 120 min. After completion of all reaction steps for each conjugate, the product was purified via reversed phase preparative HPLC using a 218TP1022 C18 column (2.2 cm ID × 25 cm L, 10 μm; Vydac), with a mobile phase gradient from 2% to 65% (vol/vol) of solvent B (0.043% trifluoroacetic acid/acetonitrile, 20/80) with solvent A (trifluoracetic acid/water, 0.05/99.95). Fractions were collected and lyophilized to provide a white product. The product was characterized by deconvolution electrospray ionization using a QSTAR hybrid Q-TOF, performed at the Koch Institute

Swanson Biotechnology Center Biopolymers and Proteomics core. Masses obtained were as follows: C1, expected 6246.85, actual 6210.2; C2, expected 6264.84, actual 6228.3; C3, expected 6258.86, actual 6240.3; C4, expected 6303.95, actual 6267.7; C5, expected 6218.80, actual 6182.2; C6, expected 6236.79, actual 6200.2; C7, expected 6230.81, actual 6211.8; C8, expected 6275.89, actual 6239.7; C9, expected 6331.02, actual 6294.2; C10, expected 6349.01, actual 6312.2; C11, expected 6343.03, actual 6324.3; C12, expected 6388.11, actual 6351.2; C25, expected 6246.85, actual 6210.5; C26, expected 6264.84, actual 6228.3; C27, expected 6258.86, actual 6240.7; C28, expected 6303.95, actual 6267.9; C29, expected 6218.80, actual 6182.4; C30, expected 6236.79, actual 6200.5; C31, expected 6230.81, actual 6212.5; C32, expected 6275.89, actual 6324.8; C33, expected 6331.02, actual *n.d.*; C34, expected 6349.01, actual *n.d.*; C35, expected 6343.03, actual *n.d.*; C36, expected 6388.11, actual 6351.98; n.d. denotes *not determined* due to limitations in yield. It is noted that these masses are consistent with MS for PBA-modified peptides, where the mono- (i.e., -18) or double- (i.e., -36) dehydrated masses are observed due to gas phase anhydro formation of the boronic acid.[75]

To confirm site-specific, di-conjugated modification on the ε-amine of the B29 lysine residue and the N-terminal primary amine of the A1 glycine, purified insulin conjugates were reduced using DTT, followed by alkylation of free thiols and subsequent protein digestion with trypsin. Proteomics analysis was performed using a QSTAR hybrid Q-TOF with tandem MS/MS analysis, with a search conducted for masses of the digested products with free amines at the N-terminal A1Gly, N-terminal B1Phe, and the ε-amine B29Lys positions, as well as for the small molecule-conjugated masses. All purification

and characterization were performed at the Koch Institute Swanson Biotechnology Center Biopolymers and Proteomics core.

Circular Dichroism. To assess whether the protein modifications resulted in any alteration of insulin secondary structure, near-UV circular dichroism (CD) spectroscopy was performed with a Jasco J-1500 high-performance CD spectrometer over a wavelength range of 205–250 nm using a transparent 0.1-cm path length quartz cuvette. Quantifying relative protein stability of the insulin conjugates was also performed with the same Jasco J-1500 high-performance CD spectrometer instrument following a denaturation study involving titration of each insulin sample with the chemical denaturant guanidine hydrochloride (GHCl). For measuring secondary structure, each insulin sample was dissolved at a concentration of 4 mg/mL in a buffer containing 0.12 M $NaHCO_3$ and 0.12 M Na_2CO_3 (pH 9.4). Each sample was then titrated to a final pH of 7.4 using minimal HCl. Determination of relative protein stability was performed following a series of GHCl titrations with each respective insulin sample, at intervals of denaturant concentration spanning a range from 0.0 M GHCl to 7.5 M GHCl. For the stability study, each insulin sample was dissolved at a concentration of 4 mg/mL in a buffer containing 0.12 M $NaHCO_3$ and 0.12 M Na_2CO_3 (pH 9.4). Each sample was diluted to a final concentration of 0.25 mg/mL using varying mixtures of DI water and 8.0M GHCl solutions to ensure the full range of denaturant concentration necessary for the study. All measurements were taken at pH 7.4. Alterations in secondary structure were observed at wavelength 222 nm at each GHCl concentration. For glucose and sorbitol incorporated denaturation studies, appropriate amounts of each sugar were added to both the DI water and 8.0 M GHCl solutions in order to ensure a consistent final concentration of 500 mg/dL glucose or 5,000

mg/dL sorbitol. Thermodynamic stabilities were inferred from fitting normalized CD-detected protein denaturation to a nonlinear least squares two-state model, as described previously,[17] and statistical significance determined by one-way ANOVA for comparing the fit statistics of ΔG_u for all samples relative to the native protein. All analysis was performed using GraphPad Prism 6.0.

Thermal Aggregation Assay. Recombinant human insulin and insulin conjugates were dissolved at a concentration of 344 μM in a buffer containing 0.12 M $NaHCO_3$ and 0.12 M Na_2CO_3. Insulins were then diluted to a final concentration of 172 μM in 1X PBS and final pH of 7.4. Samples were plated at 150 μL per well (n = 4/group) in a clear 96- well plate (Thermo Scientific Nunc) and sealed with optically clear and thermally stable seal (VWR). The plate was immediately placed into an Infinite M1000 plate reader (Tecan Group) and shaken continuously at 37 °C. Absorbance readings at 540 nm were collected every 6 min for 100 h, and absorbance values were subsequently converted to transmittance. The aggregation of insulin leads to light scattering, which results in reduction of sample transmittance. The time for aggregation (t_A) was defined as a >10% reduction in transmittance from the initial transmittance. Following the 100-h kinetic study, the plate was maintained under continuous agitation at 37 °C, and absorbance at 540 nm was monitored daily to approximate t_A for the insulin bioconjugates.

In Vitro Insulin Receptor Activation. C2C12 cells were purchased from the American Type Culture Collection (ATCC) and confirmed free of mycoplasma contamination before use. Cells were cultured in Dulbecco's modified Eagle medium(DMEM) containing L-glutamine, 4.5 g/L D-glucose, and 110 mg/L sodium pyruvate, and supplemented with 10% FBS and 1% penicillin–streptomycin. Incubations occurred in a 5% CO_2/water-

saturated incubator at 37 °C. Cells were seeded in 96-well plates at a density of 5,000 cells per well. Twenty-four hours after plating, the cells were washed three times with 200 µL of DMEM containing L-glutamine, 4.5 g/L glucose, and 110 mg/L sodium pyruvate, and starved for at least 4 h at 37 °C in the same serum-free conditions. After 4 h, the media was removed, and cells were stimulated with 100 µL of insulin samples of various concentrations for 30 min at 37 °C. After 30 min, cells were washed three times with 100 µL of cold Tris-buffered saline (1X), followed by lysing the cells for 10 min with 100 µL of cold Lysis Buffer (Perkin-Elmer). Levels of phosphorylated AKT 1/2/3 (Ser473) and Total AKT 1 were determined from cell lysates using the AlphaLISA SureFire ULTRA kits (Perkin-Elmer) according to the manufacturer's instructions. Intra-well normalized data of phosphorylated AKT 1/2/3 (Ser473) and Total AKT 1 were analyzed using GraphPad Prism 6.0, with dose–response curves fitted to a variable slope (four-parameter) stimulation model to determine the EC_{50} of each insulin sample, and statistical significance determined by an extra sum-of-squares F test for comparing the fit statistics of LogEC50 for all samples relative to the native protein.

Diabetic mouse model. Male C57BL/6J mice, age 8 wk, were purchased from Jackson Laboratory. After acclimation, mice were fasted overnight before intraperitoneal injection of 150 mg/kg STZ. Preparation of STZ for injection involved dissolving the chemical at a concentration of 15 mg/mL in sodium citrate buffer (114 mM, pH 4.5) immediately before injection. Food was withheld for 2 h post-injection, after which mice were allowed to eat and drink ad libitum. Glucose levels were monitored by peripheral tail vein bleeds using a portable glucose meter (Clarity Plus, Clarity Diagnostics) daily until unfasted glucose levels were >400 mg/dL. For the *in vivo* diabetic study, STZ-induced diabetic mice were

fasted overnight before performing studies. Mice were bled at the beginning of the study, and any mouse with a fasting blood glucose level <300 mg/dL was triaged from the study. Mice were then randomized and injected subcutaneously with native insulin or insulin conjugate at a dose of 5 IU/kg (1 IU = 5.97 nmol). Blood glucose readings were collected every 30 min using a handheld glucose meter for a total of 3 hours. Responsiveness was quantified by measuring the area-under-the-curve with a baseline at the point of initial injection and integrating across a 3-h window following administration. All statistical comparisons were performed using two-tailed, unpaired t-tests (GraphPad Prism 6.0).

3.8 *Acknowledgements*

This work was supported by a grant from the Leona M. and Harry B. Helmsley Charitable Trust Foundation (Grant No. 2017PG-T1D027). We acknowledge technical support from the Nuclear Magnetic Resonance core facility in the Department of Chemistry, as well as the Structural Biology Core Facility and the Koch Institute Swanson Biotechnology Center, with specific gratitude for use of the Biopolymers & Proteomics Core Facility, all at the Massachusetts Institute of Technology.

Chapter 4: Site-specific Conjugation of Zwitterionic Polymers to Insulin for the Development of Ultra Long-Acting Insulin Therapies

The work presented in this chapter is in preparation for publication:

V. Yesilyurta*, A. B. Cortinas*, L. S. Thapa, S. D. Truong, R. S. Langer, D. G. Anderson, Site-specific conjugation of zwitterionic polymers to insulin improves the bioactivity in STZ-diabetic mice. *In preparation*.

4.1 *Introduction*

Diabetes mellitus is a global epidemic that affects more than 400 million individuals worldwide, with that number expected to increase by almost 50% by 2045. [4] For insulin-dependent diabetes, the predominant standard-of-care requires patients to carefully monitor their sugar levels by sampling their own blood multiple times per day, followed by performing multiple self-administered insulin injections, until glycemic goals are achieved. Despite following such a strictly regimented insulin therapy, which can be as unique as the individual itself, a majority of patients still suffer from complications that arise from poor adherence to therapy or from inadequate glycemic control.[133] Although several advances have been made throughout the decades to engineer basal insulins, there remains a pressing need for enhanced basal therapies that are safer, more efficacious, and require far less frequent injections.[91,134]

Like many other therapeutic proteins or peptides, insulin suffers from various issues ranging from short circulation half-life, poor stability, and rare cases of immunogenicity.[135] Extensive effort and resources have been devoted to the development of new insulin analogues with tunable pharmacokinetics (PK), which have led to the commercialization of multiple insulin variants with fast-acting and long-acting activity for personalized therapy. Engineered insulin analogs with an extended time-action profile have been particularly useful as a once- or twice-daily injection formulation that attempts to mimic the basal secretion profile of the healthy pancreas. For example, insulin detemir (Novo Nordisk), a des-B30 myristic acid acylated insulin conjugate, is a basal insulin that binds to hydrophobic regions of circulating serum proteins such as albumin, enabling the enhancement of circulatory half-life to approximately 6 hours.[136,137] Insulin glargine

(Sanofi-Aventis), an isoelectric-point-shifted insulin analogue engineered to precipitate at the subcutaneous injection site for delayed solubilization and absorption, has a half-life of approximately 13 hours.[138] Most recently, insulin degludec (Novo Nordisk) was designed to facilitate ligand-mediated multi-hexamer assembly after subcutaneous injection for enhanced protraction of disassembly and absorption, allowing for circulation half-life of more than 24 hours.[109]

Alternative to protein engineering, bioconjugation of water soluble polymers to the insulin protein has served as a general approach to achieving augmented protraction mechanisms. These modifications are typically intended to enhance pharmacokinetic (PK) profiles and improve shelf-life stability of insulin, a protein highly susceptible to aggregation if not subjected to proper storage conditions.[139–142] Dextran, chitosan, trehalose glycopolymer, and polyethylene glycol (PEG) are a few examples of polymers typically conjugated to insulin to modulate PK profiles.[143–145] Among all polymers, PEGylation is the most widely used polymer conjugation method to enhance the circulation half-life, stability, and solubility of protein therapeutics.[146,147] Although numerous PEGylated therapeutic drugs have been approved by the U.S. Food and Drug Administration, with numerous others in development, there are currently no insulin polymer conjugates approved for clinical use. Perhaps the most recent candidate to almost achieve that designation was insulin peglispro (Eli Lilly), an ultra long-acting insulin derivative formed from the conjugation of a 20 kDa molecular weight linear PEG polymer to the B28Lys ε-amine of insulin lispro.[148] Although this derivative showed substantial promise in demonstrating hepato-preferential action and single-dosing steady state PK profiles up to 7-10 days, with an apparent half-life of 2-3 days, Eli Lilly terminated its

development in 2015 due to unfavorable lipid and liver function tests from a FDA Phase III clinical trial.[149–151]

Although PEGylation still remains one of the primary methods utilized to achieve protein stabilization and enhanced blood circulation half-life, there are limitations. PEG polymers exhibit temperature sensitive solution behavior, causing the precipitation of polymer at its lower critical solution temperature.[152,153] And despite PEG being a water-soluble polymer, it also possesses amphiphilic characteristics due to its solubility in nonpolar organic solvents such as toluene. Moreover, several recent studies have shown that PEG conjugates may induce immunogenicity and antibody responses, which could potentially accelerate blood clearance of PEGylated protein therapeutics.[147,154] These drawbacks have led to the development of alternative biocompatible polymers for protein conjugation, with the prospect of possessing less potential for immunogenicity.[155] To this end, zwitterionic materials have emerged as a new class of non-fouling biomaterials that are super hydrophilic and prevent non-specific protein adsorption. Recently, it has been shown that zwitterionic polymer coated nanoparticles and conjugated proteins have enhanced blood circulation half-life and reduced immunogenicity compared to PEGylated analogs.[154,156–160]

Here, we report the systematic design, synthesis, *in vitro* assessment, and *in vivo* functional evaluation of a small library of insulin-zwitterionic polymer conjugates, ultimately aimed towards the generation of an ultra long-acting insulin therapy. Three zwitterionic polymers were synthesized utilizing reversible addition-fragmentation chain transfer (RAFT) polymerization for the ultimate designation of site-specific, bio-orthogonal conjugation to insulin. The resulting library is demonstrated to afford equivalent biological

potency relative to native human insulin, augmented thermal and chemical stability capable of withstanding aggregation for over 80 days, as well as ultra long-acting basal insulin potential, capable of enhanced protraction and *in vivo* activity comparable to a pegylated insulin inspired by ultra long-acting insulin peglispro. Overall, it is envisioned that zwitterionic functionalization of insulin could provide a potentially improved therapeutic strategy for the development of ultra long-acting insulin therapeutics for diabetes management.

4.2 *Synthesis of Insulin Zwitterionic Polymer Conjugates*

The desired insulin zwitterionic polymer conjugates were synthesized in two steps according to methods outlined in Figure 4. 1 and Figure A. 8. Using N-hydroxysuccinimide (NHS) coupling under basic conditions, a dibenzocyclooctyne (DBCO) group bearing a short oligoethyleneglycol linker was reacted preferentially to the ε-amine of the B29 lysine residue (Figure 4. 1a), as previously demonstrated, to preserve functionality and biological activity of the resulting conjugate.[75–77,146,161,162] The resulting insulin-DBCO conjugate (Ins-DBCO) was purified using preparative HPLC to afford Ins-DBCO specifically modified at the B29Lys residue. Characterization was performed using whole-protein electrospray ionization (ESI) as well as protein fragment tandem MS/MS ESI analysis to confirm both the mono- and site-specific conjugation of the DBCO small molecule to the insulin protein (Figure A. 9). Next, zwitterionic polymers based on carboxybetaine (CB), sulfobetaine (SB), and phosphorylcholine (PC) functionalities were prepared through RAFT polymerization using an azido functionalized chain transfer agent (CTA). Performing aqueous RAFT with zwitterionic methacrylate monomers enabled us

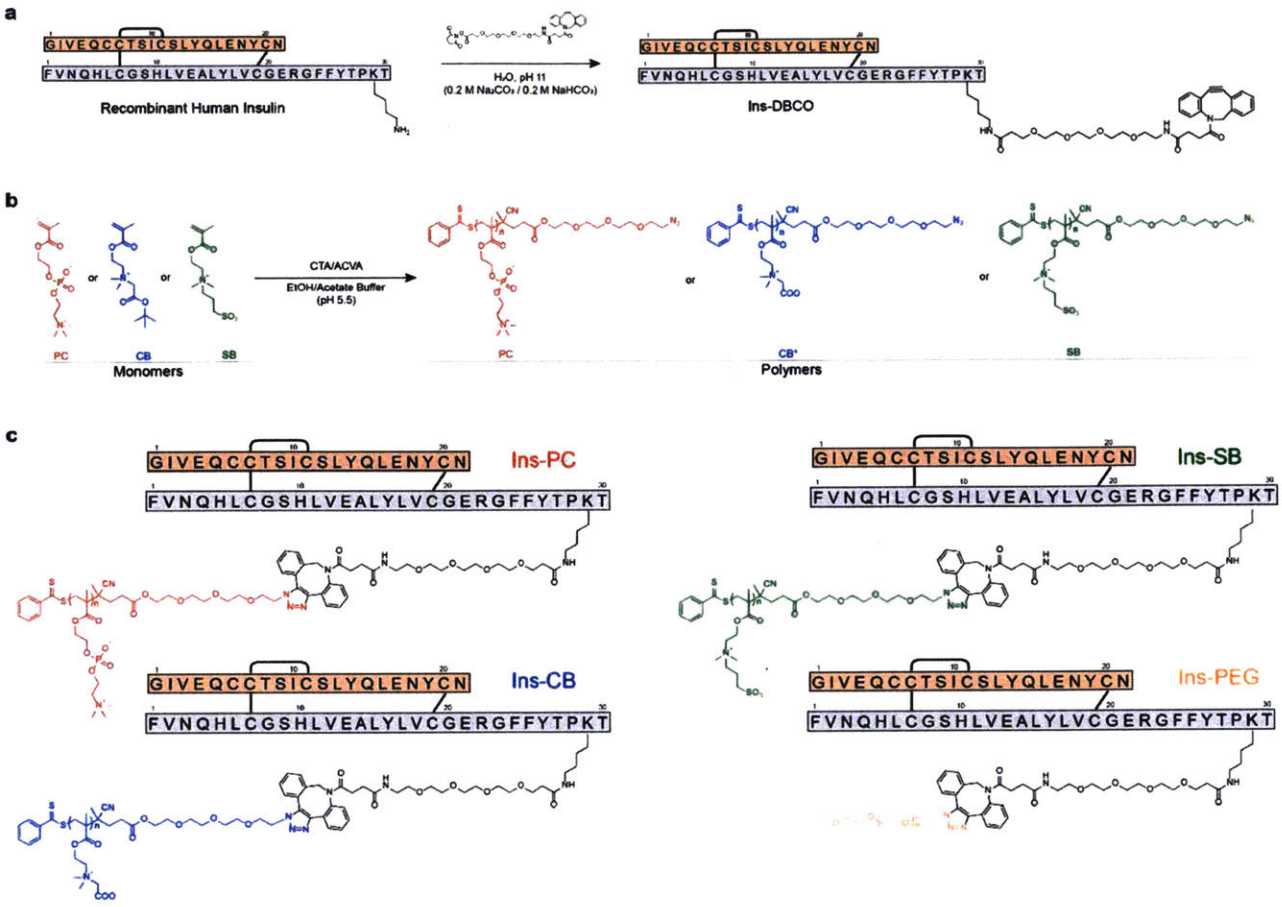

Figure 4. 1 Strategy for synthesizing insulin-zwitterionic conjugates. (a) Reaction of the DBCO small molecule to the B29 lysine residue ε-amine for site-preferential conjugation and synthesis of the Ins-DBCO core molecule. (b) Generalized scheme for preparation of zwitterionic polymers utilizing RAFT polymerization, to be used for Ins-DBCO orthogonal conjugation. *Note: Final CB polymer was obtained after the removal of tert-butyl ester with trifluoroacetic acid. (c) Structures of the three insulin-zwitterionic conjugates used in this work along with the positive control, Ins-PEG, a pegylated insulin inspired by the clinically tested ultra long-acting insulin peglispro.

to achieve quantitative conversion of monomers yielding the target molecular weights of 10 kDa for all zwitterionic homopolymers while maintaining the polydispersity (PDI) at a reasonably low value [Mn(^{1}H NMR): 10 kDA; PDI (SEC): 1.1-1.2; Figure A. 10]. Polymerization reactions (Figure 4. 1b) took place in acetate buffer, pH 5.5, to prevent the hydrolysis of dithioesters on the RAFT CTA.[163] The purified zwitterionic polymers were subsequently conjugated to Ins-DBCO by simple mixing via a bio-orthogonal copper-free

click reaction scheme to afford three insulin-zwitterionic polymer conjugates (Figure 4. 1c): Ins-PC, Ins-CB, and Ins-SB. Similarly, the Ins-PEG conjugate was also prepared through the reaction of Ins-DBCO with commercially available, linear mPEG-azide (Mn: 10 kDa). The described reaction strategy allowed for the site-specific functionalization of exactly one polymer chain per insulin molecule via the copper-free click chemistry scheme. The resulting conjugations were confirmed qualitatively by native polyacrylamide gel electrophoresis (PAGE) (Figure A. 11), and the insulin-polymer conjugates were used directly, with no further purification performed on the reaction mixture to remove unreacted excess polymers.

4.3 *Functional Characterization In Vitro*

To assess whether the insulin modification strategy ultimately altered the secondary structure of all resulting insulin polymer conjugates, a series of in vitro assessment assays were utilized for both qualitative and quantitative functional validation. First, near-UV circular dichroism (CD) spectroscopy was utilized to determine post-modification retention of alpha-helical secondary structure (Figure 4. 2a). Overall, all synthesized conjugates demonstrated no detrimental evidence that the synthesis strategy had any effect on the alpha-helical character of native insulin. Additionally, an in vitro cell-based insulin receptor activation assay was performed to ensure that all insulin-polymer conjugates maintained full receptor binding and activation potential relative to the native protein (Figure 4. 2b and c). The dose-response studies indicate no statistically significant changes in downstream AKT phosphorylation events, and ultimately confirm full retention of *in vitro* potency.

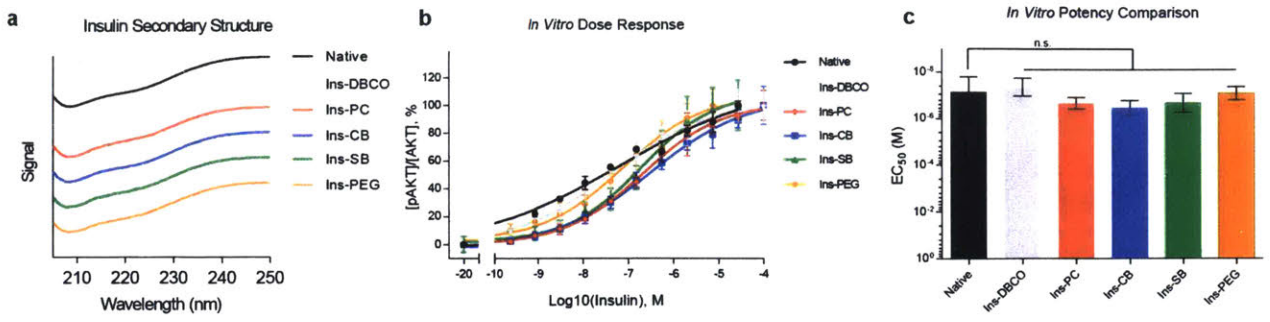

Figure 4. 2 *In vitro* functional characterization of synthesized insulin polymer conjugates. (a) Near-UV circular dichroism comparison demonstrated no qualitative loss of alpha-helical secondary structure relative to the native protein, observed by retention of the characteristic local minima detected at 208 nm and 222 nm.[164] (b) *In vitro* cell stimulation assay for all insulin samples, measuring the ratio of phosphorylated AKT (Ser473) relative to total AKT as a function of insulin concentration. Error bars represent standard deviation. (c) Determination of differences in potency by comparing dose response derived EC_{50} values for all insulin polymer conjugates relative to the native protein. Results verified no loss of biological activity. Error bars represent 95% confidence intervals.

4.4 *In Vivo Studies of Insulin Polymer Conjugates*

To assess the glucose-correcting efficacy of the prepared insulin polymer conjugates under hyperglycemic conditions, an STZ-induced Type 1 diabetic mouse model was used.[106] All polymer-insulin conjugates reduced average blood glucose levels to normoglycemic levels, <200 mg/dL, following a single subcutaneous injection of 5 IU/kg native human insulin, or molar equivalent of insulin polymeric conjugates. At three hours post-subcutaneous administration, an intraperitoneal glucose tolerance test (IPGTT) was performed. Following the IPGTT, all insulin-zwitterionic polymer conjugates, as well as the Ins-PEG control, demonstrated recovery of blood glucose concentrations to normoglycemia (< 200 mg/dL). However, all other insulin controls (Native, Ins-DBCO, and Ins-PEG 2k) did not demonstrate glucose-correcting effects and resulted in blood glucose concentrations rising above 400 mg/dL (Figure 4. 3a). Of note, despite the linear PEG polymer of Ins-PEG having the same molecular weight as all synthesized zwitterionic

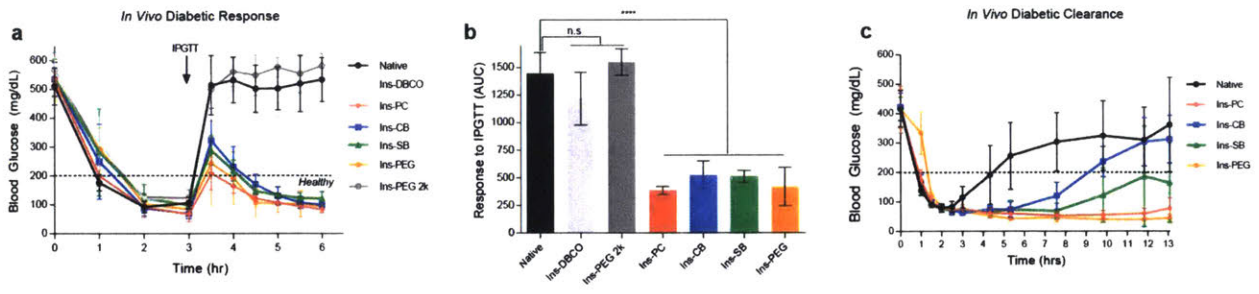

Figure 4. 3 *In vivo* diabetic functional characterization of synthesized insulin polymer conjugates. (a) Glucose-correcting efficacy and recovery study of insulin samples injected at 5 IU/kg (29.9 nmol/kg) in an STZ-induced diabetic mouse model, with the IPGTT administered at 3 hours post insulin administration. After IPGTT challenge, Ins-PC, Ins-CB, Ins-SB, and Ins-PEG demonstrated normoglycemic recovery. (b) Quantification of *in vivo* diabetic response study based on measuring the area-under-the-curve from 3 to 6 hours, with the baseline set at the 3-hour blood glucose value. ANOVA with Turkey multiple comparisons post hoc test was performed for measuring statistical significance, **** $P < 0.0001$. (c) Clearance study, for all samples demonstrating normoglycemic recovery from previous study, over thirteen hours, with Ins-PC and Ins-PEG demonstrating highest potential for long-acting efficacy. Error bars for all graphs represent standard deviation.

polymers, the degree of polymerization (DP), proportional to the hydrodynamic radius, is ~ 7-fold higher than that of CB, SB, and PC polymers.[165] Therefore, to better account for the potential size effects of these metrics, Ins-PEG 2k, which has a DP value equivalent to all zwitterionic polymers, was incorporated into the diabetic response study. To quantify the IPGTT response of all insulin samples, the area-under-the-curve (AUC) was calculated for each group (Figure 4. 3b). As corroborated in the blood glucose profiles, all insulin-zwitterionic polymer conjugates and Ins-PEG demonstrate significantly higher sequestration, and therefore longer-acting activity, relative to Native, Ins-DBCO, and Ins-PEG 2k, as shown by the AUC comparison ($P < 0.0001$). To further probe the long-acting potential of insulin samples demonstrating significant recovery from the IPGTT study, insulin clearance was investigated. Following an initial subcutaneous injection of 5 IU/kg native insulin, or the molar equivalent of Ins-PC, Ins-CB, Ins-SB, and Ins-PEG, blood glucose concentrations were measured over a thirteen-hour window. Based on the results

of this study, Native and Ins-CB failed to correct average blood glucose concentrations to normoglycemic levels after 4 hours and 10 hours, respectively. Ins-SB maintained a normoglycemic state throughout the study but observed fluctuating blood glucose levels after eight hours. Only Ins-PC and Ins-PEG demonstrated a consistent normoglycemic effect with little to no sign of potential failure throughout the duration of the study, with no statistical difference between final average blood glucose concentrations at hour thirteen between the two groups (Figure 4. 3c).

To assess the potential of the insulin-zwitterionic polymer conjugates to induce hypoglycemia, dosing studies were performed on healthy, normoglycemic mice (Figure 4. 4). Doses of 1 IU/kg, 3 IU/kg, and 5 IU/kg of native insulin, or the molar equivalent of insulin polymer conjugates, were chosen to be the therapeutically relevant dose range. The extent by which insulin induced a hypoglycemic response, characterized by a blood glucose concentration below 70 mg/dL, was evaluated for all insulin zwitterionic conjugates, with native insulin chosen to be the negative control and Ins-PEG chosen to be the positive control, based on the *in vivo* diabetic efficacy study. The hypoglycemic response for each insulin was quantified using the hypoglycemia index, a unitless metric measured by the drop from initial blood glucose concentration to the nadir (i.e., the lowest observed value) divided by the initial blood glucose concentration. A variation of this metric is used clinically to help diagnose incidence of hypoglycemia in diabetic patients.[104] For healthy mice dosed at 1 IU/kg, the hypoglycemia index for Ins-SB was equivalent to that of native insulin, whereas Ins-PC, Ins-CB, and Ins-PEG demonstrated statistically higher incidence of hypoglycemia ($P<0.05$). At a dose of 3 IU/kg, Ins-SB maintained a significantly lower level of induced hypoglycemia relative to native insulin ($P<0.001$) and

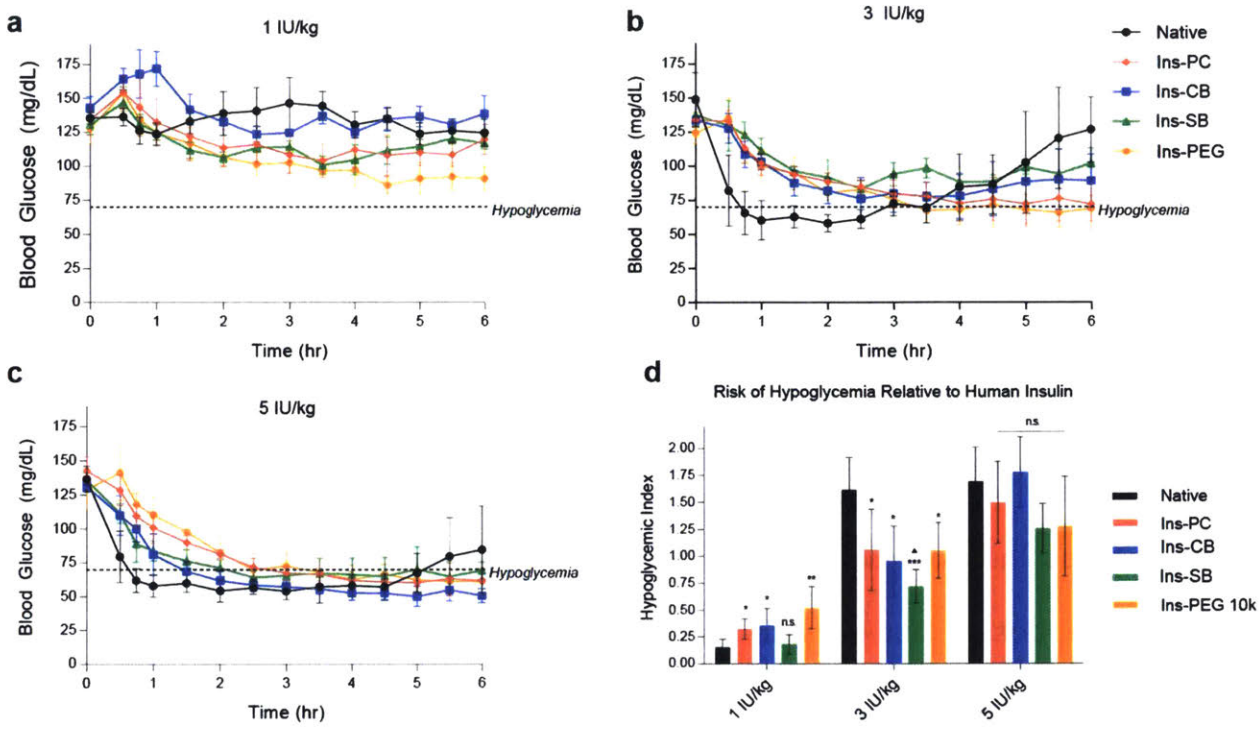

Figure 4. 4 Dose escalation studies in healthy, normoglycemic mice for the evaluation of hypoglycemia risk. All insulins were dosed at (a) 1 IU/kg, (b) 3 IU/kg, and (c) 5 IU/kg, with blood glucose monitoring occurring over a six-hour window and hypoglycemia defined as a drop in blood glucose concentration below 70 mg/dL. (d) Quantification of hypoglycemia index, determined from the difference between the initial and nadir blood glucose values divided by the nadir (i.e., lowest observed concentration). Two-tailed, unpaired t tests were performed for statistical comparison. n.s. $P > 0.05$, * $P < 0.05$, ** $P < 0.01$, and *** $P < 0.001$ refer to comparisons to native insulin at the 3 IU/kg dose; ▲ $P < 0.05$ refers to Ins-SB compared with Ins-PEG. Error bars for all graphs represent standard deviation.

Ins-PEG (*P<0.05)*, as well as a generally safer profile compared to all other insulin zwitterionic conjugates. At the highest dosing concentration, 5 IU/kg, all insulin polymer conjugates demonstrated statistically equivalent hypoglycemia incidence as compared to native insulin. The effect seen at the highest dose demonstrates a potential concentration-dependent plateau in therapeutic index, as seen previously, whereby possible safety effects are overcome by the relatively high concentration of insulin present in the biological system.[77] Altogether, the healthy mice dosing studies reveal Ins-SB to have a similar hypoglycemic effect to native at the lowest dose (1 IU/kg), a lower risk of

hypoglycemia incidence relative to native and Ins-PEG at 3 IU/kg, and all insulin samples having similar hypoglycemic profiles relative to each other at the highest dose (5 IU/kg).

4.5 *Chemical and Thermal Stability*

To determine the potential stabilization effects of the zwitterionic polymer conjugation to the insulin protein, chemical denaturation and thermal aggregation assays were performed at physiological pH and temperature at near-clinically-formulated concentrations. To assess thermodynamic stability, titration of native insulin, Ins-PC, Ins-CB, and Ins-SB with guanidine hydrochloride was performed, with normalized changes in alpha-helical secondary structure measured by circular dichroism at 222 nm, as previously described.[17] Augmentation in thermodynamic stability is observed by the rightward shift in the observed unfolding transition as a function of guanidine concentration for all insulin zwitterionic conjugates relative to native insulin (Figure 4. 5a). Quantitative analysis of the protein denaturation assay utilized a two-state model to extrapolate inferred thermodynamic parameters.[17,166] In contrast to native insulin, direct comparison of the inferred free energy of unfolding (ΔG_u) for all insulin zwitterionic polymer conjugates (Figure 4. 5b) exhibited statistically robust enhancement in stability ($P<0.0001$). Furthermore, comparison of the fitted slope parameter, m, correlated with the extent of exposure of non-polar surfaces upon unfolding, reveals that the observed increase between native insulin and the insulin zwitterionic polymer conjugates is consistent with a greater burial of non-polar surfaces in the native state, denoting a resistance to unfolding and ultimately to denaturation.[17]

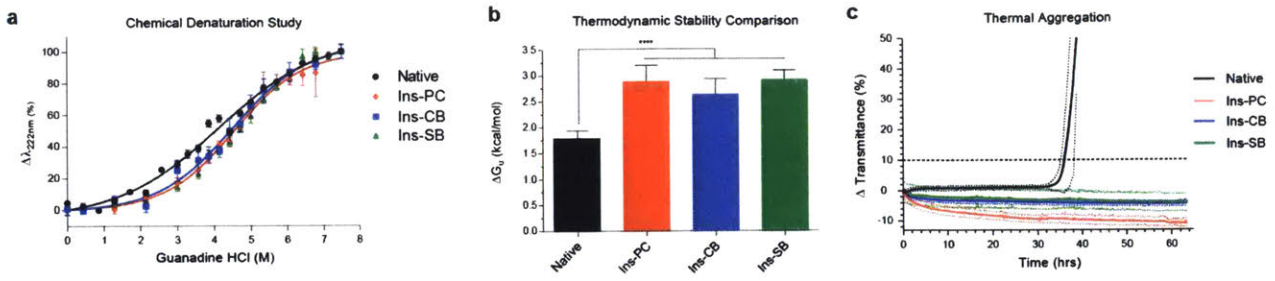

Figure 4. 5 Protein stability evaluation of native insulin and all insulin zwitterionic polymer conjugates. (a) Assessment of secondary structure changes as a function of titration with chemical denaturant guanidine hydrochloride. Observed shift to the right for all insulin zwitterionic polymer conjugates denotes resistance to unfolding transition and therefore an enhancement in thermodynamic stability. Error bars represent standard deviation. (b) Inferred free energy of unfolding (ΔGu) quantified using a two-state model demonstrated statistically robust augmentation in chemical stability ($P<0.0001$) of all insulin zwitterionic polymer conjugates relative to native insulin. Furthermore, increases in the fitted slope parameter, m, denote a greater burial of non-polar surface in the native state, consistent with higher resistance to destabilization and denaturation. Fitted slope parameters for insulin samples are as follows (Mean ± SEM, kcal/mol/M): Native, 0.43 ± 0.02; Ins-PC, 0.64 ± 0.04; Ins-CB, 0.58 ± 0.04; Ins-SB, 0.61 ± 0.02. Error bars in the graph represent 95% confidence intervals. (c) Kinetic aggregation profile of native insulin and insulin zwitterionic polymer conjugates through measurement of changes in solution transmittance at pH 7.4 and 37°C under continuous agitation. Native insulin observed physical aggregation after ~36 hours while all insulin zwitterionic polymer conjugates did not throughout the entire 60-hour kinetic trial. It should be noted that after the kinetic trial, all insulin samples were monitored daily for a period of 80 days, with all insulin zwitterionic polymer conjugates demonstrating no changes in transmittance. Dotted error bars represents standard deviation.

Building upon the observations of enhanced thermodynamic stability, determination of whether these augmentations translate to an increased resistance to thermal aggregation was assessed by using a continuous agitation assay on all insulin zwitterionic polymer conjugates and native insulin.[129] Performed under physiological pH and temperature, continuous agitation was employed to determine the kinetics of insulin aggregation in a solution of 172 μM protein (1 mg/mL native insulin and molar equivalent of all insulin zwitterionic polymer conjugates) with changes in optical transmittance measured at 540 nm in order to detect the formation of aggregates over time. With the aggregation time (t_A) defined as a change in optical transmittance greater than 10% of the initial absorbance value, native insulin aggregated after ~36 hours while all other

insulin zwitterionic polymer conjugates did not exhibit any aggregation throughout the entire 60-hour kinetic study (Figure 4. 5c). After the initial kinetic study, transmittance of the insulin samples was measured once daily until termination of the study after 80 days. No aggregation of any of the insulin zwitterionic polymer conjugates was observed at the 80-day endpoint of the study, enhancing the stability in solution of native insulin from ~36 hours to over 80 days.

4.6 *Discussion and Conclusions*

Long-acting insulins are a critical component of the therapeutic toolbox used by insulin-dependent diabetics, allowing for supplementation or replacement of the stable basal insulin concentrations required throughout the day normally provided by the healthy pancreas. Advances in basal insulin technology has led to the advent of once- or twice-daily long-acting insulin therapies. However, further development of basal insulins towards an ultra long-acting protraction profile could potentially reduce the injection frequency from once- or twice-daily to once- or twice-weekly, thereby dramatically alleviating the burden and potential for regimen noncompliance for insulin-dependent diabetics. This study systematically assesses the effects of zwitterionic functionalization on the insulin protein towards an ultra long-acting insulin therapy, focusing on the *in vitro* potency, *in vivo* efficacy and safety, as well as chemical and thermal stability of the resulting conjugates. After validating the complete retention of secondary structure and receptor activation-based potency for all insulin zwitterionic polymer conjugates, functional evaluation was performed in diabetic and healthy mice. In diabetic mice, an *in vivo* response study revealed the recovery potential of all zwitterionic candidates, Ins-PC,

Ins-CB, and Ins-SB, to be comparable to that of Ins-PEG, a pegylated insulin inspired by the clinically tested ultra long-acting insulin peglispro. And despite having a degree of polymerization ~7-fold lower than Ins-PEG, a parameter that is proportional to hydrodynamic radius and largely responsible for the enhanced protraction effects of insulin peglispro [92,167–169], all insulin zwitterionic polymer conjugates were shown to have a comparable IPGTT response, successfully reducing blood glucose concentrations back to normoglycemic levels as demonstrated by the AUC comparison. Further testing of all insulin zwitterionic polymer conjugates in a clearance-based study revealed Ins-PC to have the most ultra-long acting potential based on its comparable profile to Ins-PEG. All other zwitterionic candidates demonstrated longer protraction profiles relative to native insulin, but either failed to maintain normoglycemia (Ins-CB) or observed blood glucose fluctuations within a normoglycemic range (Ins-SB) over the thirteen-hour study. In healthy mice, the hypoglycemia index for Ins-SB was consistently lower relative to Ins-PC and Ins-CB, whereas Ins-PC and Ins-CB possessed similar risk for hypoglycemia relative to each other and to Ins-PEG. These studies point towards zwitterionic polymer SB possessing the most potential for both long-acting efficacy and reduced risk of hypoglycemia relative to Ins-PEG. Lastly, all zwitterionic polymer functionalities facilitated improved protein stability and inhibited thermal aggregation, an important parameter in the storage and deployment of insulin therapeutics around the world, especially in regions with poor cold-chain infrastructure. Overall, this approach provides meaningful context in that zwitterionic polymers provide a clinical opportunity for therapeutic protein development, and could prove especially beneficial in the pursuit of clinically relevant ultra long-acting insulin therapies.

4.7 *Materials and Methods*

Materials. All commercially available reagents and lab supplies were purchased from Sigma Aldrich, unless otherwise specified. DBCO-PEG4-NHS (Cat# A134-100) and Azide-PEG3-Hydroxyl were purchased from Click Chemistry tools. 2-(Methacryloyloxy)ethyl 2-(Trimethylammonio)ethyl Phosphate (Cat# M2005) was purchased from TCI America. Azido-PEG10k (Cat# PG1-AZ-10k) and Azido-PEG2k (Cat# PG1-AZ-2k) were purchased from Nanocs. Recombinant human insulin was purchased from Life Technologies Corporation. Dialysis tubing of MWCO 2 kDa (Cat# 132109) was purchased from Spectrum Labs.

Synthesis of Raft Chain Transfer Agent (CTA-Azide). Azide-PEG3-Hydroxyl (4.56 mmol) and 4-Cyano-4-(thiobenzoylthio)pentanoic acid (9.13 mmol) were combined in 60 mL of anhydrous dichloromethane (DCM). EDC (9.13 mmol), HOBt (9.13 mmol) and triethylamine (18.24 mmol) were added sequentially. After 20 hours at room temperature, the reaction mixture was partitioned between 1N HCl and DCM. The organic layer was subsequently washed with H_2O and then with brine before being dried with Na_2SO_4. The resultant crude mixture was purified using combi flash chromatography system using 80 gram silica column (10 to 60% EtOAc/hexanes) to obtain a red viscous oil compound (1.1g, 50% yield). ^{1}H NMR (400 MHz, $CDCl_3$): 7.91 (d, 2H), **7.56** (t, 1H), 7.40 (t, 2H), 4.27 (t, 2H), 3.71 (t, 2H), 3.6-3.7 (m, 10H), 3.39 (t, 2H), 2.5-2.75 (m, 3H), 2.44 (m, 1H), 1.94 (s, 3H) HRMS: calculated $C_{21}H_{28}N_4O_5S_2$ 480.60; found 480.1728 [M^+].

Synthesis of Carboxybetaine Monomer (CB). To a 250 mL round bottom flask, 2-(dimethylamino)ethyl-methacrylate (10.7 mL, 63.61 mmol), acetonitrile (60 mL) and *tert*-Butyl bromoacetate (18.8 mL, 127.22 mmol) were added at RT under N_2. The reaction

solution was heated at 50 °C for 48 h, cooled to RT, and then concentrated on rotavap to leave viscous oil, which was solidified by adding and mixing with diethyl ether (50 mL) followed by evaporation to have a solid, which was filtered by vacuum suction, washed with diethyl ether thoroughly and dried to give 23 g (100%) of the product as a white solid. ^{1}H NMR (400 MHz, $CDCl_3$): d 6.15 (s, 1H), 5.67 (s, 1H), 4.78 (s, 2H), 4.68-4.61 (m, 2H), 4.42-4.36 (m, 2H), 3.73 (s, 6H), 1.95 (s, 3H), 1.48 (s, 9H); ^{13}C NMR (500 MHz, CD_3OD): d 167.5, 165.1, 136.8, 127.5, 86.2, 64.6, 63.4, 59.2, 53.1, 28.2, 18.5; HRMS calculated for $C_{14}H_{26}NO_4$ 272.1856, found 272.1857 [M^+].

Synthesis of PC-Azide Polymer. CTA-Azide (46.5 mg, 0.096 mmol) and 4,4'-azobis(4-cyanovaleric acid) (ACVA) (9 mg, 0.031 mmol) were transferred into a glass vial and dissolved in 3.5 mL of ethanol. This solution was then transferred to a 10 mL Schlenk flask containing 2-(Methacryloyloxy)ethyl 2-(Trimethylammonio)ethyl Phosphate (1 g, 3.39 mmol) in 2.5 mL of pH 5.5 acetate buffer (0.3M). The flask was sealed with a rubber septum and purged with nitrogen for 20 minutes. The flask was then immersed in a preheated oil bath at 70 °C. The reaction was terminated at 20 hours by rapid cooling and exposure to air. The polymer was precipitated from diethyl ether, filtered, dissolved in DI water and dialyzed against water for 24 hours using 2 kDa MWCO dialysis bag. After lyophilization, a pink powder was obtained, and stored at –20 °C until further use (M_n(SEC): 8.5 kDa, PDI: 1.10, DP(^{1}H NMR: 33).

Synthesis of SB-Azide Polymer. CTA-Azide (43 mg, 0.089 mmol) and 4,4'-azobis(4-cyanovaleric acid) (ACVA) (8 mg, 0.029 mmol) were transferred into a glass vial and dissolved in 3.5 mL of ethanol. This solution was then transferred to a 10 mL Schlenk flask containing 2-(*N*-3-Sulfopropyl-*N*,*N*-dimethyl ammonium)ethyl methacrylate (1.0 g,

3.58 mmol) in 3.5 mL of pH 5.5 acetate buffer (0.3M) containing 0.5 M of NaBr. The flask was sealed with a rubber septum and purged with nitrogen for 20 minutes. The flask was then immersed in a preheated oil bath at 65 °C. The reaction was terminated at 13 hours by rapid cooling and exposure to air. The polymer was dissolved in DI water and dialyzed against water for 24 hours using 2 kDa MWCO dialysis bag. After lyophilization, a pink powder was obtained, and stored at –20 °C until further use (M_n (SEC): 9.1 kDa, PDI: 1.20, DP(^{1}H NMR): 36).

Synthesis of CB-Azide Polymer. CTA-Azide (35 mg, 0.073 mmol) and 4,4'-azobis(4-cyanovaleric acid) (ACVA) (7 mg, 0.024 mmol) were transferred into a glass vial and dissolved in 3.5 mL of ethanol. This solution was then transferred to a 10 mL Schlenk flask containing carboxybetaine monomer (CB) (1.0 g, 3.67 mmol) in 2.5 mL of pH 5.5 acetate buffer (0.3M). The flask was sealed with a rubber septum and purged with nitrogen for 20 minutes. The flask was then immersed in a preheated oil bath at 70 °C. The reaction was terminated at 20 hours by rapid cooling and exposure to air. The polymer was precipitated with diethyl ether, filtered, and dried to get a pinkish solid. The resultant polymer was stirred in trifluoroacetic acid (TFA, 25 mL) at room temperature for 2 hours to remove *tert*-butyl ester. TFA was evaporated under vacuum to dryness. The resultant solid was dissolved in DI water and dialyzed against water for 24 hours using 2 kDa MWCO dialysis bag. After lyophilization, a pink powder was obtained, and stored at –20 °C until further use (M_n (SEC): 8.7 kDa, PDI: 1.25, DP(^{1}H NMR): 46).

Synthesis of Insulin-DBCO Core. Recombinant human insulin (100 mg, 17.22 μmol) was dissolved in a buffer containing 0.12 M $NaHCO_3$ and 0.12 M Na_2CO_3 (3 mL) at pH 11. The small molecule DBCO-PEG4-NHS ester (112 mg, 172.2 μmol) was dissolved in

1 mL of anhydrous DMSO and added to the gently stirred insulin solution in three increments (333 μL at 0 min, 20 min, and 40 min). After 60 min, 1 M CH_3NH_2 (1 mL) was added to the reaction mixture. The product was purified via reversed phase preparative HPLC using a 218TP1022 C18 column (2.2 cm ID × 25 cm L, 10 μm; Vydac), with a mobile phase gradient from 2% to 65% (vol/vol) of solvent B (0.043% trifluoroacetic acid/acetonitrile, 20/80) with solvent A (trifluoracetic acid/water, 0.05/99.95). Fractions were collected and lyophilized to provide a white product. The product was characterized by deconvolution electrospray ionization using a QSTAR hybrid Q-TOF, performed at the Koch Institute Swanson Biotechnology Center Biopolymers and Proteomics core. Whole protein MS for $C_{287}H_{417}N_{67}O_{84}S_6$ provided a molecular mass of 6341.91 Da (calculated, 6342.24 Da).

To confirm site-specific, mono-conjugated modification on the ε-amine of the B29 lysine residue, purified Insulin-DBCO was reduced using DTT, followed by alkylation of free thiols and subsequent protein digestion with trypsin. Proteomics analysis was performed using a QSTAR hybrid Q-TOF with tandem MS/MS analysis, with a search conducted for masses of the digested products with free amines at the N-terminal A1Gly, N-terminal B1Phe, and the ε-amine B29Lys positions, as well as for the DBCO small molecule-conjugated masses. All purification and characterization were performed at the Koch Institute Swanson Biotechnology Center Biopolymers and Proteomics core.

Synthesis of Insulin-Polymer Conjugates utilizing Copper-Free Click Chemistry. Insulin-DBCO (2.5 mg, 0.39 μmol) was dissolved in a buffer containing 0.12 M $NaHCO_3$ and 0.12 M Na_2CO_3 (0.25 mL). For each polymer conjugate, 0.25 mL of Insulin-DBCO was mixed with 0.25 mL of appropriate amount of polymer stock solutions prepared in 1M

Hepes buffer, pH 7.4. Four moles excess (1.56 μmol) of each polymer was utilized in each reaction to ensure complete conjugation of Insulin-DBCO, with a final reaction mixture pH of 7.4. Directly after mixing, the reaction mixture was placed at 4°C overnight under gentle orbital shaking (50 rpm). The resulting insulin-polymer conjugates were used directly from the reaction mixture with no further purification performed to remove unreacted, excess polymer.

Instrumentation. ^{1}H NMR spectra were recorded on Varian Inova 500 MHz NMR spectrometer, using the residual proton resonance of the solvent as the internal standard. Chemical shifts are reported in parts per million (ppm). High-resolution mass spectral (HRMS) data were obtained on 7 Tesk Bruker Fourier-Transform Ion Cyclotron Resonance Mass Spectrometer. Molecular weight and PDI values of the water soluble zwitterionic polymers were estimated by Gel Permeation Chromatography (GPC) in aqueous buffer containing 0.05 M sodium nitrate. Poly(ethylene glycol) standards were used to calibrate GPC for molecular weight measurements. One guard column and three Tosoh TSKgel GMPWxL columns were calibrated with PEG standards. Flow rate was set to 1.0 mL/min and Viscotek refractive index detector was used for conventional calibration. Flash chromatography was performed on a Teledyne Isco CombiFlash Rf-200 chromatography equipped with UV-Vis and evaporative light scattering detectors (ELSD).

Circular Dichroism. To assess whether polymer modification of native insulin to Insulin-DBCO, Insulin-PC, Insulin-CB, Insulin-SB, and Insulin-PEG yielded alteration of insulin secondary structure, near-UV circular dichroism (CD) spectroscopy was performed with a Jasco J-1500 high-performance CD spectrometer over a wavelength range of 205–250

nm using a transparent 0.1-cm path length quartz cuvette. Quantifying relative protein stability of the insulin conjugates was also performed with the same Jasco J-1500 high-performance CD spectrometer instrument following a denaturation study involving titration of each insulin sample with the chemical denaturant guanidine hydrochloride (GHCl). For measuring secondary structure, each insulin sample was dissolved at a concentration of 4 mg/mL in a buffer containing 0.12 M $NaHCO_3$ and 0.12 M Na_2CO_3 (pH 9.4). Each sample was then diluted to a final concentration of 0.25 mg/mL using 100 mM HEPES buffer. All measurements were taken at pH 7.4 and 37 °C. Comparison of native insulin spectra with all conjugates demonstrated no compromising of insulin protein alpha helical secondary structure due to chemical modification. Determination of relative protein stability was performed following a series of GHCl titrations with each respective insulin sample, at intervals of denaturant concentration spanning a range from 0.0 M GHCl to 7.5 M GHCl. For the stability study, each insulin sample was dissolved at a concentration of 4 mg/mL in a buffer containing 0.12 M $NaHCO_3$ and 0.12 M Na_2CO_3 (pH 9.4). Each sample was diluted to a final concentration of 0.25 mg/mL using varying mixtures of 100 mM HEPES and 8.0M GHCl solutions to ensure the full range of denaturant concentration necessary for the study. All measurements were taken at pH 7.4 and 37 °C. Alterations in secondary structure were observed at wavelength 222 nm at each GHCl concentration. Thermodynamic stabilities were inferred from fitting normalized CD-detected protein denaturation to a nonlinear least squares two-state model, as described previously,[17] and statistical significance determined by an extra sum-of-squares F test for comparing the global fit statistics of ΔG_u for all samples relative to the native protein. All analysis was performed using GraphPad Prism 6.0.

Thermal Aggregation Assay. Recombinant human insulin and Insulin-DBCO were dissolved at a concentration of 344 μM in a buffer containing 0.12 M $NaHCO_3$ and 0.12 M Na_2CO_3. Recombinant human insulin was diluted to a final concentration of 172 μM in 1 M HEPES. Insulin-DBCO was individually mixed with each respective polymer (PC-Azide, CB-Azide, SB-Azide, and PEG-Azide), present at a concentration of 1.38 mM in 1 M HEPES (4X molar excess). Samples were plated at 150 μL per well (n = 3/group) in a clear 96- well plate (Thermo Scientific Nunc) and sealed with optically clear and thermally stable seal (VWR). The plate was immediately placed into an Infinite M1000 plate reader (Tecan Group) and shaken continuously at 37 °C. Absorbance readings at 540 nm were collected every 6 min for 60 h, and absorbance values were subsequently converted to transmittance. The aggregation of insulin leads to light scattering, which results in reduction of sample transmittance. The time for aggregation (t_A) was defined as a >10% reduction in transmittance from the initial transmittance. Following the 60-h kinetic study, the plate was maintained under continuous agitation at 37 °C, and absorbance at 540 nm was monitored daily to approximate t_A for the insulin polymer conjugates. At 80 d, with no indication of a change in absorbance for insulin polymer conjugates, the aggregation study was terminated.

In Vitro Insulin Receptor Activation. C2C12 cells were purchased from the American Type Culture Collection (ATCC) and confirmed free of mycoplasma contamination before use. Cells were cultured in Dulbecco's modified Eagle medium(DMEM) containing L-glutamine, 4.5 g/L D-glucose, and 110 mg/L sodium pyruvate, and supplemented with 10% FBS and 1% penicillin–streptomycin. Incubations occurred in a 5% CO_2/water-saturated incubator at 37 °C. Cells were seeded in 96-well plates at a density of 5,000

cells per well. Twenty-four hours after plating, the cells were washed three times with 200 µL of DMEM containing L-glutamine, 4.5 g/L glucose, and 110 mg/L sodium pyruvate, and starved for at least 4 h at 37 °C in the same serum-free conditions. After 4 h, the media was removed, and cells were stimulated with 100 µL of insulin samples of various concentrations for 30 min at 37 °C. After 30 min, cells were washed three times with 100 µL of cold Tris-buffered saline (1X), followed by lysing the cells for 10 min with 100 µL of cold Lysis Buffer (Perkin-Elmer). Levels of phosphorylated AKT 1/2/3 (Ser473) and Total AKT 1 were determined from cell lysates using the AlphaLISA SureFire ULTRA kits (Perkin-Elmer) according to the manufacturer's instructions. Intra-well normalized data of phosphorylated AKT 1/2/3 (Ser473) and Total AKT 1 were analyzed using GraphPad Prism 6.0, with dose–response curves fitted to a variable slope (four-parameter) stimulation model to determine the EC_{50} of each insulin sample, and statistical significance determined by an extra sum-of-squares F test for comparing the fit statistics of LogEC50 for all samples relative to the native protein.

Diabetic mouse model. Male C57BL/6J mice, age 8 wk, were purchased from Jackson Laboratory. After acclimation, mice were fasted overnight before intraperitoneal injection of 150 mg/kg STZ. Preparation of STZ for injection involved dissolving the chemical at a concentration of 15 mg/mL in sodium citrate buffer (114 mM, pH 4.5) immediately before injection. Food was withheld for 2 h post-injection, after which mice were allowed to eat ad libitum. Glucose levels were monitored by peripheral tail vein bleeds using a portable glucose meter (Clarity Plus, Clarity Diagnostics) daily until unfasted glucose levels were >400 mg/dL. For healthy mouse studies, age-matched healthy C57BL/6J mice were used.

Glucose tolerance test. STZ-induced diabetic mice were fasted overnight before performing studies. Mice were bled at the beginning of the study, and any mouse with a fasting blood glucose level <300 mg/dL was triaged from the study. Mice were then randomized and injected subcutaneously with native insulin or insulin polymer conjugates at doses ranging from 1 to 5 IU/kg (1 IU = 5.97 nmol), with insulin concentration determined by comparing analytical HPLC area under the curve (AUC) signal to a standard curve. Blood glucose readings were collected every 15–30 min using a handheld glucose meter (Clarity Plus, Clarity Diagnostics). A glucose tolerance test was performed via intraperitoneal injection of 1 g/kg glucose dissolved in PBS (1X), and blood glucose was monitored. Responsiveness was quantified by measuring the area-under-the-curve with a baseline at the point of glucose injection and integrating across a 3-h window following the challenge. For dosing studies in healthy mice, insulin injections were performed via identical methods, but no glucose tolerance test was performed. The induction of hypoglycemia was quantified as the difference between the initial and the nadir (i.e., lowest observed) blood glucose readings divided by the nadir to determine the hypoglycemia index.

Gel Electrophoresis. Native PAGE was carried out using Bio-Rad, PROTEAN® TGX™ Precast Protein Gels to confirm conjugation. Sample stock solutions of all insulin and polymer samples to be tested were dissolved at a concentration of 5 mg/ml, using the same buffers as described above. All samples were diluted to 0.5 mg/ml with Bio-Rad, Native sample buffer, with 25ul of each sample to be used for loading into the appropriate well. Gel running conditions were set to 150V for 45 minutes in Bio-Rad Tris/Glycine buffer. After gel electrophoresis was complete, the gel was washed three times with de-

ionized water and stained using Invitrogen SimplyBlue SafeStain. Image of the gel was taken using Bio-Rad Imager with the ChemiDoc™ Imaging Systems.

4.8 *Acknowledgements*

This work was supported by a grant from the Leona M. and Harry B. Helmsley Charitable Trust Foundation (Grant No. 2017PG-T1D027). We acknowledge technical support from the Koch Institute Swanson Biotechnology Center and are specifically grateful for use of the Biopolymers & Proteomics Core Facility, at the Massachusetts Institute of Technology.

Chapter 5: Conclusions

5.1 *Thesis Summary*

The unifying theme of this Thesis is the design, synthesis, and optimization of novel insulin bioconjugates for the application of enhanced basal and glucose-responsive activity. First, we conceived of a method to perform screen-based optimization of a novel class of unimolecular GRI constructs, which ultimately led to the identification of a lead candidate possessing a unique combination of properties: glucose-mediated solubility, safety, and *in vivo* activity. We envision this synergistic combination of properties to provide an ideal basis for further development of a truly state-responsive insulin therapeutic. Next, we pioneered the first experimental example of an innovative library of dynamically tethered insulin conjugates possessing enhanced chemical and thermal stability, ultimately demonstrating the potential, with further development and optimization, to achieve GRI constructs capable of sugar-mediated insulin receptor interactions. Finally, we incorporate zwitterionic polymers into an ultra long-acting insulin design strategy to create a potentially new therapeutic class of basal insulins. It is the hope that this work will contribute to the development of unimolecular insulin technologies and therapeutics by increasing their overall safety and efficacy, as well as in accelerating the discovery and optimization processes of novel GRI constructs for the autonomous glycemic management of insulin-dependent diabetes.

5.2 *Future Perspectives for Unimolecular GRI Constructs*

To conclude this Thesis, I describe three areas of topical interest for future work involving unimolecular glucose-responsive insulin therapy.

5.2.1 Intelligent Design In Silico

One of the largest bottlenecks currently experienced in drug design and evaluation, especially within the glucose-responsive insulin technology space, is the iterative nature of exploration. Time- and resource-consuming practices are required to design, synthesize, and evaluate individual GRI constructs at various levels of the preclinical development process, both *in vitro* and *in vivo*, the results of which may or may not be directly correlative or translatable to human patients. And despite the advent of high-throughput screening technology, the fact remains that there exists numerously diverse mechanisms-of-action that GRI technologies can exploit, many of which have yet to be conceived. This prospect makes designing universal screen-based approaches less applicable and difficult to develop, especially when taking into account the mechanism-specific kinetics and thermodynamics that would be desirable for a specific construct, as well as the translation of those parameters to an appropriate therapeutic index. *In silico* mathematical modeling possesses the potential and promise of streamlining this exploration process, helping to identify performance parameters desired for the successful synthesis, safety, efficacy, and translation of current and future GRI constructs. Current examples of this goal exist today, as seen with the adaptation of the Sorensen model as well as the work by Bisker et al.; however, a relatively large set of obstacles that must be overcome is the experimental validation that still remains for many of these theoretical models.[34,43]

5.2.2 Glucose-Selective Boronic Acid Motifs

A very common inorganic strategy for incorporating sugar-sensing properties onto the insulin protein is through the use of boronic acid motifs, due to their binding affinities

being in the millimolar concentration range. However, this property is afforded by the universal interaction of boronic acids to create reversible covalent bonds with *cis*-1,2 and *cis*-1,3 diols, of which glucose is a prime example. The disadvantage of this is the fact that many biological sugars possess the same binding motif, allowing for the possibility for non-specific competition that could inadvertently activate a glucose-responsive insulin, thereby creating the potential of inducing a hypoglycemia event. Two common examples of freely-circulating diols that could pose a threat to boronic-acid-incorporated constructs are fructose and lactic acid.[48] Fructose is generally not present as a freely-circulating diol in the bloodstream, even after a fructose-rich meal.[170] However, the binding constant of fructose with boronic acid is significant, almost 50X higher than that of glucose, and therefore posing a serious risk that must be taken into consideration when developing boronic-acid-enabled GRI constructs.[59] Lactic acid, on the other hand, is naturally present within the human body. The concentration of lactic acid in the bloodstream can be amplified under various conditions, such as after intense exercise, as well as in cases of the diabetic disease state in combination of oral antidiabetic medications such as metformin.[171–173] Although the binding constant of boronic acids with lactic acid is orders-of-magnitude lower than that of fructose, the potentially higher concentration of lactic acid could also induce undesired activation of a boronic-acid-activated GRI construct.[53] A strategy that has been used to improve selectivity has incorporated either bulky hydrophobic scaffolds or di-boronic frameworks, both of which significantly decrease water solubility.[60,61] To this end, continued development of more selective boronic acid motifs will be necessary in the advancement of GRI constructs that utilize boronic acid motifs.

5.2.3 Artificial Lectins

As an alternative to boronic acids, artificial lectins are complex, inorganic constructs that utilize a macrocycle design to promote strategic hydrogen-bonding with the various alcohols found on sugars, in particular glucose. Previous success of designing and synthesizing artificial lectins with selectivity towards glucose has been demonstrated, albeit under extremely non-scalable synthesis routes.[174–176] Progress has been made to advance this technology to produce artificial macrocycles capable of selectively binding to glucose at physiologically-relevant ranges with more accessible and scalable strategies possessing sufficient yields;[177] however, toxicity and overall biological safety remains to be determined both *in vitro* or *in vivo*. No examples exist of a bioconjugation strategy between the insulin protein and an artificial lectin to-date. Nonetheless, the successful development of artificial lectins and macrocycles capable of physiologically relevant binding to glucose could provide a powerful alternative to boronic acids towards the generation of a glucose-responsive insulin construct.

Appendix A: Supplementary Figures

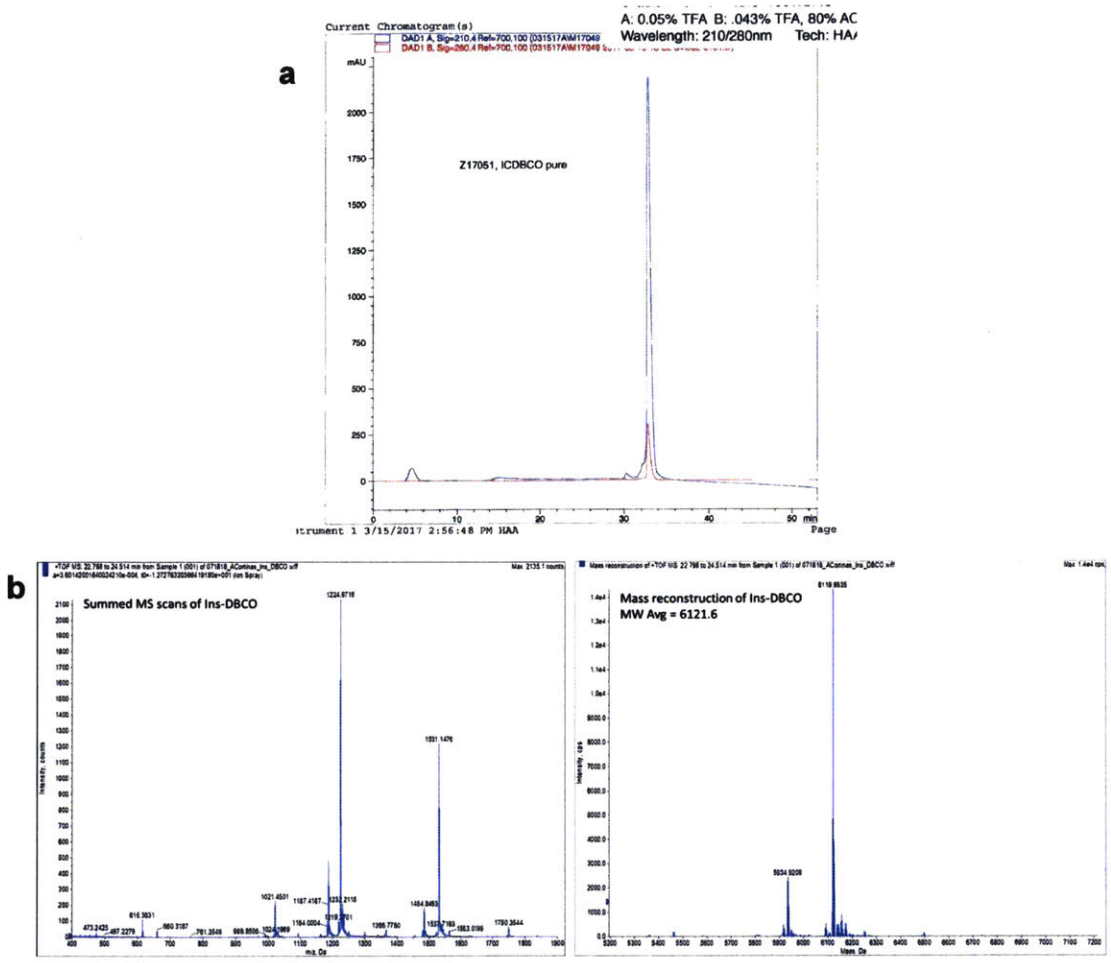

Figure A. 1 Analytical characterization of the purified Insulin-DBCO core molecule. (a) Reverse-phase HPLC chromatogram of purified Insulin-DBCO at wavelength 210 nm. (b) Electrospray ionization MS scan of purified Insulin-DBCO (left) and resulting deconvoluted whole protein molecular weight (right).

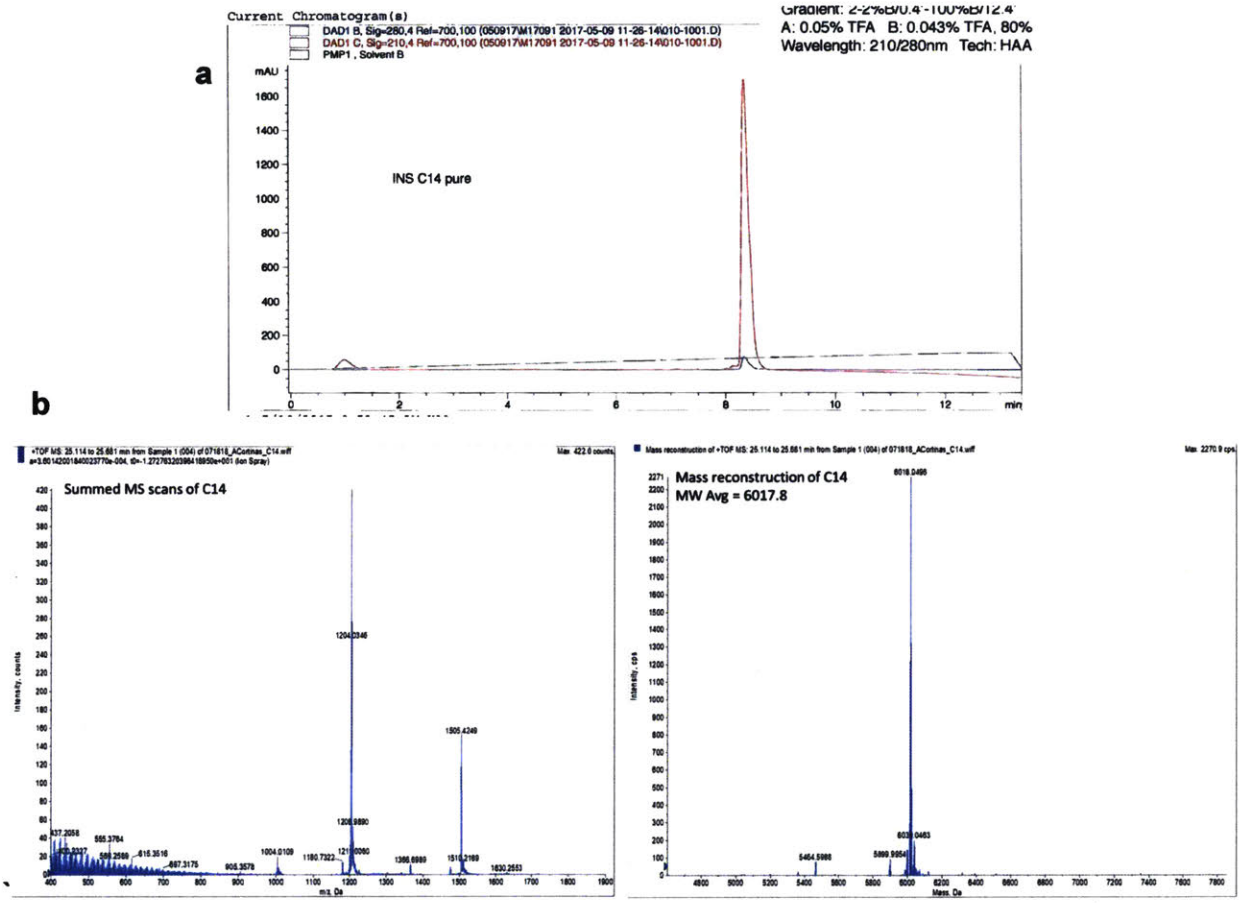

Figure A. 2 Analytical characterization of the purified insulin detemir. (a) Reverse-phase HPLC chromatogram of purified insulin detemir at wavelength 210 nm. (b) Electrospray ionization MS scan of purified insulin detemir (left) and resulting deconvoluted whole protein molecular weight (right).

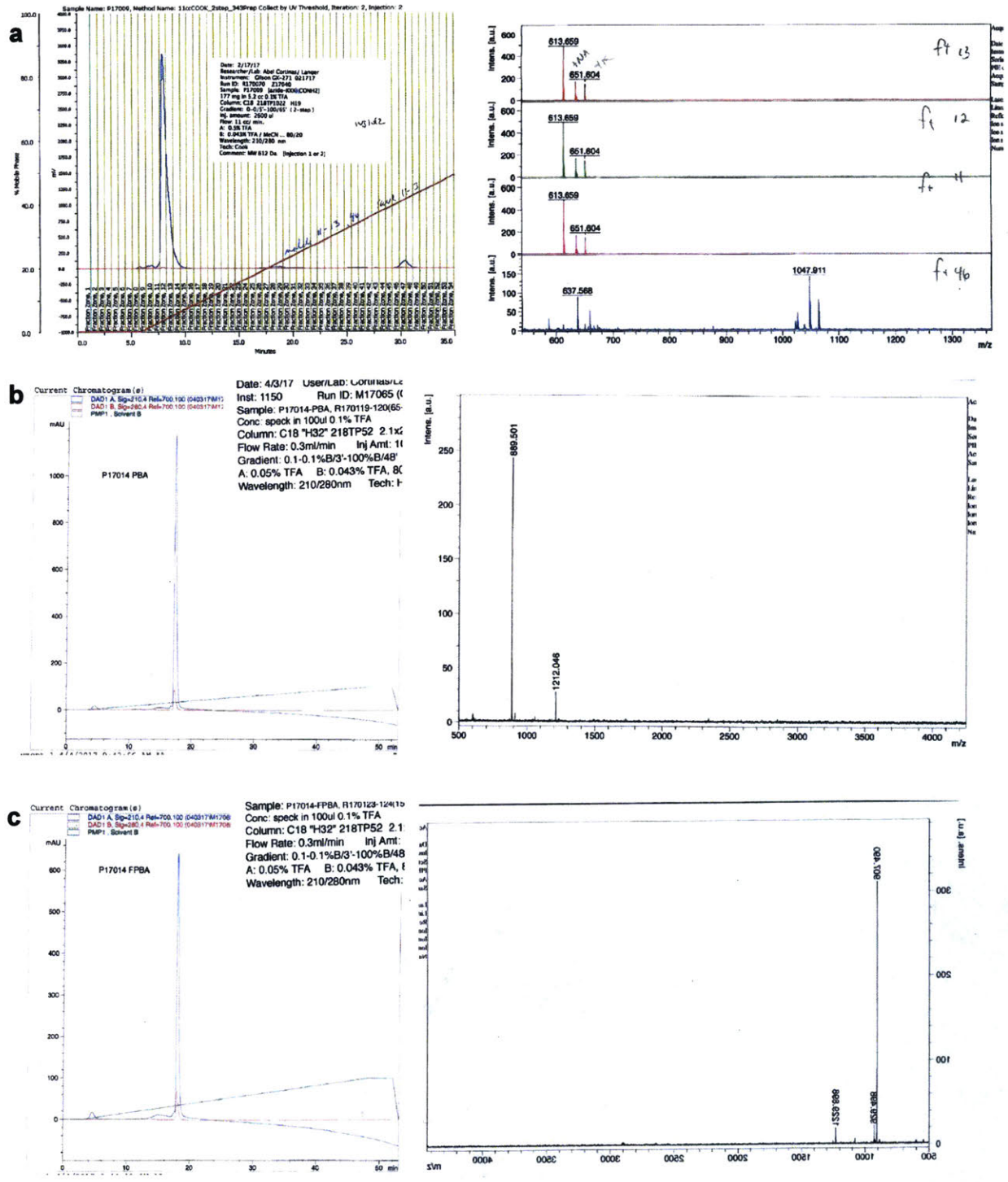

Figure A. 3 Analytical characterization of the oligopeptide constructs. Reverse-phase HPLC chromatogram (left) and MALDI-TOF MS (right) of purified (a) PL, (b) PL-PBA, and (c) PL-FPBA

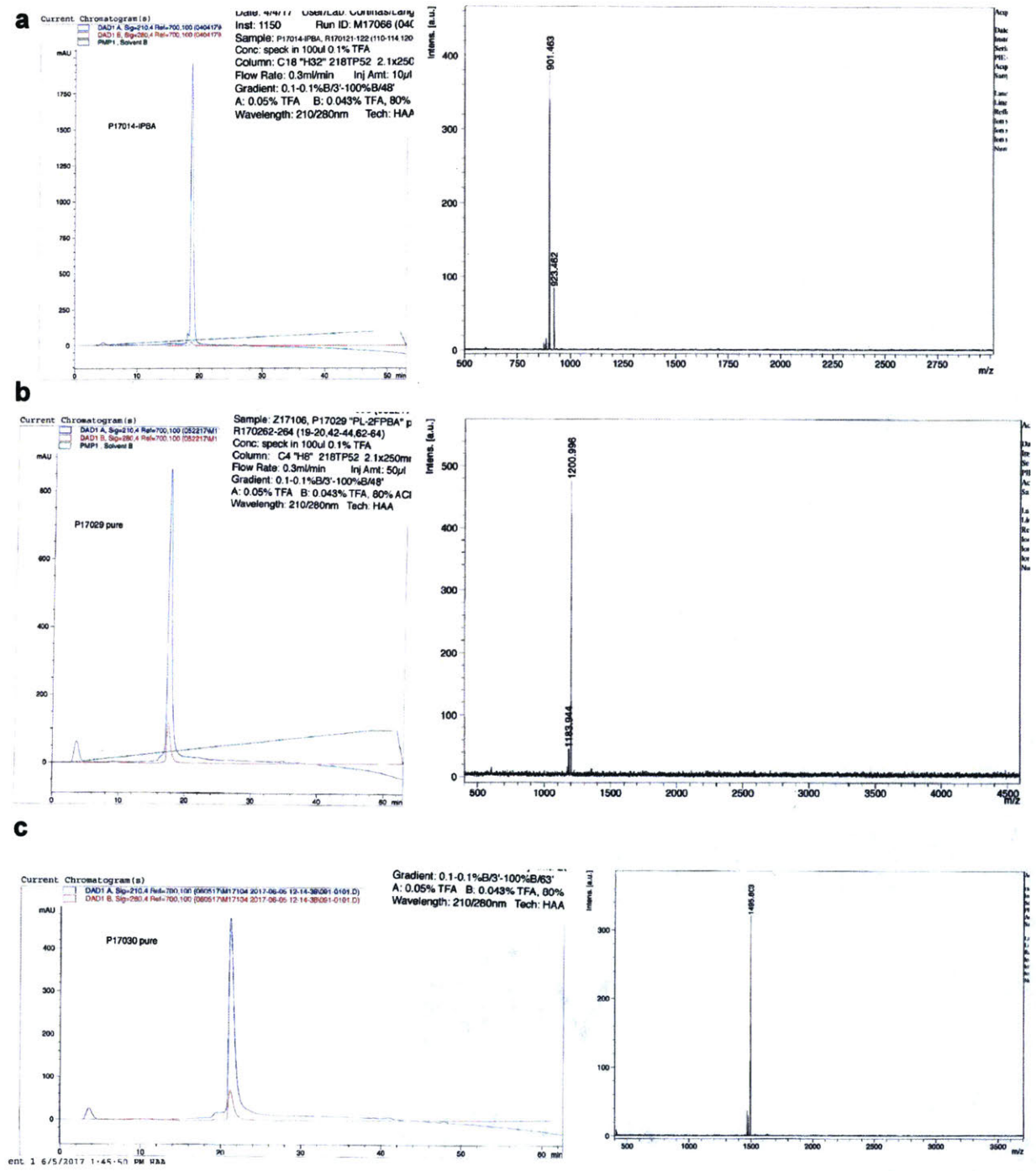

Figure A. 3 (continued) Analytical characterization of the oligopeptide constructs. Reverse-phase HPLC chromatogram (left) and MALDI-TOF MS (right) of purified (a) PL-OHPBA, (b) PL-2FPBA, and (c) PL-3FPBA

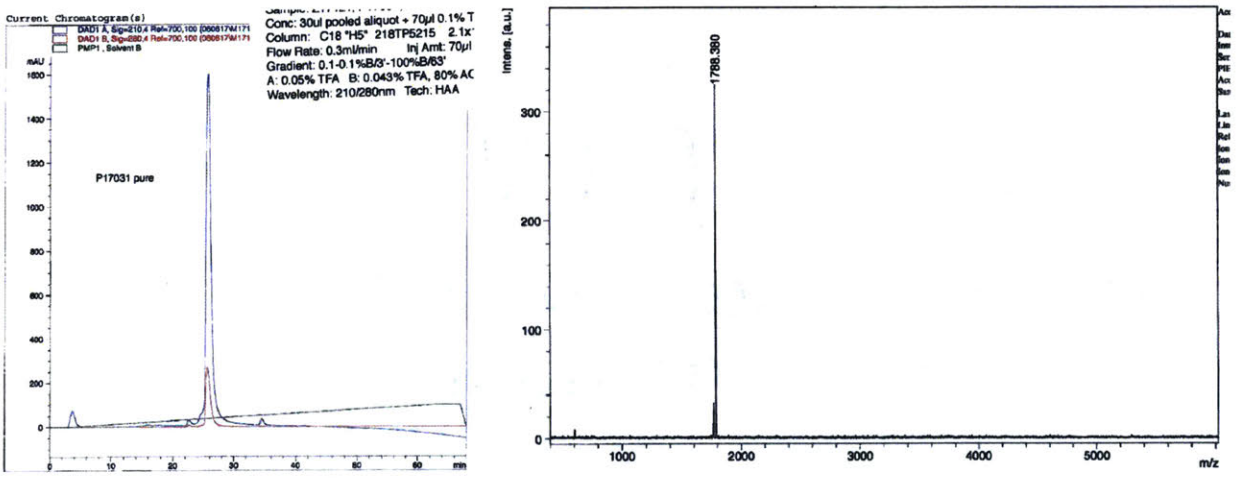

Figure A. 3 (continued) Analytical characterization of the oligopeptide constructs. Reverse-phase HPLC chromatogram (left) and MALDI-TOF MS (right) of purified PL-4FPBA

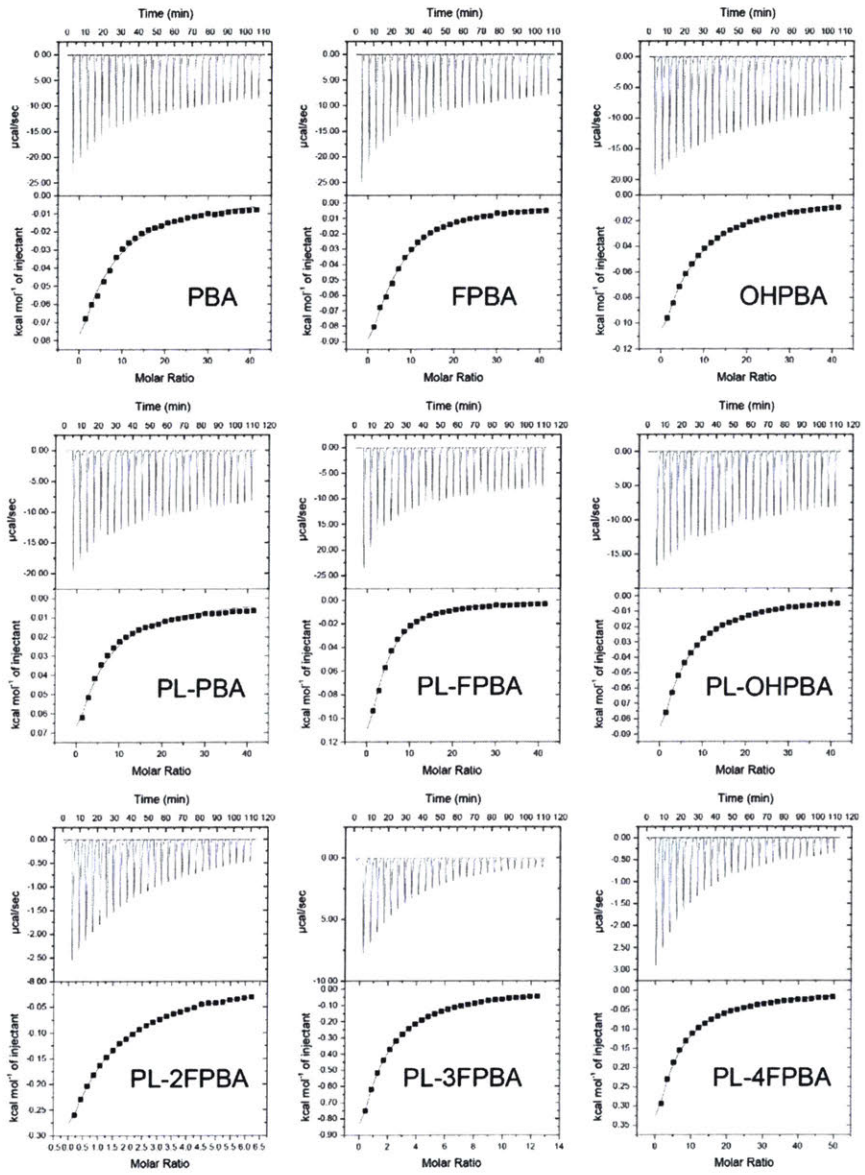

Figure A. 4 Representative, background-subtracted isothermal titration calorimetry profiles. Experiments performed at 310.15 K in PBS (1X, pH 7.4) for the binding of glucose to phenylboronic acid small molecules (PBA, FPBA, and OHPBA) and to oligopeptide constructs bearing phenylboronic acid molecules (PL-PBA, PL-FPBA, PL-OHPBA, PL-2FPBA, PL-3FPBA, and PL-4FPBA).

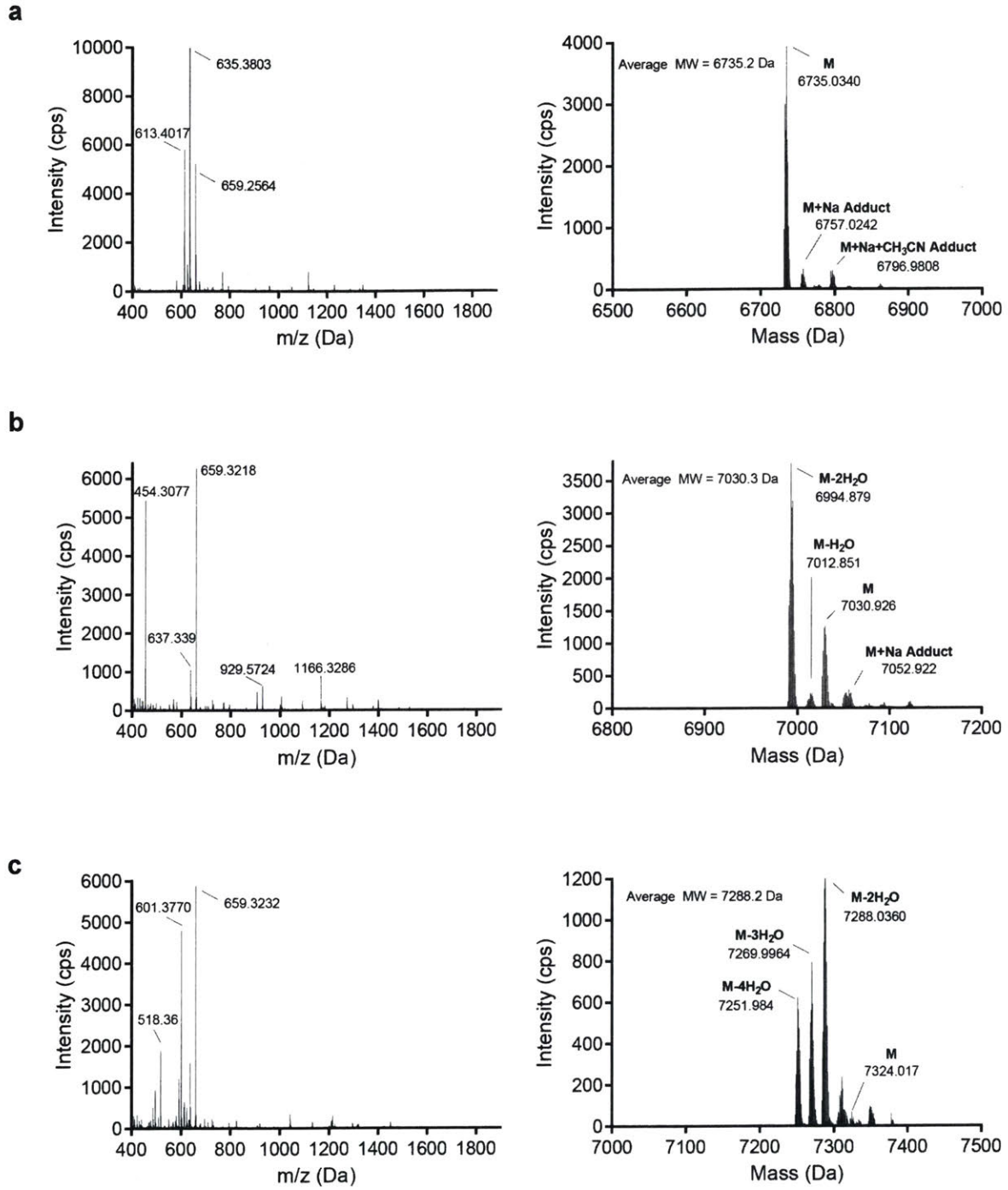

Figure A. 5 Analytical characterization of glucose-responsive insulin conjugates. Electrospray ionization MS scan (left) and resulting deconvoluted whole protein molecular weight (right) of purified (a) Ins-PL, (b) Ins-PL-FPBA, and (c) Ins-PL-2FPBA

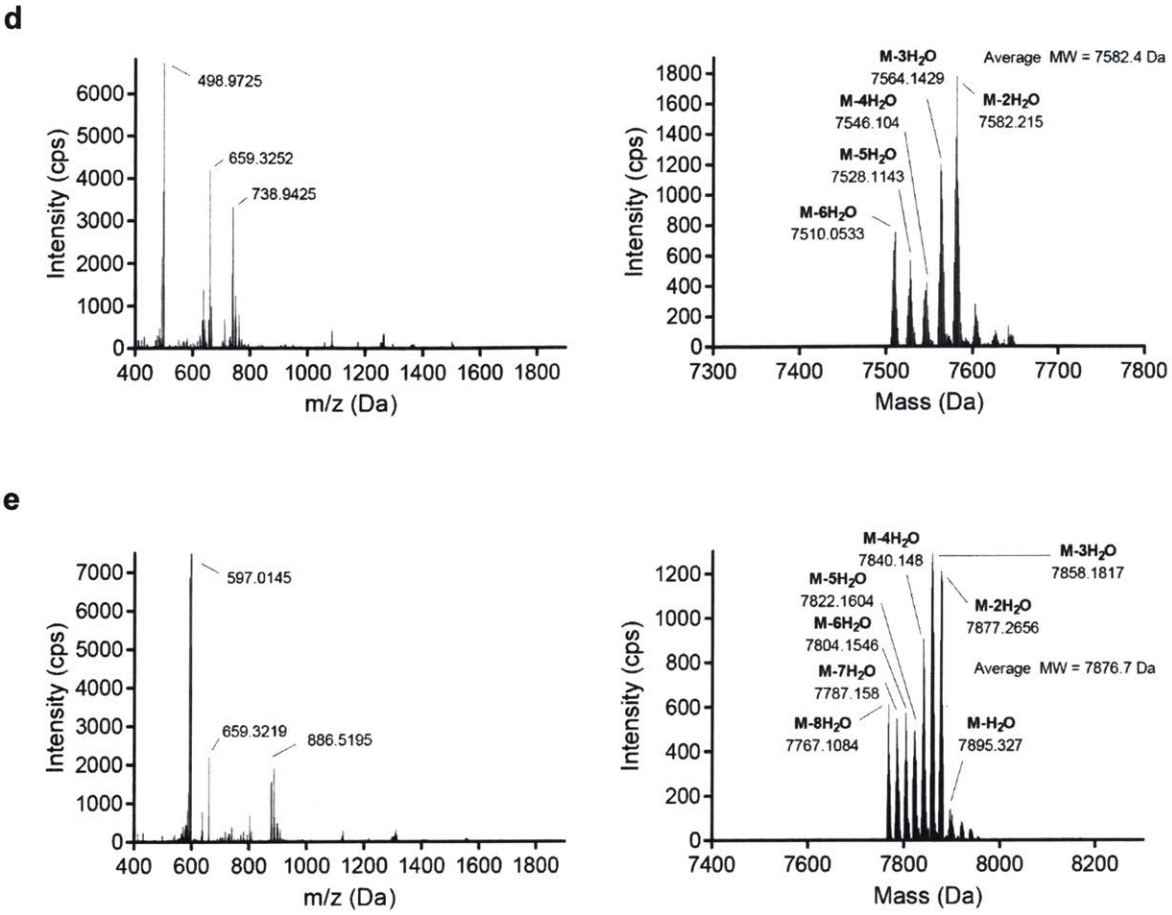

Figure A. 5 (continued) Analytical characterization of glucose-responsive insulin conjugates. Electrospray ionization MS scan (left) and resulting deconvoluted whole protein molecular weight (right) of purified (d) Ins-PL-3FPBA, and (e) Ins-PL-4FPBA.

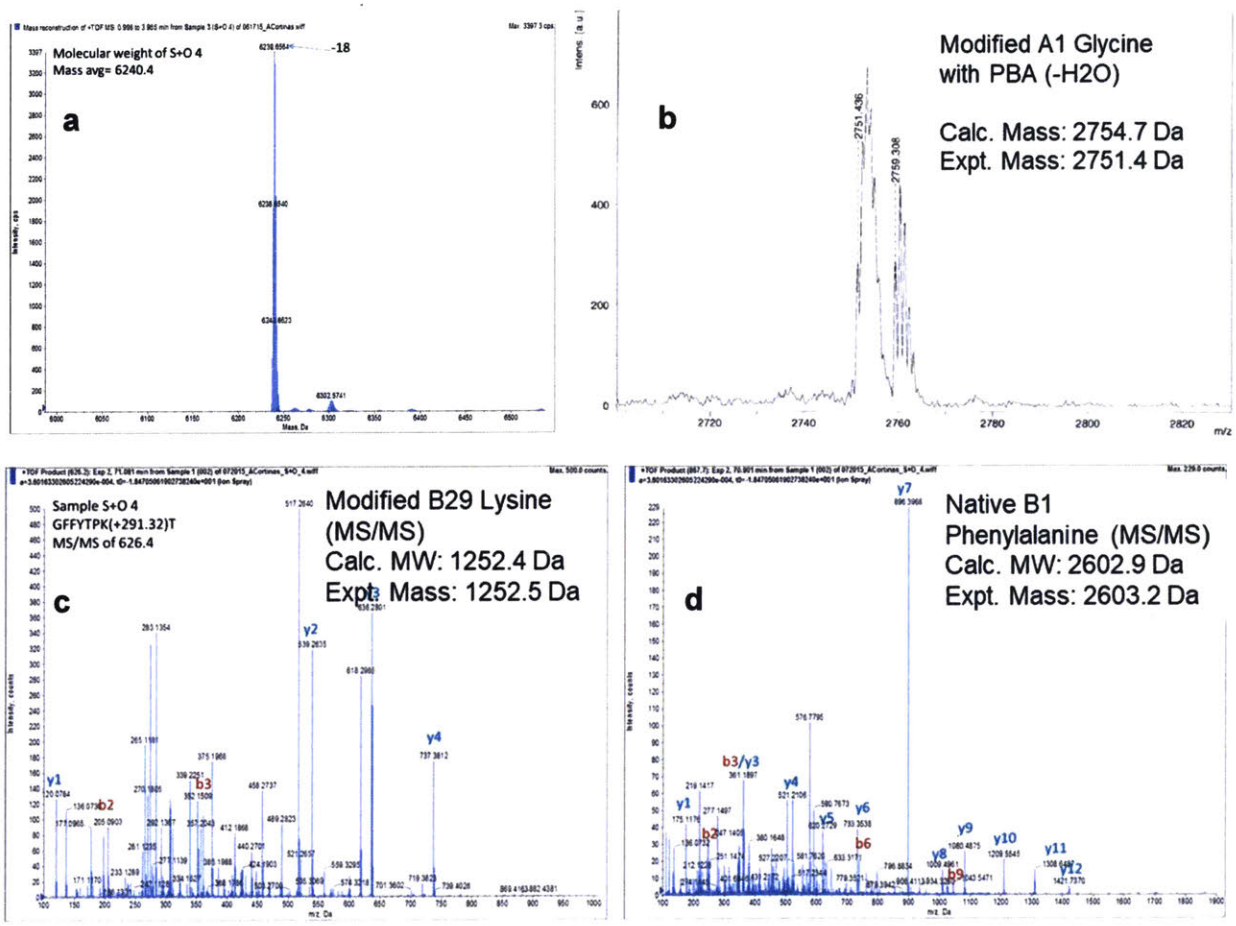

Figure A. 6 Representative MS characterization of the purified, dynamically tethered insulin conjugates. (a) Whole protein electrospray ionization MS scan of purified Conjugate 3; (b-d) fragment tandem MS/MS analysis of DTT/trypsin protein digestion of Conjugate 3, confirming site-specific di-conjugation via the (b) N-terminal A1 glycine modification with OHPBA, the (c) modification of the ε-amine of the B29 lysine residue with S2, and d) identification of a lack of modification on the B1 phenylalanine.

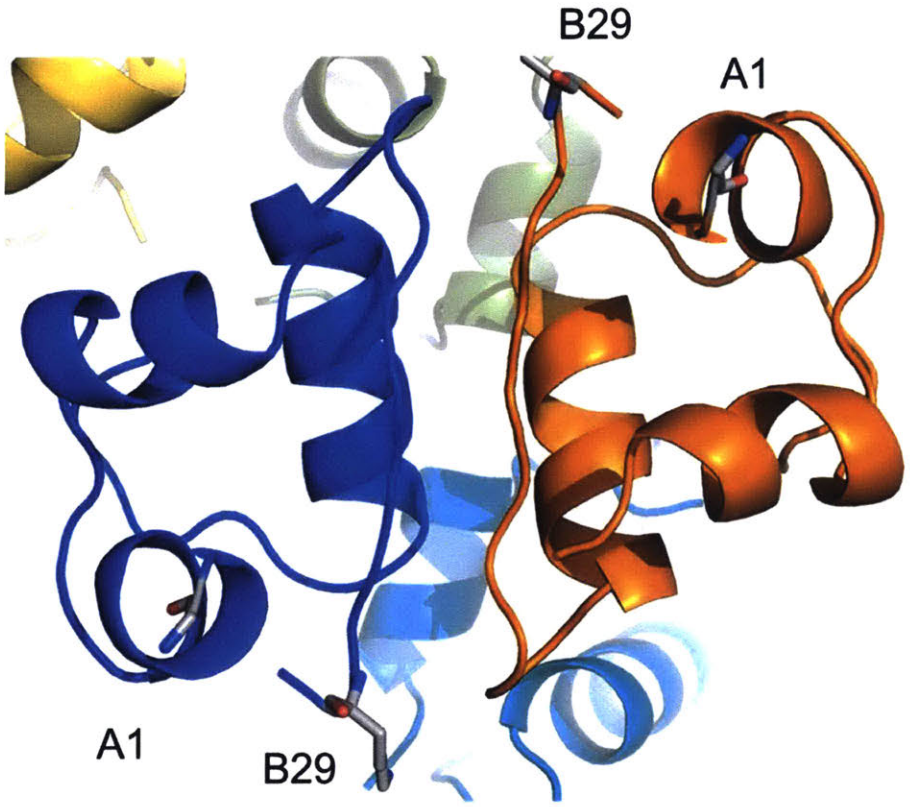

Figure A. 7 Crystal structure packing data of Conjugate 3. Overall, the data demonstrates retention of tertiary structure as well as retained monomeric packing structure relative to the native protein, indicating no adverse effects in monomeric interactions due to the synthesis and purification routes. Additionally, the packing of Conjugate 3, as shown here, also supports the proposed intra-protein stability mechanism by demonstrating no complimentary alignment of small molecule conjugates relative to the neighboring protein (B29 position of one conjugate is not directly next to the A1 position of the neighboring conjugate; which is where PBA and polyol conjugations occurred), suggesting that dynamic interactions occur within the same conjugate and not with neighboring conjugates. If stabilization interactions were due to nearest-neighbor stabilization, the B29 position of one conjugate would need to be directly neighboring the A1 position of another conjugate.

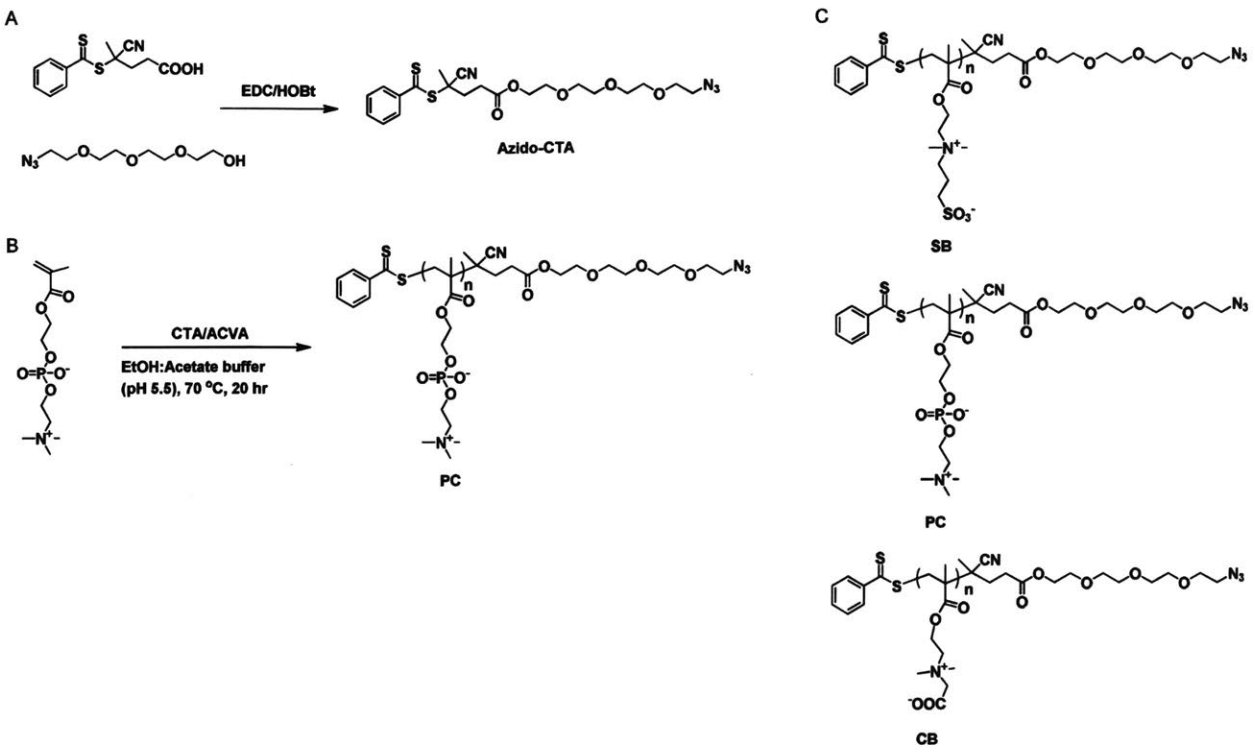

Figure A. 8 Synthesis route of zwitterionic polymer products. (a) Synthesis of azido-RAFT agent. (b) Representative RAFT polymerization reaction of the zwitterionic phosphoryl choline monomer. (c) Structures of all synthesized zwitterionic homopolymers.

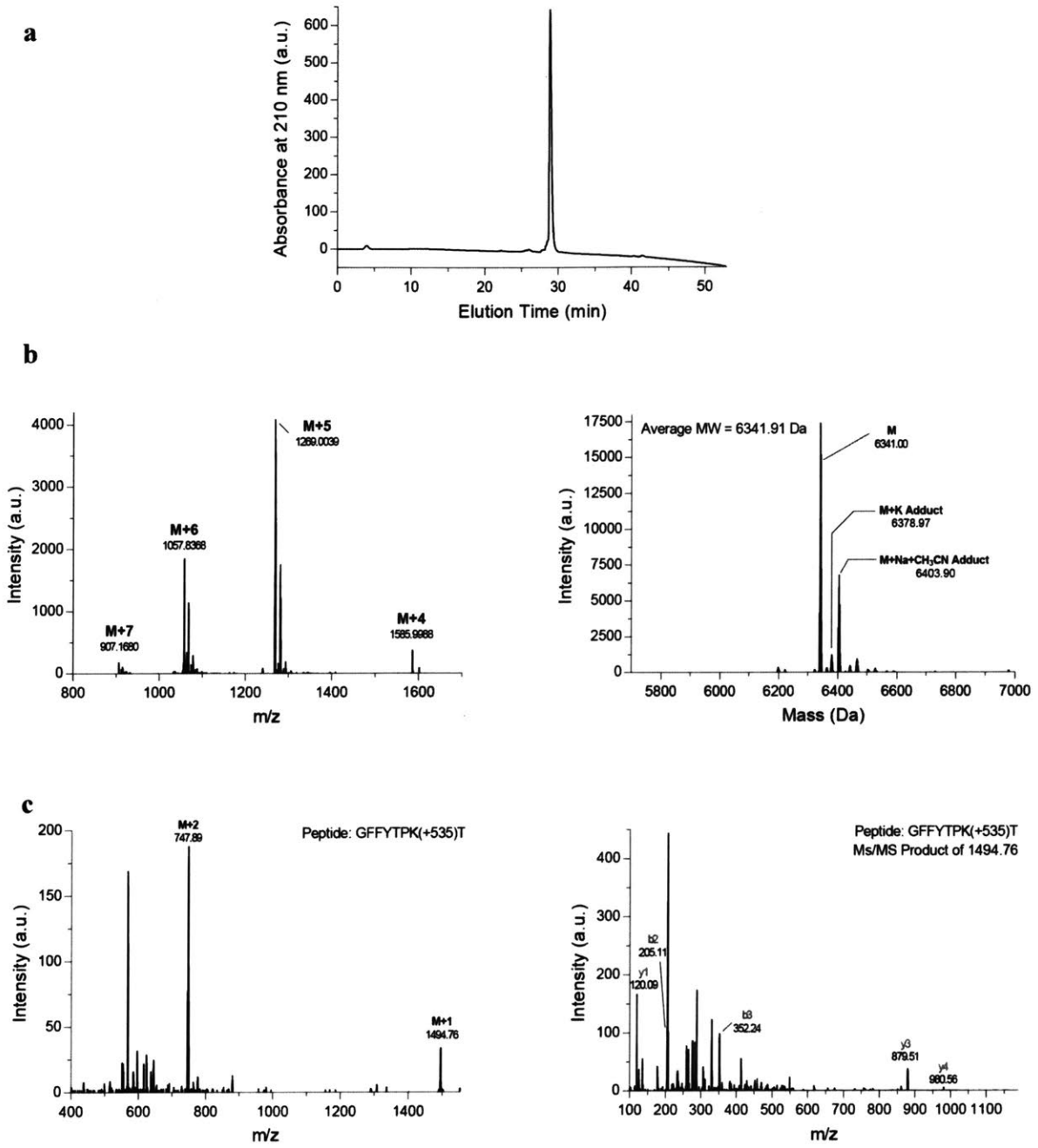

Figure A. 9 Analytical characterization of the purified Ins-DBCO core molecule. (a) Reverse-phase HPLC chromatogram of purified Ins-DBCO at wavelength 210 nm. (b) Electrospray ionization MS scan of purified Ins-DBCO (left) and resulting deconvoluted whole protein molecular weight (right). (c) Electrospray ionization MS scan (left) and fragment tandem MS/MS analysis (right) of DTT/trypsin protein digestion of Ins-DBCO molecule, identifying the ε-amine of the B29 lysine residue as the site of mono-conjugation.

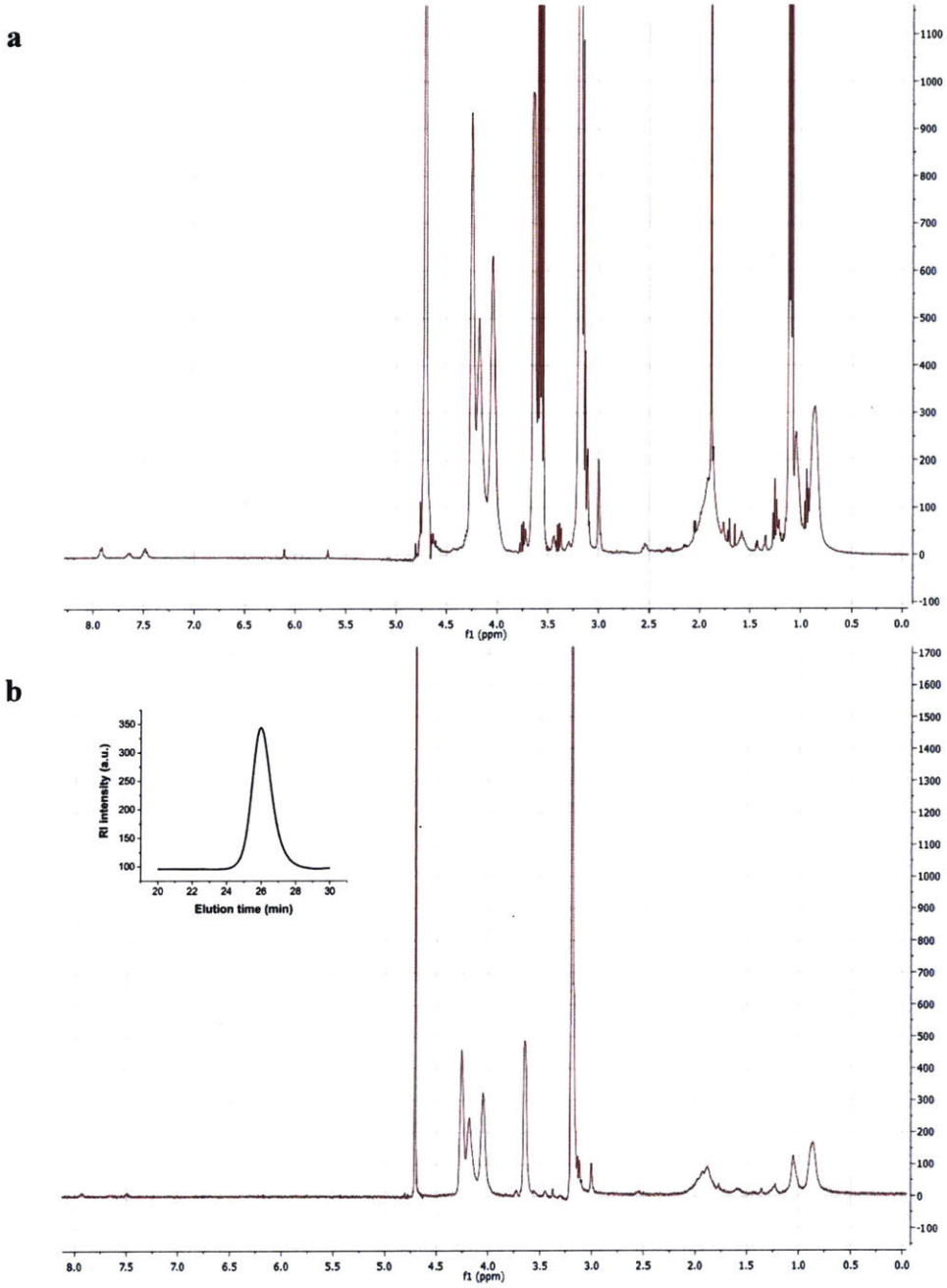

Figure A. 10 Representative ^{1}H NMR spectra of crude and purified polymer products. Representative spectra of crude (a) and purified (b) PC polymer in D_2O is shown. Inset: Aqueous GPC trace of PC polymer. The monomer conversion was determined by comparing the vinyl resonance of monomer peaks in crude reaction mixture at 5.6 and 6.10 ppm to quaternary methyl resonance of polymer at 3.20 ppm, suggesting more than 98% conversion.

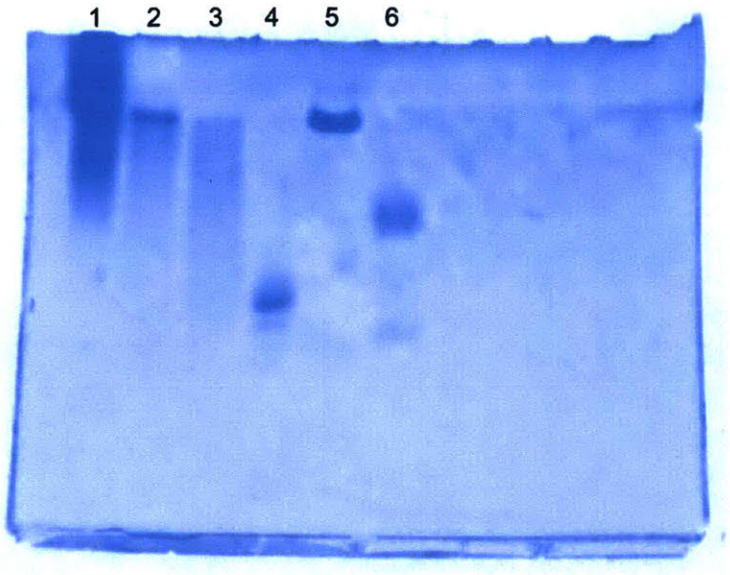

Figure A. 11 Native polyacrylamide gel electrophoresis (PAGE) of polymer conjugation mixture after Coomassie staining. Lane 1: Ins-CB; Lane 2: Ins-PC; Lane 3: Ins-SB; Lane 4: Ins-DBCO; Lane 5: Ins-PEG; Lane 6: Ins-PEG 2k. Results indicate complete conjugation of Ins-DBCO and polymer, demonstrated by the lack of residual Ins-DBCO band seen in any of the lanes apart from reference lane 4.

Appendix B: References

1. Owens, D. R., Zinman, B. & Bolli, G. B. Insulins today and beyond. *Lancet* **358,** 739–46 (2001).

2. *IDF Diabetes Atlas, 6th Edition*. (2013).

3. Heller, S., Kozlovski, P. & Kurtzhals, P. Insulin's 85th anniversary--An enduring medical miracle. *Diabetes Res. Clin. Pract.* **78,** 149–58 (2007).

4. *IDF Diabetes Atlas, 8th Edition*. (2017).

5. Barnett, A. H. & Owens, D. R. Drug profile: Insulin analogues. *Lancet* **349,** 47–51 (1997).

6. Evans, M., Schumm-Draeger, P. M., Vora, J. & King, a B. A review of modern insulin analogue pharmacokinetic and pharmacodynamic profiles in type 2 diabetes: improvements and limitations. *Diabetes. Obes. Metab.* **13,** 677–84 (2011).

7. Heise, T. & Pieber, T. R. Towards peakless, reproducible and long-acting insulins. An assessment of the basal analogues based on isoglycaemic clamp studies. *Diabetes. Obes. Metab.* **9,** 648–59 (2007).

8. Zaykov, A. N., Mayer, J. P. & DiMarchi, R. D. Pursuit of a perfect insulin. *Nat. Rev. Drug Discov.* (2016). doi:10.1038/nrd.2015.36

9. Sheldon, B., Russell-Jones, D. & Wright, J. Insulin analogues: an example of applied medical science. *Diabetes. Obes. Metab.* **11,** 5–19 (2009).

10. Kurtzhals, P. *et al.* Albumin binding of insulins acylated with fatty acids: characterization of the ligand-protein interaction and correlation between binding affinity and timing of the insulin effect in vivo. *Biochem. J.* **312,** 725–731 (1995).

11. Home, P. Insulin glargine: the first clinically useful extended-acting insulin in half a century? *Expert Opin. Investig. Drugs.* **8,** 307–314 (1999).

12. Jonassen, I. *et al.* Biochemical and Physiological Properties of a Novel Series of Long-Acting Insulin Analogs Obtained by Acylation with Cholic Acid Derivatives. *Pharm. Res.* **23,** 49–55 (2006).

13. Kurtzhals, P., Kiehr, B. & Sørensen, a R. The cobalt(III)-insulin hexamer is a prolonged-acting insulin prodrug. *J. Pharm. Sci.* **84,** 1164–8 (1995).

14. Malik, L. *et al.* Perfluoroalkyl chains direct novel self-assembly of insulin. *Langmuir* **28,** 593–603 (2012).

15. Jonassen, I. *et al.* Design of the novel protraction mechanism of insulin degludec, an ultra-long-acting basal insulin. *Pharm. Res.* **29,** 2104–14 (2012).

16. Vienberg, S. G. *et al.* Receptor-isoform-selective insulin analogues give tissue-preferential effects. *Biochem. J.* **440,** 301–308 (2011).

17. Hua, Q. X. *et al.* Design of an active ultrastable single-chain insulin analog: Synthesis, structure, and therapeutic implications. *J. Biol. Chem.* **283,** 14703–

14716 (2008).

18. Edgerton, D. S. *et al.* Changes in glucose and fat metabolism in response to the administration of a hepato-preferential insulin analog. *Diabetes* **63,** 3946–3954 (2014).

19. Veiseh, O., Tang, B. C., Whitehead, K. a, Anderson, D. G. & Langer, R. Managing diabetes with nanomedicine: challenges and opportunities. *Nat. Rev. Drug Discov.* **14,** 45–57 (2015).

20. Brownlee, M. & Cerami, A. A glucose-controlled insulin-delivery system: semisynthetic insulin bound to lectin. *Science (80-.).* **206,** 1190–1191 (1979).

21. Tiegs, G., Hentschel, J. & Wendel, A. AT cell-dependent experimental liver injury in mice inducible by concanavalin A. *J. Clin. Invest.* **90,** 196 (1992).

22. Bull, S. D. *et al.* Exploiting the Reversible Covalent Bonding of Boronic Acids: Recognition, Sensing, and Assembly. *Acc. Chem. Res.* **46,** 312–326 (2013).

23. Matsumoto, A. *et al.* A Synthetic Approach Toward a Self-Regulated Insulin Delivery System. *Angew. Chemie Int. Ed.* **51,** 2124–2128 (2012).

24. Fischel-Ghodsian, F., Brown, L., Mathiowitz, E., Brandenburg, D. & Langer, R. Enzymatically controlled drug delivery. *Proc. Natl. Acad. Sci.* **85,** 2403–2406 (1988).

25. Podual, K., Iii, F. J. D. & Peppas, N. A. Glucose-sensitivity of glucose oxidase-containing cationic copolymer hydrogels having poly (ethylene glycol) grafts. *J. Control. Release* **67,** 9–17 (2000).

26. Tai, W. *et al.* Bio-Inspired Synthetic Nanovesicles for Glucose-Responsive Release of Insulin. *Biomacromolecules* **15,** 3495–3502 (2014).

27. Gu, Z. *et al.* Injectable nano-network for glucose-mediated insulin delivery. *ACS Nano* **7,** 4194–201 (2013).

28. Gu, Z. *et al.* Glucose-responsive microgels integrated with enzyme nanocapsules for closed-loop insulin delivery. *ACS Nano* **7,** 6758–6766 (2013).

29. Podual, K., III, F. J. D. & Peppas, N. A. Preparation and Dynamic Response of Cationic Copolymer Hydrogels containing Glucose Oxidase. *Polymer (Guildf).* **41,** 3975–3983 (2000).

30. Holtz, J. H. & Asher, S. A. Polymerized colloidal crystal hydrogel films as intelligent chemical sensing materials. *Nature* **389,** 829–832 (1997).

31. Goldraich, M. & Kost, J. Glucose-sensitive polymeric matrices for controlled drug delivery. *Clin. Mater.* **13,** 135–142 (1993).

32. Yu, J. *et al.* Microneedle-array patches loaded with hypoxia-sensitive vesicles provide fast glucose-responsive insulin delivery. *Proc. Natl. Acad. Sci. U. S. A.* **112,** 8260–8265 (2015).

33. Grodsky, G. M., Curry, D., Landahl, H. & Bennett, L. [Further studies on the dynamic aspects of insulin release in vitro with evidence for a two-compartmental storage system]. *Acta Diabetol Lat* **6 Suppl 1,** 554–578 (1969).

34. Bakh, N. A., Bisker, G., Lee, M. A., Gong, X. & Strano, M. S. Rational Design of Glucose-Responsive Insulin Using Pharmacokinetic Modeling. *Adv. Healthc. Mater.* **1700601,** 1700601 (2017).

35. Bakh, N. A. *et al.* Glucose-responsive insulin by molecular and physical design. *Nat. Chem.* **9,** 937–943 (2017).

36. Lee, D. & Yannakakis, M. Principles and methods of testing finite state machines-a survey. *Proc. IEEE* **84,** 1090–1123 (1996).

37. Man, C. D., Raimondo, D. M., Rizza, R. A. & Cobelli, C. GIM, Simulation Software of Meal Glucose--Insulin Model. *J. Diabetes Sci. Technol.* **1,** 323–330 (2007).

38. Cobelli, C., Renard, E. & Kovatchev, B. Artificial pancreas: Past, present, future. *Diabetes* **60,** 2672–2682 (2011).

39. Kovatchev, B. P., Breton, M., Dalla Man, C. & Cobelli, C. In Silico Preclinical Trials: A Proof of Concept in Closed-Loop Control of Type 1 Diabetes. *J. Diabetes Sci. Technol.* **3,** 44–55 (2009).

40. Dalla Man, C., Rizza, R. A. & Cobelli, C. Meal simulation model of the glucose-insulin system. *IEEE Trans. Biomed. Eng.* **54,** 1740–1749 (2007).

41. Boutayeb, a & Chetouani, a. A critical review of mathematical models and data used in diabetology. *Biomed. Eng. Online* **5,** 43 (2006).

42. Sorensen, J. T. Ph.D dissertation, Department of Chemical Engineering, MIT. (1985).

43. Bisker, G., Iverson, N. M., Ahn, J. & Strano, M. S. A pharmacokinetic model of a tissue implantable insulin sensor. *Adv. Healthc. Mater.* **4,** 87–97 (2015).

44. Heller, J., Chang, A. C., Rood, G. & Grodsky, G. M. Release of insulin from pH-sensitive poly(ortho esters). *J. Control. Release* **13,** 295–302 (1990).

45. Albin, G., Horbett, T. A. & Ratner, B. Glucose Sensitive Membranes for Controlled Delivery of Insulin: Insulin Transport Studies. *J. Control. Release* **2,** 153–164 (1985).

46. Ishihara, K., Kobayashi, M., Ishimaru, N. & Shinohara, I. Glucose Induced Permeation Control of Insulin through a Complex Membrane Consisting of Immobilized Glucose Oxidase and a Poly(amine). *Polym. J.* **16,** 625–631 (1984).

47. Webber, M. J. & Anderson, D. G. Smart Approaches to Glucose-Responsive Drug Delivery. *J. Drug Target.* **23,** 651–655 (2015).

48. Hansen, J. S., Christensen, J. B., Petersen, J. F., Hoeg-Jensen, T. & Norrild, J. C. Arylboronic acids: A diabetic eye on glucose sensing. *Sensors Actuators B Chem.* **161,** 45–79 (2012).

49. Peppas, N. A. Is there a future in glucose-sensitive, responsive insulin delivery systems? *J. Drug Del. Sci. Tech.* **14,** 247–256 (2004).

50. Webber, M. J., Anderson, D. G. & Langer, R. S. Engineering Synthetically Modified Insulin for Glucose-Responsive Diabetes Therapy. *Expert Rev. Endocrinol. Metab.* **10,** 483–489 (2015).

51. James, T. D., Phillips, M. D. & Shink, S. in *Boronic Acids in Saccharide Recognition* 3–176 (The Royal Society of Chemistry, 2006).

52. Huang, Y.-J. *et al.* Glucose sensing via aggregation and the use of 'knock-out' binding to improve selectivity. *J. Am. Chem. Soc.* **135,** 1700–3 (2013).

53. Springsteen, G. & Wang, B. A detailed examination of boronic acid–diol complexation. *Tetrahedron* **58,** 5291–5300 (2002).

54. Springsteen, G. & Wang, B. Alizarin Red S. as a general optical reporter for studying the binding of boronic acids with carbohydrates. *Chem. Commun.* 1608–1609 (2001). doi:10.1039/b104895n

55. Arimori, S., Ward, C. J. & James, T. D. A D-glucose selective fluorescent assay. *Tetrahedron Lett.* **43,** 303–305 (2002).

56. Dowlut, M. & Hall, D. G. An improved class of sugar-binding boronic acids, soluble and capable of complexing glycosides in neutral water. *J. Am. Chem. Soc.* **128,** 4226–7 (2006).

57. Hansen, J. S., Christensen, J. B., Solling, T. I., Jakobsen, P. & Hoeg-Jensen, T. Ortho-substituted aryl monoboronic acids have improved selectivity for d-glucose relative to d-fructose and l-lactate. *Tetrahedron* **67,** 1334–1340 (2011).

58. Martinez-Aguirre, M. A., Villamil-Ramos, R., Guerrero-Alvarez, J. A. & Yatsimirsky, A. K. Substituent Effects and pH Profiles for Stability Constants of Arylboronic Acid Diol Esters. *J. Org. Chem.* **78,** 4674–4684 (2013).

59. Yan, J., Springsteen, G., Deeter, S. & Wang, B. The relationship among pKa, pH, and binding constants in the interactions between boronic acids and diols—it is not as simple as it appears. *Tetrahedron* **60,** 11205–11209 (2004).

60. Hoeg-Jensen, T. Preparation and Screening of Diboronate Arrays for Identification of Carbohydrate Binders. *QSAR Comb. Sci.* **23,** 344–351 (2004).

61. Yang, W., He, H. & Drueckhammer, D. G. Computer-Guided Design in Molecular Recognition : Design and Synthesis of a Glucopyranose Receptor. *Angew Chem Int Ed* **40,** 1714–1718 (2001).

62. Davis, A. P. & James, T. D. in *Functional Synthetic Receptors* (eds. Schrader, T. & Hamilton, A. D.) 45–109 (2005).

63. Walsh, G. Therapeutic insulins and their large-scale manufacture. *Appl. Microbiol. Biotechnol.* **67,** 151–159 (2005).

64. Baeshen, N. A. *et al.* Cell factories for insulin production. 1–9 (2014).

65. Keasling, J. D., Mendoza, A., Baran, P. S. & Bernstein, H. D. Synthesis: A Constructive Debate. *Nature* **492,** 188–189 (2012).

66. Liu, F., Zaykov, A. N., Levy, J. J., Dimarchi, D. & Mayer, J. P. Chemical synthesis of peptides within the insulin superfamily. *J. Pept. Sci.* **22,** 260–270 (2016).

67. Liu, F., Luo, E. Y., Flora, D. B. & Mezo, A. R. A synthetic route to human insulin using isoacyl peptides. *Angew. Chemie - Int. Ed.* **53,** 3983–3987 (2014).

68. Liu, F., Luo, E. Y., Flora, D. B. & Mayer, J. P. Concise synthetic routes to human insulin. *Org. Lett.* **15,** 960–963 (2013).

69. Mayer, J. P., Zhang, F. & DiMarchi, R. D. Insulin Structure and Function. *Pept. Sci.* **88,** 687–713 (2007).

70. Tofteng, A. P., Jensen, K. J., Schäffer, L. & Hoeg-Jensen, T. Total synthesis of desB30 insulin analogues by biomimetic folding of single-chain precursors. *Chembiochem* **9,** 2989–2996 (2008).

71. Avital-Shmilovici, M. *et al.* Fully convergent chemical synthesis of ester insulin: Determination of the high resolution X-ray structure by racemic protein crystallography. *J. Am. Chem. Soc.* **135,** 3173–3185 (2013).

72. Zaykov, A. N., Mayer, J. P., Gelfanov, V. M. & Dimarchi, R. D. Chemical synthesis of insulin analogs through a novel precursor. *ACS Chem. Biol.* **9,** 683–691 (2014).

73. Royo, M., Alsina, J., Giralt, E., Slomcyznska, U. & Albericio, F. S-Phenylacetamidomethyl (Phacm): an orthogonal cysteine protecting group for Boc and Fmoc solid-phase peptide synthesis strategies. *J. Chem. Soc. Perkin Trans.* 1095–1102 (1995).

74. Karas, J. A. *et al.* 2-Nitroveratryl as a Photocleavable Thiol-Protecting Group for Directed Disulfide Bond Formation in the Chemical Synthesis of Insulin. *Chem. - A Eur. J.* **20,** 9549–9552 (2014).

75. Hoeg-Jensen, T. *et al.* Insulins with built-in glucose sensors for glucose responsive insulin release. *J. Pept. Sci.* **11,** 339–46 (2005).

76. Hoeg-Jensen, T., Havelund, S., Nielsen, P. K. & Markussen, J. Reversible insulin self-assembly under carbohydrate control. *J. Am. Chem. Soc.* **127,** 6158–9 (2005).

77. Chou, D. H.-C. *et al.* Glucose-responsive insulin activity by covalent modification with aliphatic phenylboronic acid conjugates. *Proc. Natl. Acad. Sci. U. S. A.* 1–6 (2015). doi:10.1073/pnas.1424684112

78. Standards of Medical Care in Diabetes - 2018: Abridged for Primary Care Providers. *Clin. Diabetes* **36,** 14–37 (2018).

79. Classification and Diagnosis of Diabetes: Standards of Medical Care in Diabetes - 2018. *Diabetes Care* **41,** S13–S27 (2018).

80. Reichard, P., Nilsson, B.-Y. & Rosenqvist, U. The Effect of Long-Term Intensified Insulin Treatment on the Development of Microvascular Complications of Diabetes

Mellitus. *New Engl. J. Med.* **329,** 304–309 (1993).

81. Jacqueminet, S., Masseboeuf, N., Rolland, M., Grimaldi, A. & Sachon, C. Limitations of the so-called 'intensified' insulin therapy in type 1 diabetes mellitus. *Diabetes Metab.* **31,** 4S45-4S50 (2005).

82. Gerstein, H. C. *et al.* Basal Insulin and Cardiovascular and Other Outcomes in Dysglycemia. *N. Engl. J. Med.* **367,** 319–328 (2012).

83. Pathak, R. D. *et al.* Severe hypoglycemia requiring medical intervention in a large cohort of adults with diabetes receiving care in U.S. integrated health care delivery systems: 2005-2011. *Diabetes Care* **39,** 363–370 (2016).

84. Hirsch, I. B. Insulin Analogues. *N. Engl. J. Med.* **352,** 174–183 (2005).

85. Zinman, B. Newer insulin analogs: Advances in basal insulin replacement. *Diabetes, Obes. Metab.* **15,** 6–10 (2013).

86. Burn, P. Type 1 diabetes. *Nat. Rev. Drug Discov.* **9,** 187–188 (2010).

87. Valla, V. Therapeutics of diabetes mellitus: focus on insulin analogues and insulin pumps. *Exp. Diabetes Res.* **2010,** 178372 (2010).

88. Kurtzhals, P. *et al.* Albumin binding and time action of acylated insulins in various species. *J. Pharm. Sci.* **85,** 304–8 (1996).

89. Jonassen, I. *et al.* Design of the novel protraction mechanism of insulin degludec, an ultra-long-acting basal insulin. *Pharm. Res.* **29,** 2104–2114 (2012).

90. Hilgenfeld, R., Seipke, G., Berchtold, H. & Owens, D. R. The evolution of insulin glargine and its continuing contribution to diabetes care. *Drugs* **74,** 911–927 (2014).

91. Grunberger, G. The need for better insulin therapy. *Diabetes, Obes. Metab.* **15,** 1–5 (2013).

92. Madsbad, S. LY2605541—A Preferential Hepato-Specific Insulin Analogue. *Diabetes* **63,** 390–392 (2014).

93. Kaur, Z. P., Ochman, A. R., Mayer, J. P., Gelfanov, V. M. & Dimarchi, R. D. Discovery of high potency, single-chain insulin analogs with a shortened B-chain and nonpeptide linker. *ACS Chem. Biol.* **8,** 1822–1829 (2013).

94. Number (in Millions) of Adults with Diabetes by Diabetes Medication Status, United States, 1997–2011. *Center for Disease Control and Prevention: Diabetes Public Health Resource* (2013). Available at: https://www.cdc.gov/diabetes/statistics/meduse/fig1.htm. (Accessed: 26th June 2018)

95. Guan, Y. & Zhang, Y. Boronic acid-containing hydrogels: synthesis and their applications. *Chem. Soc. Rev.* **42,** 8106–21 (2013).

96. Yang, H. *et al.* Glucose-responsive complex micelles for self-regulated release of insulin under physiological conditions. *Soft Matter* **9,** 8589 (2013).

97. Zhang, G., Zhang, X., Shen, H., Yang, J. & Yang, J. Smarter glucose-sensitivity of polymeric micelles formed from phenylborate ester-co-pyrenylboronic ester for insulin delivery at physiological pH. *Rsc Adv.* **4,** 49964–49973 (2014).

98. Yesilyurt, V. *et al.* Injectable Self-Healing Glucose-Responsive Hydrogels with pH-Regulated Mechanical Properties. *Adv. Mater.* **28,** 86–91 (2016).

99. Poon, K. & King, A. B. Glargine and detemir: Safety and efficacy profiles of the long-acting basal insulin analogs. *Drug. Healthc. Patient Saf.* **2,** 213–23 (2010).

100. Sanofi-aventis. *Product Monograph: Lantus® (insulin glargine)*. (2017).

101. United States Pharmacopeia. *USP Monograph: Human Insulin*. (2018).

102. United States Pharmacopeia. *Insulin Glargine*. (2016).

103. Novo Nordisk. *Product Monograph: Levemir® (insulin detemir)*. (2017).

104. Hadji-Georgopoulos, A., Schmidt, M. I., Margolis, S. & Kowarski, A. A. Elevated Hypoglycemic Index and Late Hyperinsulinism in Symptomatic Postprandial Hypoglycemia. *J. Clin. Endocrinol. Metab.* **50,** 371–376 (1980).

105. International Hypoglycaemia Study Group. Glucose Concentrations of Less Than 3.0 mmol/L (54 mg/dL) Should Be Reported in Clinical Trials: A Joint Position Statement of the American Diabetes Association and the European Association for the Study of Diabetes: Table 1. *Diabetes Care* **40,** 155–157 (2017).

106. Wu, K. K. & Huan, Y. Streptozotocin-induced diabetic models in mice and rats. *Curr. Protoc. Pharmacol.* **40,** 5.47.1-5.47.14 (2008).

107. Brange, J. & Vølund, A. Insulin analogs with improved pharmacokinetic profiles. *Adv. Drug Deliv. Rev.* **35,** 307–335 (1999).

108. Hirose, T. Development of new basal insulin peglispro (LY2605541) ends in a disappointing result. *Diabetol. Int.* **7,** 16–17 (2016).

109. Gough, S. C. L., Harris, S., Woo, V. & Davies, M. Insulin degludec: Overview of a novel ultra long-acting basal insulin. *Diabetes, Obes. Metab.* **15,** 301–309 (2013).

110. Polonsky, W. H. & Henry, R. R. Poor medication adherence in type 2 diabetes: Recognizing the scope of the problem and its key contributors. *Patient Prefer. Adherence* **10,** 1299–1306 (2016).

111. García-Pérez, L.-E., Álvarez, M., Dilla, T., Gil-Guillén, V. & Orozco-Beltrán, D. Adherence to Therapies in Patients with Type 2 Diabetes. *Diabetes Ther.* **4,** 175–194 (2013).

112. Ravaine, V., Ancla, C. & Catargi, B. Chemically controlled closed-loop insulin delivery. *J. Control. Release* **132,** 2–11 (2008).

113. Chen, W. *et al.* Microneedle-array patches loaded with dual mineralized protein/peptide particles for type 2 diabetes therapy. *Nat. Commun.* **8,** (2017).

114. Ahmed, N. & Thornalley, P. J. Advanced glycation endproducts: what is their

relevance to diabetic complications? *Diabetes. Obes. Metab.* **9,** 233–45 (2007).

115. Menting, J. G. *et al.* How insulin engages its primary binding site on the insulin receptor. *Nature* **493,** 241–5 (2013).

116. Menting, J. G. *et al.* Protective hinge in insulin opens to enable its receptor engagement. *Proc. Natl. Acad. Sci. U. S. A.* **111,** E3395-404 (2014).

117. Derewenda, U. *et al.* X-ray analysis of the single chain B29-A1 peptide-linked insulin molecule. A completely inactive analogue. *J. Mol. Biol.* **220,** 425–33 (1991).

118. Hua, Q. X. *et al.* Mini-proinsulin and mini-IGF-I: homologous protein sequences encoding non-homologous structures. *J. Mol. Biol.* **277,** 103–118 (1998).

119. Nakagawa, S. H. & Tagers, H. S. Perturbation of Insulin-Receptor Interactions by Intramolecular Hormone Cross-linking. *J. Biol. Chem.* **264,** 272–279 (1989).

120. Brems, D. N., Brown, P. L., Nakagawa, S. H. & Tager, H. S. The conformational stability and flexibility of insulin with an additional intramolecular cross-link. *J. Biol. Chem.* **266,** 1611–1615 (1991).

121. Zion, T. C. & Lancaster, T. M. Soluble non-depot insulin conjugates and uses thereof. *U.S Pat. Appl.* **2014003769,** (2012).

122. Lin, S. *et al.* Glucose-responsive insulin conjugates. *U.S Pat. Appl.* **WO 2015051,** (2015).

123. Cutfield, J. *et al.* Evidence Concerning Insulin Activity from the Structure of a Cross-Linked Derivative. *Hoppe-Seyler's Z. Physiol. Chem.* 755–761 (1981).

124. Berenson, D., Weiss, A. R., Wan, Z.-L. & Weiss, M. A. Insulin analogs for the treatment of diabetes mellitus: therapeutic applications of protein engineering. *Ann. N. Y. Acad. Sci.* **1243,** E40–E54 (2012).

125. Drejer, K. The bioactivity of insulin analogues from in vitro receptor binding to in vivo glucose uptake. *Diabetes Metab. Rev.* **8,** 259–285 (1992).

126. Weiss, M. A. & Ph, D. Insulin Fibrillation and Protein Design: Topological Resistance of Single-Chain Analogs to Thermal Degradation with Application to a Pump Reservoir. *J. Diabetes Technol.* **6,** 277–288 (2012).

127. Millican, R. L. & Brems, D. N. Equilibrium intermediates in the denaturation of human insulin and two monomeric insulin analogs. *Biochemistry* **33,** 1116–1124 (1994).

128. Phillips, N. B., Whittaker, J., Ismail-Beigi, F. & Weiss, M. A. Insulin Fibrillation and Protein Design: Topological Resistance of Single-Chain Analogs to Thermal Degradation with Application to a Pump Reservoir. *J. Diabetes Sci. Technol.* **6,** 277–288 (2012).

129. Webber, M. J. *et al.* Supramolecular PEGylation of biopharmaceuticals. *Proc. Natl. Acad. Sci.* 201616639 (2016). doi:10.1073/pnas.1616639113

130. Whittingham, J. L., Havelund, S. & Jonassen, I. Crystal Structure of a Prolonged-Acting Insulin with Albumin-Binding Properties. *Biochemistry* **36,** 2826–2831 (1997).

131. Whittingham, J. L. *et al.* Crystallographic and Solution Studies of N -Lithocholyl Insulin : A New Generation of Prolonged-Acting Human Insulins. *Biochemistry* **43,** 5987–5995 (2004).

132. Steensgaard, D. B. *et al.* Ligand-controlled assembly of hexamers, dihexamers, and linear multihexamer structures by the engineered acylated insulin degludec. *Biochemistry* **52,** 295–309 (2013).

133. Davies, M. J. *et al.* Real-world factors affecting adherence to insulin therapy in patients with Type 1 or Type 2 diabetes mellitus: A systematic review. *Diabet. Med.* **30,** 512–524 (2013).

134. Peyrot, M., Barnett, A. H., Meneghini, L. F. & Schumm-Draeger, P. M. Insulin adherence behaviours and barriers in the multinational Global Attitudes of Patients and Physicians in Insulin Therapy study. *Diabet. Med.* **29,** 682–689 (2012).

135. Fineberg, S. E. *et al.* Immunological responses to exogenous insulin. *Endocr. Rev.* **28,** 625–652 (2007).

136. Elsadek, B. & Kratz, F. Impact of albumin on drug delivery - New applications on the horizon. *J. Control. Release* **157,** 4–28 (2012).

137. Sleep, D., Cameron, J. & Evans, L. R. Albumin as a versatile platform for drug half-life extension. *Biochim. Biophys. Acta - Gen. Subj.* **1830,** 5526–5534 (2013).

138. Becker, R. H. A. *et al.* New insulin glargine 300 Units/mL provides a more even activity profile and prolonged glycemic control at steady state compared with insulin glargine 100 Units/mL. *Diabetes Care* **38,** 637–643 (2015).

139. Sluzky, V., Klibanov, A. M. & Langer, R. Mechanism of insulin aggregation and stabilization in agitated aqueous solutions. *Biotechnol. Bioeng.* **40,** 895–903 (1992).

140. Nielsen, L., Frokjaer, S., Brange, J., Uversky, V. N. & Fink, A. L. Probing the mechanism of insulin fibril formation with insulin mutants. *Biochemistry* **40,** 8397–8409 (2001).

141. Nielsen, L. *et al.* Effect of environmental factors on the kinetics of insulin fibril formation: Elucidation of the molecular mechanism. *Biochemistry* **40,** 6036–6046 (2001).

142. Malik, R. & Roy, I. Probing the mechanism of insulin aggregation during agitation. *Int. J. Pharm.* **413,** 73–80 (2011).

143. Baudys, M. *et al.* Extending insulin action in vivo by conjugation to carboxymethyl dextran. *Bioconjug. Chem.* **9,** 176–83 (1998).

144. Lee, E., Lee, J. & Jon, S. A novel approach to oral delivery of insulin by conjugating with low molecular weight chitosan. *Bioconjug. Chem.* **21,** 1720–1723 (2010).

145. Mansfield, K. M. & Maynard, H. D. Site-Specific Insulin-Trehalose Glycopolymer Conjugate by Grafting from Strategy Improves Bioactivity. *ACS Macro Lett.* **7,** 324–329 (2018).

146. Uchio, T., Baudys, M., Liu, F., Song, S. & Kim, S. Site-specific insulin conjugates with enhanced stability and extended action profile. *Adv. Drug Deliv. Rev.* **35,** 289–306 (1999).

147. Turecek, P. L., Bossard, M. J., Schoetens, F. & Ivens, I. A. PEGylation of Biopharmaceuticals: A Review of Chemistry and Nonclinical Safety Information of Approved Drugs. *J. Pharm. Sci.* **105,** 460–475 (2016).

148. Jacober, S. J. *et al.* Basal insulin peglispro: Overview of a novel long-acting insulin with reduced peripheral effect resulting in a hepato-preferential action. *Diabetes, Obes. Metab.* **18,** 3–16 (2016).

149. Henry, R. R. *et al.* Basal insulin peglispro demonstrates preferential hepatic versus peripheral action relative to insulin glargine in healthy subjects. *Diabetes Care* **37,** 2609–2615 (2014).

150. Caparrotta, T. M. & Evans, M. PEGylated insulin Lispro, (LY2605541)-A new basal insulin analogue. *Diabetes, Obes. Metab.* **16,** 388–395 (2014).

151. Muñoz-Garach, A., Molina-Vega, M. & Tinahones, F. J. How Can a Good Idea Fail? Basal Insulin Peglispro [LY2605541] for the Treatment of Type 2 Diabetes. *Diabetes Ther.* **8,** 9–22 (2017).

152. Israelachvili, J. The different faces of poly(ethylene glycol). *Proc. Natl. Acad. Sci.* **94,** 8378–8379 (1997).

153. Keefe, A. J. & Jiang, S. Poly(zwitterionic)protein conjugates offer increased stability without sacrificing binding affinity or bioactivity. *Nat. Chem.* **4,** 59–63 (2012).

154. Zhang, P., Sun, F., Liu, S. & Jiang, S. Anti-PEG antibodies in the clinic: Current issues and beyond PEGylation. *J. Control. Release* **244,** 184–193 (2016).

155. van Witteloostuijn, S. B., Pedersen, S. L. & Jensen, K. J. Half-Life Extension of Biopharmaceuticals using Chemical Methods: Alternatives to PEGylation. *ChemMedChem* **11,** 2474–2495 (2016).

156. Lewis, A., Tang, Y., Brocchini, S., Choi, J. W. & Godwin, A. Poly(2-methacryloyloxyethyl phosphorylcholine) for protein conjugation. *Bioconjug. Chem.* **19,** 2144–2155 (2008).

157. Jackson, M. A. *et al.* Zwitterionic Nanocarrier Surface Chemistry Improves siRNA Tumor Delivery and Silencing Activity Relative to Polyethylene Glycol. *ACS Nano* **11,** 5680–5696 (2017).

158. Xie, J. *et al.* Simple Protein Modification Using Zwitterionic Polymer to Mitigate the Bioactivity Loss of Conjugated Insulin. *Adv. Healthc. Mater.* **6,** 1–5 (2017).

159. Bhattacharjee, S. *et al.* Site-Specific Zwitterionic Polymer Conjugates of a Protein

Have Long Plasma Circulation. *ChemBioChem* **16,** 2451–2455 (2015).

160. Li, Y., Liu, R., Shi, Y., Zhang, Z. & Zhang, X. Zwitterionic poly(carboxybetaine)-based cationic liposomes for effective delivery of small interfering RNA therapeutics without accelerated blood clearance phenomenon. *Theranostics* **5,** 583–596 (2015).

161. Lindsay, D. G. & Shall, S. The acetylation of insulin. *Biochem. J.* **121,** 737–45 (1971).

162. Kavimandan, N. J., Losi, E., Wilson, J. J., Brodbelt, J. S. & Peppas, N. a. Synthesis and characterization of insulin-transferrin conjugates. *Bioconjug. Chem.* **17,** 1376–84 (2006).

163. McCormick, C. L. & Lowe, A. B. Aqueous RAFT polymerization: Recent developments in synthesis of functional water-soluble (Co)polymers with controlled structures. *Acc. Chem. Res.* **37,** 312–325 (2004).

164. Greenfield, N. J. Using circular dichroism spectra to estimate protein secondary structure. *Nat. Protoc.* **1,** 2876–2890 (2006).

165. Duenweg, B., Reith, D., Steinhauser, M. & Kremer, K. Corrections to Scaling in the Hydrodynamic Properties of Dilute Polymer Solutions. *J. Chem. Phys.* **117,** 914–924 (2002).

166. Sosnick, T. R., Fang, X. & Shelton, V. M. Application of Circular Dichroism to Study RNA Folding Transitions. *Methods Enzymol.* **317,** 393–409 (2000).

167. Beals, J. M. *et al.* LY2605541: leveraging hydrodynamic size to develop a novel basal insulin (Abstract). *Diabetes* **61 (Suppl.,** A228 (2012).

168. Moore, M. C. *et al.* Novel PEGylated basal insulin LY2605541 has a preferential hepatic effect on glucose metabolism. *Diabetes* **63,** 494–504 (2014).

169. Shao, J., Zaro, J. L. & Shen, W. C. Tissue barriers and novel approaches to achieve hepatoselectivity of subcutaneously-injected insulin therapeutics. *Tissue Barriers* **4,** 1–6 (2016).

170. Kawasaki, T., Akanuma, H. & Yamanouchi, T. Increased Fructose Concentrations in Blood and Urine in Patients With Diabetes . *Diabetes Care* **25,** 353–357 (2002).

171. Blough, B., Moreland, A. & Mora Jr., A. Metformin-induced lactic acidosis with emphasis on the anion gap. *Proc (Bayl Univ Med Cent)* **28,** 31–33 (2015).

172. Vecchio, S. & Protti, A. Metformin-induced lactic acidosis: No one left behind. *Crit. Care* **15,** 1–2 (2011).

173. Goodwin, M. L., Harris, J. E., Hernández, A. & Gladden, L. B. Blood lactate measurements and analysis during exercise: A guide for clinicians. *J. Diabetes Sci. Technol.* **1,** 558–569 (2007).

174. Jin, S., Cheng, Y., Reid, S., Li, M. & Wang, B. Carbohydrate Recognition by Boronolectins, Small Molecules, and Lectins. *Med. Res. Rev.* **30,** 171–257 (2011).

175. Kubik, S. Synthetic Lectins. *Angew. Chem. Int. Ed.* **48,** 1722–1725 (2009).

176. Davis, A. P. Synthetic lectins. *Org. Biomol. Chem.* **7,** 3629–3638 (2009).

177. Ke, C., Destecroix, H., Crump, M. P. & Davis, A. P. A simple and accessible synthetic lectin for glucose recognition and sensing. *Nat. Chem.* **4,** 718–723 (2012).